

**VERIFICATION OF THERMOGRAPHIC BRIDGE  
INSPECTION TECHNOLOGIES**

---

A Thesis presented to the Faculty of the Graduate School  
at the University of Missouri - Columbia

---

In Partial Fulfillment of the Requirements for the Degree  
Master of Science

---

by

Alan Michael Jungnitsch

Dr. Glenn Washer, Graduate Advisor

MAY 2015

The undersigned, appointed by the Dean of the Graduate School, have examined the thesis entitled

**VERIFICATION OF THERMOGRAPHIC BRIDGE  
INSPECTION TECHNOLOGIES**

Presented by **Alan Michael Jungnitsch**

A candidate for the degree of **Master of Science**,

And hereby certify, in their opinion, it is worthy of acceptance.

---

Professor Glenn Washer

---

Professor Sarah Orton

---

Professor Roger Fales

## **ACKNOWLEDGEMENTS**

I would first and foremost like to thank Dr. Glenn Washer, Associate Professor and my graduate advisor in the Department of Civil & Environmental Engineering at the University of Missouri-Columbia. Dr. Washer's guidance and confidence in my abilities have been invaluable to me. He is the reason I chose to attend graduate school and I am truly indebted to him for giving me the opportunity to work with him for the last 3 years.

Thanks also to my fellow students at Mizzou; Seth Nelson, Rilya Rumbayan, Dan Looten, Steven Brooks, Justin Schmidt, Pedro Ruiz Fabian, Scott Feldt and Ali Sultan who donated their time and efforts to our needs.

Additionally, I would like to thank Mike Trial and all the State Department of Transportation personnel who assisted in the success of this research.

Furthermore, I am grateful to the Graduate support staff in the Civil Engineering Office for always being available, helpful and caring, in particular Mary McCush and Connie Taylor

# TABLE OF CONTENTS

Acknowledgements.....	ii
List of Figures .....	vi
List of Tables .....	xiii
Abstract .....	xiv
1 Introduction.....	1
1.1 Purpose .....	7
1.2 Goals .....	8
1.3 Objectives.....	8
1.4 Approach .....	8
1.5 Individual Contributions.....	9
2 Background .....	11
2.1 Introduction.....	11
2.2 Concrete and corrosion.....	11
2.3 IR Theory.....	15
2.3.1 IR Radiation .....	16
2.3.2 Heat Transfer .....	18
2.3.3 Environmental Factors .....	23
3 Training.....	27
3.1 Ohio.....	29
3.2 Kentucky.....	31
3.3 Florida .....	33
4 Hand held Verification Results .....	36
4.1 Tools for Inspection .....	36
4.1.1 Lens Selection.....	36

4.1.2	Wind Speed Analysis .....	40
4.1.3	Shared Data Site .....	41
4.1.4	Weather Checker .....	42
4.2	Kansas City .....	42
4.3	Providence Road .....	47
4.4	Iowa .....	49
4.5	Georgia .....	55
4.6	Pennsylvania .....	60
4.7	Texas .....	63
4.8	Oregon .....	65
4.9	Kentucky .....	70
4.10	New York .....	73
4.11	Ohio .....	77
4.12	Comparison of Results .....	81
5	IR-UTD Verification .....	84
5.1	Test Blocks .....	87
5.1.1	Lab Test Block .....	87
5.1.2	RTF Test Block .....	89
5.2	Providence Road .....	93
5.3	Kansas City, MO .....	97
5.3.1	Test One .....	97
5.3.2	Test Two .....	100
5.4	Lamoni, IA .....	103
5.4.1	Epoxy Injection Pretest .....	105

5.4.2	Epoxy Injection Test.....	108
5.5	University of Missouri-Columbia Columns.....	115
5.5.1	South Face.....	116
5.5.2	North Face .....	118
5.6	West Boulevard .....	120
6	Analysis .....	123
7	Implementation .....	132
8	Conclusions .....	134
8.1	Results .....	134
8.2	Future Work.....	137
	References .....	138
	Appendix A .....	141

## LIST OF FIGURES

Figure 2-1: Delamination at the embedded steel level.....	13
Figure 2-2: IR energy emitted from a concrete deck under day and night time conditions.....	16
Figure 3-1: IR (A) and digital (B) images of deck delaminations captured during Ohio training .....	30
Figure 3-2: Ambient temperature surrounding Figure 3-1 during Ohio training.....	31
Figure 3-3: IR (A) and digital (B) images of a pier cap delamination captured during Kentucky training .....	32
Figure 3-4: Ambient temperature surrounding Figure 3-3 during Kentucky training.....	33
Figure 3-5: Infrared (A) and digital (B) images of a deck delamination in Florida .....	34
Figure 3-6: Ambient temperature on April 30, 2014 for Tampa, FL.....	35
Figure 4-1: Critical dimension as a function of target distance.....	38
Figure 4-2: Critical dimension study setup.....	39
Figure 4-3: Target distances of 25 ft with the wide lens (A) and 50 ft with the regular lens (B) .....	40
Figure 4-4: Correlation of experimental wind data to NWS wind data.....	41
Figure 4-5: Chain drag results for the North span of Bridge A0295 .....	44
Figure 4-6: Infrared (A) and digital (B) images of a deck delamination in Kansas City .....	45

Figure 4-7: Infrared (A) and Digital (B) images of a group of delaminations in Kansas City.....	46
Figure 4-8: Ambient Temperature for Kansas City, MO on March 9th, 2014 .....	47
Figure 4-9: Infrared (A) and Digital (B) images of Providence Rd. Bridge (northbound) over Hinkson Creek.....	48
Figure 4-10: Ambient temperature on May 6th, 2014 for Columbia, MO..	49
Figure 4-11: Hammer sound result (A) and Infrared (B) images of a deck delamination in Lamoni, IA .....	50
Figure 4-12: Infrared (A) and Digital (B) images from the soffit of the delamination in Figure 4-11 .....	51
Figure 4-13: Drilled hole locations for borescope measurements .....	52
Figure 4-14: Borescope image of a deck delamination .....	53
Figure 4-15: Schematic diagram of how the borescope is used for inspection .....	54
Figure 4-16: Ambient temperature for verification in Lamoni, IA .....	55
Figure 4-17: Ambient air temperature for the verification trip to Georgia (2012).....	56
Figure 4-18: Ambient air temperature for the verification trip to Georgia (2014).....	57
Figure 4-19: IR (A) and digital (B) images of a deck delamination on Johnstonville Rd. ....	58



Figure 4-20: IR (A) and digital (B) images of a deck delamination over Ocmulgee River.....	59
Figure 4-21: IR (A) and digital (B) images of a deck delamination over a railroad on Dames Ferry Rd. ....	59
Figure 4-22: Ambient air temperature for the verification trip to Pennsylvania .....	60
Figure 4-23: Thermal image (A) and digital image (B) of a pier cap delamination .....	61
Figure 4-24: Boom truck utilized for imaging a bridge deck from an elevated location .....	62
Figure 4-25: IR (A) and digital (B) images from a boom of a deck in Pennsylvania .....	63
Figure 4-26: Ambient temperature for the verification trip to Texas .....	64
Figure 4-27: Ambient temperature for the verification trip to Oregon .....	66
Figure 4-28: Hammer sounding results of a drain delamination from the WJE report.....	67
Figure 4-29: Thermal image (A) and digital image (B) of a drain delamination .....	68
Figure 4-30: IR (A) and digital (B) image of a possible parge coat delamination .....	69
Figure 4-31: Thermal (A) and Digital (B) images of a delaminated abutment wall under I-265 .....	71

Figure 4-32: IR (A) and digital (B) images of hammer sounding results on a pier in Kentucky .....	71
Figure 4-33: Ambient temperature for the verification trip to Kentucky ....	73
Figure 4-34: Previous and forecasted weather conditions of Albany, NY provided by the weather checker.....	74
Figure 4-35: IR (A) and digital (B) images of a delaminated column on Pier 1 of South Bridge.....	75
Figure 4-36: Illustration of how thermal gradient can affect an image.....	76
Figure 4-37: Afternoon infrared (A) and digital (B) images of a soffit delamination in Columbus, Ohio.....	78
Figure 4-38: Morning infrared (A) and digital (B) images of a soffit delamination in Columbus, Ohio.....	78
Figure 4-39: Thermal images of delaminations in the soffit of a wide slab bridge, showing morning (top) and afternoon (bottom) results .....	79
Figure 4-40: Thermal images showing damage along a longitudinal joint in a 159 ft wide slab bridge.....	80
Figure 4-41: Ambient temperature for June 23, 2014 in Columbus Ohio .	81
Figure 5-1: Components of the IR-UTD system.....	85
Figure 5-2: Lab test block setup.....	88
Figure 5-3: Post-processed infrared (A) and digital (B) images of a lab IR-UTD test .....	89
Figure 5-4: Test setup for the IR-UTD test conducted at the University of Missouri RTF .....	90

Figure 5-5: Concrete block constructed for testing nondestructive evaluation technologies .....	91
Figure 5-6: Processed results of IR-UTD test conducted on September 4, 2014 .....	92
Figure 5-7: Demonstration of IR-UTD spatial resolution .....	93
Figure 5-8: Test setup for IR-UTD test of Providence Road bridge .....	95
Figure 5-9: Processed results of Providence Road test conducted on May 6, 2014 .....	96
Figure 5-10: Setup for IR-UTD test in Kansas City .....	98
Figure 5-11: Processed results of IR-UTD test conducted on June 5, 2014 .....	99
Figure 5-12: Deck temperature of June 5, 2014 test measured with a data logger and thermocouple .....	100
Figure 5-13: Camera head with lenses positioned in a vertical orientation .....	101
Figure 5-14: Processed IR-UTD results of the June 5, 2014 (left) and August 20, 2014 (right) tests.....	102
Figure 5-15: Components of the IR-UTD test setup for Lamoni, IA .....	104
Figure 5-16: Full view of the Lamoni, IA IR-UTD pretest setup.....	106
Figure 5-17: Close-up of the plate series used for mounting the camera head .....	107
Figure 5-18: Generator used to power the IR-UTD system during the pretest .....	107

Figure 5-19: Close up of the pan and tilt mount and rain hood .....	110
Figure 5-20: Battery box used to power the IR-UTD system during the epoxy injection test.....	110
Figure 5-21: Contents of the battery box.....	111
Figure 5-22: Processed IR-UTD results (left), hammer sounding results (middle) and overlay of the two (right) of the epoxy injection test .....	114
Figure 5-23: Deck temperatures of the first two days of the epoxy injection test.....	114
Figure 5-24: Deck temperatures of the last two days of the epoxy injection test.....	115
Figure 5-25: Test Setup for the Columns test on the south face .....	117
Figure 5-26: Processed results of the IR-UTD test on the south face of the Mizzou columns.....	118
Figure 5-27: Processed results of the IR-UTD test on the north face of the Mizzou columns.....	119
Figure 5-28: Setup for West Blvd. under I-70 in Columbia, MO .....	121
Figure 5-29: Result for West Blvd. soffit test.....	122
Figure 6-1: Hand held (A) and IR-UTD (B) results of the Phase I test block .....	125
Figure 6-2: Areas used to calculate total delamination of the Lamoni, IA bridge deck.....	127
Figure 6-3: Processed image of Lamoni, IA bridge deck showing relative depths of delamination .....	130

Figure A-0-1: Schematic diagram of observation angles .....	148
Figure A-0-2: Graph showing inspection windows as a function of day length.....	150
Figure A-0-3: Graph showing critical dimension as a function of distance .....	151

## LIST OF TABLES

Table 2-1: Thermal properties of typical materials found in civil structures .....	20
Table 3-1: Training survey results from Ohio, Kentucky and Florida .....	28
Table 4-1: Maximum identification distances for each object of the study	39
Table 4-2: Results of the comparison between IR and hammer sounding results.....	83
Table 6-1: Environmental conditions for training and verification testing	124
Table 6-2: Number of pixels from areas marked in Figure 6-2.....	128

## **ABSTRACT**

This thesis presents the research performed to determine the reliability of infrared technology as an inspection tool for concrete bridge components. Concrete deteriorates due to the corrosion of embedded reinforcing steel. These cracks join to form delaminations, propagate to the surface which results in spalling. The ability to detect those delaminations in the structural components of a bridge (deck, superstructure and substructure) is vital when determining when those components need to be repaired or replaced.

The objectives of the research were to quantify the capability and reliability of thermal imaging technology in the field, field test and validate inspection guidelines for the application of thermal imaging for bridge inspection, and to identify implementation barriers faced by inspectors in the field.

Infrared results were quantified using both a hand held camera and a newly developed system. Hand held results were compared to hammer sounding techniques for quantitative analysis. The analysis showed that hammer sounding is conservative when compared to infrared results. A new system was also developed to determine area and relative depth of delamination without need of further physical inspection. Results of the research show that infrared technology is an effective inspection technology under conducive environmental conditions.

# 1 INTRODUCTION

The research performed in the following paper explored the ability of infrared (IR) technology to be used as a tool for inspection of concrete bridge components. The research utilized two different instruments: a hand held camera for relatively brief bridge inspections (~1 hour) and an ultra-time domain (UTD) system utilized for inspections covering an extended period of time (6-24 hours). The overall goal of the research was to improve the safety of bridges by developing nondestructive evaluation (NDE) technologies to support and improve inspections.

Corrosion of embedded reinforcing steel is the leading cause for deterioration of concrete bridges in the United States. The deterioration of concrete due to corrosion of embedded reinforcing steel is a widespread problem for State Departments of Transportation (DOT). Cracks develop in the concrete at a subsurface level and develop into delaminations (Maser 1990). Delaminations are subsurface horizontal cracks, parallel to the concrete surface. These delaminations develop due to the expansion of the reinforcing steel during corrosion processes, and as such typically occur at the level of the reinforcing steel mat (Huston 2002). Reinforcing steel mats are typically located at a depth of 2 to 3 inches from the surface of the concrete. Depending on their composition, the volume of the corrosion products can increase 2 to 6 times more than that of the iron they are derived from (Bertolini 2004). As corrosion damage advances, these subsurface delaminations can mechanically separate from the concrete structure; this condition is typically referred to as spalling (Masliwec 1988, Maser 1990).



Spalling of the concrete further exposes the reinforcing steel to the ambient environment which results in accelerated deterioration rates. Spalling in the soffit area of an overpass bridge, or other concrete bridge components, can fall into traffic and present a hazard to motorists or pedestrians (Fenwick 2009). Condition assessment tools that are able to detect delaminations before spalling occurs are needed to ensure motorist safety and identify maintenance and repair needs.

Nondestructive evaluation (NDE) methods used to access subsurface defects in concrete vary in complexity and reliability. These methods range from simple hammer sounding for detection of characteristic tones resulting from delaminations, to advanced technologies such as ground penetrating radar (GPR) which uses electromagnetic pulses to scan a material's subsurface (Srinivasan 2012); hammer sounding is subjective based on inspector experience and GPR requires advanced technical knowledge to analyze results. Infrared Thermography (IR) has been used to detect characteristic thermal signatures associated with delaminations, primarily in concrete bridge decks (Maser 1990). Delaminations are detected by measuring the difference in surface temperature that may exist between a region of sound concrete and a delaminated region of concrete under conducive environmental conditions (Manning 1980). This method is dependent upon environmental conditions, and can become ineffective if conditions are unfavorable. As a result, IR thermography has certain limitations as an inspection tool. Weather conditions must be suitable to enable detection of subsurface features such as delaminations. One "suitable" condition includes sufficient solar loading or change in ambient temperature to produce a thermal

gradient in the concrete (Fenwick 2009). Solar loading can provide a strong radiant heating source that establishes a thermal gradient. Subsurface defects, such as a delamination, disrupt the heat transfer through concrete, and if sufficient thermal gradient exists, then a variation in the surface temperature of the concrete in the area above the delamination can be detected. The effectiveness of this technique depends on the depth of the defect; deeper defects have less effect on the surface temperature than defects located closer to the surface of the concrete. Because the ambient environmental conditions cannot be controlled, the effectiveness of the method varies significantly depending on the environmental conditions at the time the inspection is conducted (Manning 1983). As a result, experiences with this technology have been mixed.

Thermographic imaging has several advantages over other techniques; it is able to scan a large area quickly, the technology is simple to use, and it produces an image for immediate interpretation. Some other nondestructive evaluation techniques include sounding, visual inspections, impact echo (IE) and ground penetrating radar (GPR).

Sounding is a method that uses hammers, steel rods, and chains, among other things, to strike a deck surface and the inspector works progressively over the entire deck area. A delamination in the concrete will produce a dull sound contrary to a higher pitched sound when sound deck surface is struck. Methods of detecting delamination currently in routine utilize this characteristic (Manning 1980). The interpretation of the sound produced is subjectively assessed by the operator and requires hands-on access. Sounding can become a tedious task as

the inspector works in a crouched position able to cover only a small area of the deck. A large bridge deck (spanning a few hundred feet) could take hours for completion of a sounding inspection. Visual inspection is one of the most versatile methods of NDE and is usually one of the primary methods used in evaluating a structure. The primary benefits of visual inspection are the low cost, relatively quick completion time and minimal training required. However, limitations of this method include the subjectivity of the inspector, the high possibility that access vehicles will be necessary for some areas of the bridge, and deterioration must be observable on the concrete surface (Yehia 2007).

Impact echo (IE) is a process in which a mechanical impact produces a stress wave in a material. This wave is detected by a transducer on the surface and, depending on the acoustic properties of the wave, the quality of the concrete can be evaluated. The stress wave has a different frequency for different impact durations. Smaller impactors produce higher frequency stress waves, which provide greater resolution, but travel a shorter distance into the material than lower frequency stress waves (Sohanghpurwala 2006). One significant limitation of IE is that this method only measures the area where the impact is made and the surface under inspection must be fully accessible; this means that traffic control, lane closures, or access vehicles may be necessary. IE is also extremely time consuming and labor intensive. Interpretation of results can be difficult, requiring highly trained and experienced personnel.

Ground penetrating radar launches high frequency electromagnetic waves into a concrete deck; reflections caused by the changes in electromagnetic

properties of the subsurface features in the concrete (varying dielectric constants) are detected and then analyzed to determine where deterioration exists (Maierhofer 2003). This technology can be used to rapidly scan a deck to develop an image through the process of several scans or an array of sensors. Several of the limitations of GPR include complicated interpretation of results, requiring experienced personnel, the requirement of destructive testing to complete interpretation (Scott 1999, Maierhofer 2003), and lane closures.

One of the most significant advantages of IR thermography is this technology's ability to image a large area of concrete quickly and from a distance. The soffit of a bridge, for example, can be observed from the ground level, without the need for bridge access vehicles that would be required to hammer-sound the structure. The deck can be imaged from the side of road; this allows inspection of the deck without disturbing the flow of traffic. Other elements of the bridge can also be observed without gaining direct hands-on access to those locations. This has the advantage of reducing the requirements for traffic control and costs associated with using special access vehicles. Additionally, the time required to conduct the inspection may be significantly reduced because larger areas are able to be imaged. With hammer sounding, every area to be evaluated must be accessed so that the surface can be struck with the hammer. This can be a labor-intensive and time-consuming process for large areas of concrete. For areas, such as a bridge deck, traffic control must also be in place to redirect traffic so inspectors can safely access the concrete.

Another advantage of thermography is that the results are available in real-time and require little or no processing. Thermal contrasts resulting from a defect are observed on the camera screen during inspection, and additional investigation that could be required to confirm results or further explore anomalies in the image can be conducted. Furthermore, modern IR cameras are relatively easy to use with intuitive menu structures that can be easily learned. As a result, training on how to use the cameras is minimal, such that the tool could be practically implemented within a bridge inspection program.

Infrared thermography has been utilized in a variety of different test set ups. Testing the reliability of infrared has been performed on both fabricated decks, solely for testing purposes (Kee 2012), and on in-service bridges (Vaghefi 2013). A method that has not been highly utilized is capturing infrared images over an extended time period on a fixed interval and measuring the rate of change of infrared radiation. This can be done using post-processing methods that measure the change in infrared radiation of each pixel in a camera lens array. Lenses with a larger pixel array have a higher resolution and, therefore, are more accurate. Post-processing with a high resolution lens provides the ability for the detection of subtle subsurface defects by removing surrounding noise that would have made detection impossible in a raw image (Usamentiaga 2014).

The research was focused on training participating state Department of Transportation inspectors to use IR cameras effectively for inspecting concrete bridge components. The reliability of the technology was assessed, and previously

developed guidelines for field use were evaluated. The reliability results will be evaluated through a series of tests which include field verification.

## **1.1 Purpose**

This research was conducted as a continuing project designed to validate guidelines for the application of thermal imaging for highway bridge inspection. Although IR thermography has been available as a tool for the condition assessment of highway bridges, there has been limited use of the technology. This is due, in part, to the complexity of applying thermography to bridge inspection. Since the technology relies on the environmental conditions for detection of defects in concrete, the performance level and reliability of the technology can be inconsistent; the performance level depends on the particular environmental conditions of a given day or night. Therefore, to apply the technology practically, additional guidance is needed on the specific environmental conditions that are most likely to result in a high performance level and the environmental conditions that are expected to result in poor performance.

The purpose of this research is to give inspectors the tools and knowledge needed to perform thermographic inspections. With this, the research hopes to expand the use of thermographic technology as a common tool for bridge inspections.

## **1.2 Goals**

The goal of the research is to develop new technologies for the condition assessment of concrete to help ensure bridge safety and improve the effectiveness of maintenance and repair.

## **1.3 Objectives**

The objectives of the research are to:

- Quantify the capability and reliability of thermal imaging technology in the field
- Field test and validate inspection guidelines for the application of thermal imaging for bridge inspection
- Identify implementation barriers faced by inspectors in the field

## **1.4 Approach**

The objectives of the research were approached as parts of a larger study that included distribution of equipment and training for 13 State DOTs.

Each state was given two days of training that included a half day of classroom training followed by one afternoon and one morning session of field training. The states were each given a FLIR T620 camera to conduct thermographic inspections on civil structures, such as bridges, in their state.

The participating states were asked to upload the images captured during these thermal inspections to an online database. The database pooled these images together so that the research team and other inspection teams could view the images captured by inspectors. The purpose of the online database was to

provide future inspectors with examples delaminations under specific weather conditions; these examples can be used by inspectors to compare/contrast their current inspection images in terms of thermal contrast. The images were divided into categories which included state, bridge component, location, bridge ID and date uploaded.

Verification testing trips were accomplished to verify the results of the IR findings in each state. The IR findings were verified using the following techniques - chain dragging, hammer sounding, and coring. Those are the most common methods of verification, although they are not the only ones. These trips also allowed for inspectors to ask questions, discuss problems, and experience a refresher course on how to properly use the cameras to detect defects.

## **1.5 Individual Contributions**

The contributions to this project were the development of guidance on camera lens selection for infrared inspection, quantification of hand held data from verification testing, and quantification of data with a new infrared technology that was developed.

The literature review returned no results for studies performed concerning target distance of inspection with hand held infrared cameras. Utilizing the correct lens during inspection is important because damage may go undetected if the wrong lens is used. A target distance study and calculations relating critical dimension to target distance were performed as part of this project.



Quantification of infrared data with a hand held camera is difficult. It cannot be done with the camera alone and requires a separate program that can calculate area of an image. A program was used to compare areas of infrared data to areas of hammer sounding results (when achievable) to determine the accuracy of infrared technology.

Quantification of infrared data collected with a new technology was also performed during this portion of the project. The new technology is unique and nothing was found to resemble it during a literature review. The new technology provided results in which both the area and relative depth of damage could be determined.

## **2 BACKGROUND**

### **2.1 Introduction**

Corrosion of steel in concrete is a major concern when assessing the quality of a concrete bridge. When embedded steel corrodes, it increases in volume and causes cracking that can lead to delaminations and spalling. These delaminations interrupt heat flow through a structure. The disruption in heat flow can be detected using IR cameras that measure the differences in the amount of emitted infrared radiation between sound concrete and delaminated areas.

A flow pattern is transferred to concrete as the ambient environment surrounding it changes. Cracks or voids in the concrete prevent this flow which causes areas above a crack or void to warm up or cool down faster than adjacent sound areas.

There are several environmental factors that can affect IR; solar loading, ambient temperature change, and wind speed are just a few. All of these factors can be a major influence in the ability of thermography to detect subsurface defects.

### **2.2 Concrete and corrosion**

There are approximately 2.2 billion square feet of bridge deck made up of concrete in the United States (FHWA 2014). As a ubiquitous material for the construction of bridges throughout the world, concrete is utilized for primary structural members, decks, and substructures. Deterioration presents a significant

challenge for inspection and maintenance engineers. The primary cause of deterioration in concrete bridges is the corrosion of embedded reinforcing steel.

The corrosion of embedded reinforcing steel is the result of chloride intrusion into concrete at the level of the reinforcing steel, where the chlorides promote the corrosion process. A significant source of chlorides in highway bridges is the use of deicer chemicals, which can contain sodium chloride and calcium chloride (Cady 1992). Other sources could be the intrusion of marine salt water or chloride based accelerators. When chlorides penetrate concrete to the level of reinforcing steel, they allow for initiation of an electrolytic process of corrosion.

For corrosion to occur, there must be a corrosion cell containing an anode, a cathode, an electrical path connecting the anode and cathode, and an electrolyte. In a typical reinforced concrete bridge, the migration of chloride ions from deicing salts to the reinforcing bar creates anodic and cathodic areas on the bar. At first, the reinforcing bar is protected by a passive iron oxide layer over the bar due to the high concrete alkalinity (Cady 1992). Eventually the chloride ions break down the passive layer by lowering the concrete alkalinity. An electrical path is created over the bar and the concrete becomes an electrolyte. Oxygen and moisture must also be present for corrosion to occur. The iron oxide formed by the corroded steel occupies a volume two to six times greater than that of the iron they are derived from, depending on iron composition and the degree of hydration (Bertolini 2004). This leads to cracking, typically initiating at the level of embedded steel as shown in Figure 2-1 (Nelson 2013). This subsurface cracking propagates

which results in delamination in the concrete and eventually leads to spalling and disintegration.



**Figure 2-1: Delamination at the embedded steel level**

Spalling further exposes embedded steel to the environment, accelerating deterioration of the structure that may lead to a reduction in structural capacity (Vu 2000). Additionally, the spalled concrete material can provide a hazard to motorists when occurring in the soffit or parapets of bridges that span roadways. This is particularly problematic in the unreinforced soffit corners of the concrete member where corrosion of the embedded steel can lead to a separation of the concrete, which may fall into traffic below. The resulting spalling and pot holes in the deck can reduce its service level. This requires a time consuming repair to maintain a suitable riding surface. As a result, the detection of deterioration in its early stages, such that mitigation and repair strategies can be employed, is of critical importance for maintaining safe and efficient operations.

IR thermography has been applied historically to detect corrosion-induced delaminations in reinforced concrete bridges (Manning 1990). Early research into

the subject was conducted at Texas A&M and the Virginia Highway and Transportation Research Council (Arnold 1969, Clemena 1978). The researchers observed that, due to the immense difference between the volumetric heat capacity of solid concrete and that of the air gap (air void) of a delaminated region, the separated concrete was warmer than the sound concrete when exposed to solar heating. Their research suggests that more severely delaminated regions have a stronger thermal contrast.

An interpretation of this phenomenon by Holt in 1979 was that the temperature difference at the surface correlates with the depth of the delaminations (Manning 1980). In 1980, Manning & Holt investigated the use of IR thermography for delamination detection and compared the findings to results achieved with manual methods such as chain drag. Concrete cores were utilized to establish delamination depth, and thermocouples embedded 6 mm into the deck measured temperatures of sound and delaminated concrete. Deck differentials were determined both under daytime conditions as well as at night. Based on Manning & Holt's study and IR technology at the time, the results suggested that IR thermography was not as accurate as the chain drag technique (Manning 1980). It was noted, however, that thermography had the capacity to quickly scan large areas and could be used in a variety of ways including hand held, vehicle mounted, or even attached to a helicopter. Additionally, they pointed out that thermal contrast could occur at any ambient temperature, but was greatest during a period of rapid heating and cooling. Furthermore, they suggested that the surface

temperature changes were indicative of flaw depth, and larger temperature differences were, therefore, associated with shallower defects.

### **2.3 IR Theory**

The basic principle behind thermographic inspection of civil structures is that the flow of heat through the material being inspected is disrupted by the presence of a subsurface defect (Manning 1980, Yehia 2007). The disruption in heat flow can manifest as a variation in temperature at the surface of the material, which can be observed in an image created by an infrared camera. The IR camera, which measures the intensity of energy emitted from the material in the IR range, can be used to produce an image of the surface temperature of the material. Variations in the uniformity of the surface temperature resulting from the subsurface defect can be observed in the produced image (Arnold 1969). When the temperature of a material increases, such as during the daytime when the sun and ambient environment (air temperature) are heating the concrete, the surface area above a subsurface delamination warms at a faster rate than surface areas where the concrete is intact. This phenomenon is shown schematically in Figure 2-2 (Nelson 2013). Delaminations can be detected as “hot spots” on the surface of the material, relative to intact concrete. During the nighttime, when air temperatures are falling and the material is cooling, the surface area above the delaminations cool at a faster rate than the intact concrete and appear as “cold spots” relative to the intact concrete. Defects are detected by a qualitative

assessment of the thermographic image. Delaminations are determined as areas that appear to have a thermal contrast within areas that are intact.

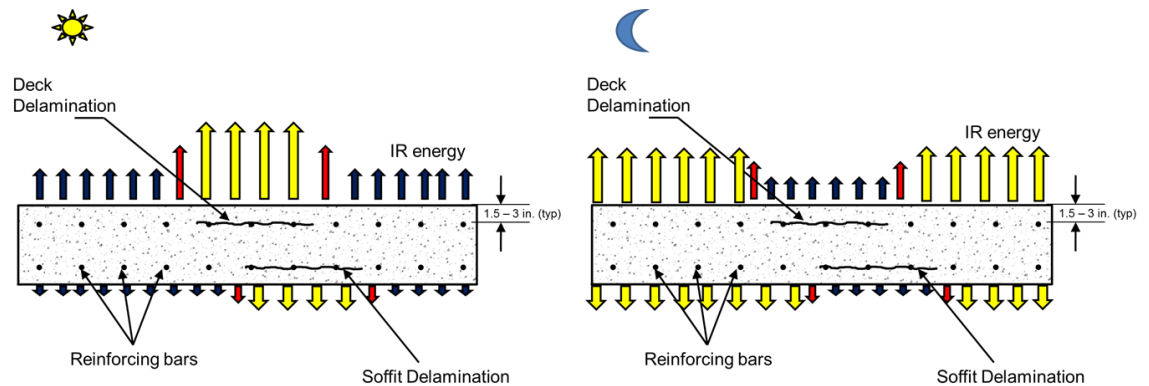


**Figure 2-2: IR energy emitted from a concrete deck under day and night time conditions**

The environmental conditions surrounding the test, such as thermal loading due to ambient temperature change or an increased wind speed, can have significant effects on the quality of the thermal image that is produced (Alqannah 2000). The effects of these environmental factors can be difficult to characterize and vary over time, such that it can be difficult to determine if the existing environmental conditions at a given point in time are adequate to produce a high quality image.

This section provides an introduction to the theory behind IR thermography with the intention of illuminating some of the challenges faced in developing this technology for application for bridge inspection.

### 2.3.1 IR Radiation

All materials emit radiation in the IR range when their temperature is above absolute zero (-273°C). The rate at which this energy is emitted is a function of

the temperature of the material and its emissivity. IR cameras can be used to infer temperature of a material, but are, in fact, not thermometers. They are radiometers, which measure the electromagnetic radiation emitted or reflected from the surface of a material (Yu 1989). The energy of emitted radiation can be expressed by the Stefan-Boltzmann equation:

$$E = \varepsilon \sigma T^4$$

### Equation 2-1

Where:

E = radiant energy emitted by a surface at all wavelengths ( $\frac{W}{m^2}$ )

$\varepsilon$  = emissivity of the materials

$\sigma$  = Stefan – Boltzmann constant ( $5.67 \times 10^{-8} \frac{W}{m^2 K^4}$ )

T = Temperature (in degrees Kelvin)

As shown in Equation 2-1, the radiant energy emitted from a material is proportional to the fourth power of its temperature, such that small variations in temperature will result in large changes in the radiant energy. The emissivity of an object is a relative measurement of the rate at which the object emits radiation; 1 represents a perfect emitter and 0 represents no emission at all. In general, concrete has a relatively high emissivity, between 0.9 and 1.0, and is a good emitter relative to other materials such as metals.

For the application of IR thermography to civil structures, where a qualitative measure of the contrast in an image is used in an attempt to identify subsurface deterioration, specific emissivity values are not required. The values of emissivity



are valuable if the absolute temperature of an object or material is needed, but to identify the contrast in a thermal image, it is not needed. However, it is important in terms of analyzing thermographic images because different materials may emit radiation at different rates, even though they may be at the same temperature (Clark 2003). If a thermal image includes different materials, such as paint on the surface of the concrete, the paint may appear at a different temperature than the concrete. This is because its emissivity is different, even though the temperatures of the two may be the same. The surface roughness of a material will also have an effect on emissivity values; rough surfaces generally have higher emissivity than smooth surfaces.

### 2.3.2 Heat Transfer

The rate of heat transfer across a solid in steady-state can be expressed using the Fourier equation:

$$q_x = -kA_x \frac{dT}{dx}$$

#### Equation 2-2

Where:

$A_x$  = surface area normal to the direction of heat flow,  $x$  ( $m^2$ )

$T$  = temperature (K)

$q_x$  = rate of heat transfer (Watts)

$k$  = thermal conductivity, Watts per meter – Kelvin ( $\frac{W}{mK}$ )

Thermal conductivity is a measure of the ability of a material to transfer heat.

Table 2-1 (Nelson 2013) highlights some typical heat transfer properties of relevant materials in civil engineering.

**Table 2-1: Thermal properties of typical materials found in civil structures**

<b>Material</b>	<b>Specific Heat (Btu lb<sup>-1</sup> °F<sup>-1</sup>)</b>	<b>Density (lb ft<sup>-3</sup>)</b>	<b>Thermal Conductivity (Btu hr<sup>-1</sup> ft<sup>-1</sup> °F<sup>-1</sup>)</b>	<b>Thermal Diffusivity (ft<sup>2</sup> Sec<sup>-1</sup>) x 10<sup>-6</sup></b>
Concrete	0.191	150	1.040	5.7
Steel	0.11	495	26.58	139.9
Air (defect)	0.17	0.075	0.014	355.2
Styrofoam	0.31	2.18	0.015	9.5
Water	1.00	62.5	0.347	1.5
Ice	0.49	57.1	1.27	0.007
Epoxy	0.29	95.5	0.717	0.004

Specific heat refers to the amount of energy required to heat a given unit of mass of a substance by one degree. Thermal conductivity is the property of a material that indicates its ability to conduct heat. Thermal diffusivity is the thermal conductivity divided by the volumetric heat capacity.

The Fourier equation (Equation 2-2) presents the most basic relationship for heat transfer in materials, representing a steady-state in which heat transfer is independent of time. For a realistic case, the situation is typically more complicated by time-varying heat input and different thermal properties (e.g. k values) of materials making up the system being examined. However, the equation is useful in that it indicates the dependence of heat transfer on the thermal gradient. The thermal gradient is the difference in temperature as a function of distance ( $\frac{dT}{dx}$ ) (Fenwick 2009). For example, if the surface of the concrete is hot and the internal temperature is cold, it is said to have a thermal gradient. This thermal gradient will cause heat to flow, and a subsurface delamination that

interrupts that heat flow will cause the heat to flow differently in the defective area. This may result in a variation in the surface temperature in that area.

For civil structures, particularly those exposed to the environment, convective heat transfer can play a significant role in heat transfer. Convective heat transfer rate away from a surface can be expressed:

$$q_c = h_c A_s (T_s - T_A)$$

**Equation 2-3**

Where:

$q_c$  = rate of heat transferred from the surface of area (J)

$A_s$  = surface area (m<sup>2</sup>)

$T_s$  = temperature of the surface (K)

$T_A$  = air temperature (K)

$h_c$  = convective heat transfer coefficient

The convective transfer coefficient,  $h_c$ , is typically an empirical value that depends on a number of factors, including the wind speed and air density (Leinhard 1981). For a large difference in temperature between the structure being inspected and the air temperature, the rate of convective heat transfer will also be large. If the wind speed is high, the convective transfer coefficient will be high, and the rate of transfer will also be high. The result of these effects is that the high rate of convective heat transfer could act to homogenize the surface temperature, masking subsurface defects. For solar exposed surfaces, convective cooling may counteract the radiant heating of the sun and reduce the thermal gradient in the concrete. For these reasons, procedures for applying IR thermography under field

conditions can typically include provisions which limit the allowable wind speed during the inspection (ASTM 2007). These procedures are directed toward solar exposed surfaces. When the surface is not exposed to radiant heating from the sun, increased convective heat transfer associated with higher wind speed may help increase the thermal gradient in the concrete, thereby increasing the detectability of a subsurface delamination. No prior literature was found discussing this effect.

Based on the findings by Manning & Holt (Manning 1980), the amount of concrete cover may also affect the inspection capability of IR thermography due to the loss of thermal contrast with target depth.

Maldague provides an equation relating the depth of a defect with observation time (Maldague 2000). Findings suggested that deeper defects will be detected at a later time with a reduced contrast, where observation time is a function of the square of the depth, indicated by the relationship:

$$t \sim \frac{z^2}{\alpha}$$

#### **Equation 2-4**

Where:

t = observation time (s)

z = depth of the target (m)

$\alpha$  = thermal diffusivity of the material ( $\frac{m^2}{s}$ )

Additionally, it was suggested there was a relationship between the loss of contrast and increasing depth, where the loss of thermal contrast is proportional to the cube of the target depth, indicated by the equation:

$$c \sim \frac{1}{z^3}$$

#### **Equation 2-5**

Where:

c = thermal contrast loss due to defect depth ( $\frac{K}{m^3}$ )

z = depth of the target (m)

Maldague also suggests, as an empirical rule of thumb, that the radius of the smallest detectable subsurface defect should be at least one to two times larger than its depth. This rule is valid for homogeneous isotropic materials. In the case of anisotropy, it is more constrained (Maldague 2000). Even though concrete is not strictly classified as such, the results may serve as a generalization for the behavior of the overall concrete structure.

### **2.3.3 Environmental Factors**

For civil structures, several different factors affect heat transfer in concrete exposed to the ambient environment. The important environmental factors which influence the ability of thermography to detect subsurface defects in concrete include solar loading, ambient temperature changes, and wind speed. Relative humidity has also been suggested in the literature as a factor (Manning 1983). This section briefly describes each of these environmental parameters and the way

in which they affect the thermal contrast developed from a subsurface defect in concrete.

A primary driving force for the development of thermal gradients in concrete is radiant energy from the sun (Washer 2010). Radiant energy from the sun transfers thermal energy into the surface of the concrete and causes the concrete to heat. The surface heats up at a much higher rate than the core of the concrete, developing a thermal gradient with high temperatures at the surface and cooler temperature at depths into the concrete. To achieve thermal equilibrium, the heat at the surface of the concrete is transferred (conducted) toward the core of the concrete. The amount of solar loading may be expressed as the radiant energy of the sun, which is the radiant energy at a given point in time.

The temperature of the air surrounding the concrete will also impart a thermal gradient. In the daytime, when temperatures are typically rising over the course of a day, the ambient air temperature is higher than the temperature of the concrete. As a result, heat is transferred into the concrete to propel the concrete toward thermal equilibrium with its surroundings (Washer 2009). This will establish a thermal gradient in the concrete since the surface warms faster than the core of the concrete. The greater the difference between the ambient air temperature and the concrete, the greater the thermal gradient. The temperature of the concrete lags in time relative to changes in the ambient environment, due to its large mass and low thermal conductivity. As a result, if there are large changes in the ambient environmental temperature, a large difference will develop between the temperature of the air and the temperature of the concrete, producing a greater

thermal gradient. For this reason, the change in the ambient temperature over the course of the day is the parameter that controls the level to which a subsurface target will affect the surface temperature of the concrete, i.e. be detectable with an IR camera, when no solar loading is present (Fenwick 2009). The actual environmental temperature is not an important factor; the thermal gradient would be the same if the air were maintained at either 75°F or at 30°F if the concrete was in thermal equilibrium with its surrounding. However, if the air temperature were to change from 30°F to 75°F over a period of 10 hours, the temperature of the concrete could not change that quickly and a thermal gradient would result. The same thermal gradient would be developed if the air temperature were to change from 40°F to 85°F or 50°F to 95°F.

Other deck conditions, such as asphalt overlay, surface emissivity, and cover thickness also influence thermographic readings. Research suggested that the presence of an asphalt overlay made it more difficult to detect defects. The effect of the overlay was to essentially decrease the thermal contrasts achieved due to the thermal mass above a potential delamination. The thicker the overlay, the greater the decreasing effect (Roddis 1987). This also has the effect of narrowing the tolerable ranges of environmental factors, i.e. if the thermal contrast were decreased, the target would be visible for less time and with smaller magnitudes.

A major concern for the reliability of IR thermography through asphalt overlay is the possible presence of a debonded area which could confuse interpretation. The debonded area could appear as a flaw in the image, in addition



to the actual delaminations in the concrete. To distinguish debonding from delaminations, it was suggested that the delaminations were circular and uniform while the debonded areas were large, non-circular, and non-uniform (Roddis 1987).

As mentioned previously, the effect of emissivity can lead to misinterpretation of readings from thermographic imaging. Surface texture, patching, debris, and oil staining are among the surface features that may complicate the identification of thermal anomalies (Maser 1990). Each of these features have different thermal properties than the surrounding concrete that create a high noise level in the thermal image, that is, thermal variations which are not related to any defect or flaw.

### **3 TRAINING**

Training was performed in each participating state of the pooled fund project. Three states were added to the project following a transition in graduate research assistants: Ohio, Kentucky, and Florida. Training was typically accomplished over a day and a half. A classroom session was conducted on the first morning to give inspectors some background to infrared technology and how it works. The classroom training for each state consisted of five modules. The first module was an introduction. It stated objectives of the project, desired results, and a brief overview of content to be covered in the other four modules. The second module covered the theoretical background of thermography and heat transfer. This section explained how heat transfers through concrete and how materials at the same temperature with different emissivity properties can appear at different temperatures. The third module covered environmental factors that affect IR images. This module discussed the many different factors the inspectors may experience while conducting IR testing. This section also discussed the findings from the research phase, phase I, of the project. Phase I consisted of collecting data on two sides of a test block, solar and non-solar loaded, with embedded styrofoam targets at depths of 1, 2, 3, and 5 inches. Guidelines for thermographic inspection were developed based on observations of how the targets appeared under various weather conditions. Module four focused on the process of capturing a good IR image. This module covered the basics of how to capture a good IR image by correctly setting the level and span of the camera in the field. Setting the appropriate level and span allows inspectors to see subsurface defects in real

time. Without correctly setting the level and span or by leaving the level and span on the automatically adjust setting, the concrete structure may not appear to have defects in locations where they exist. This module also covered the importance of focusing the camera, taking images at the proper angle, and lens selection. The last module focused on how to use the FLIR T620 camera that was provided to each participating state. Module five discussed the basic functions inspectors would have to know to when using the camera for inspections of concrete structures. After a break from classroom instruction, inspectors practiced using the technology in the field. The morning of the second day was used for further field testing at a different location to create a blind test scenario and to answer any questions members of the DOT might have.

In order to evaluate the trainees' perception and expectations of the training and IR technology, surveys were issued to each state at the end of the classroom training session. Survey questions focused on the trainees' satisfaction with the training, perception of the most/least useful module, and expectations for ease of use of the technology. The results from Ohio, Kentucky, and Florida are shown in Table 3-1.

**Table 3-1: Training survey results from Ohio, Kentucky and Florida**

<b>State DOT</b>	<b>Satisfaction with Training</b>	<b>Most/Least Useful Module</b>	<b>Will IR camera use be easy?</b>	<b>Number of Trainees</b>	<b>Number of Evaluations Received</b>
Ohio	75/100	4/1	76/100	14	10
Kentucky	84/100	4/1	87/100	10	8
Florida	85/100	4/1	80/100	8	3

Responses to the survey questions varied from strongly agree to strongly disagree and values were assigned to each answer (1 for strongly disagree to 5 for strongly agree). Averages for each state were calculated based on responses to the questions and taken out of 100 for better perception. Members of Kentucky and Florida DOTs had relatively positive views of the training. Members of Ohio DOT had a slightly less positive view of the technology. For comparison, the previous nine states where training was conducted had averages of 79 for satisfaction with training and 77 for ease of use with the IR camera. These states came in to the project later than others due to interest drawn from the initial results. More positive reactions may have been from access to knowledge of results that members of the previous states did not have. The training was also improved upon by adding new results and better examples with each conducted trip and may have also had an effect.

### **3.1 Ohio**

A training trip in Ohio was completed May 6-7, 2013. The training was conducted at a DOT location in northwestern Columbus near Ohio State University Airport. After the classroom session, inspectors were taken to a bridge 20 minutes north of the training facility. Due to rain, approximately one hour was spent in the field. Despite a relatively short amount of time spent inspecting the bridge, quality thermal images were captured of the deck. IR (A) and digital (B) images of the deck are shown in Figure 3-1.

## Delaminations

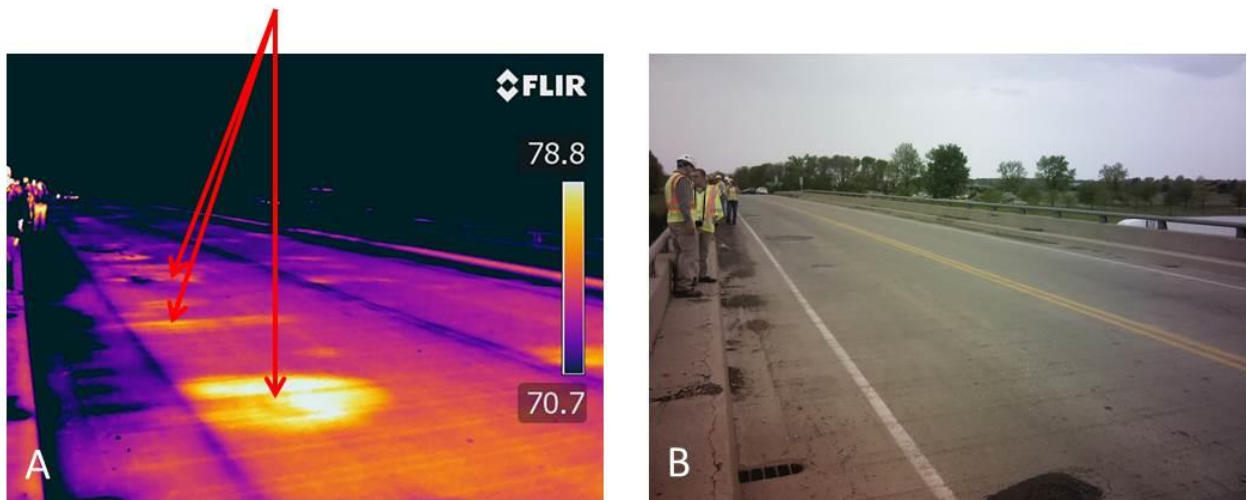


**Figure 3-1: IR (A) and digital (B) images of deck delaminations captured during Ohio training**

The second day of training was spent at another bridge located closer to central Columbus. More inspectors were in attendance for that portion of the field testing. The bridge deck was the focus of the inspection period. The weather was more conducive to infrared thermography since there was no precipitation. A graph of the ambient temperature is shown in Figure 3-2 (Wunderground 2013-2015).

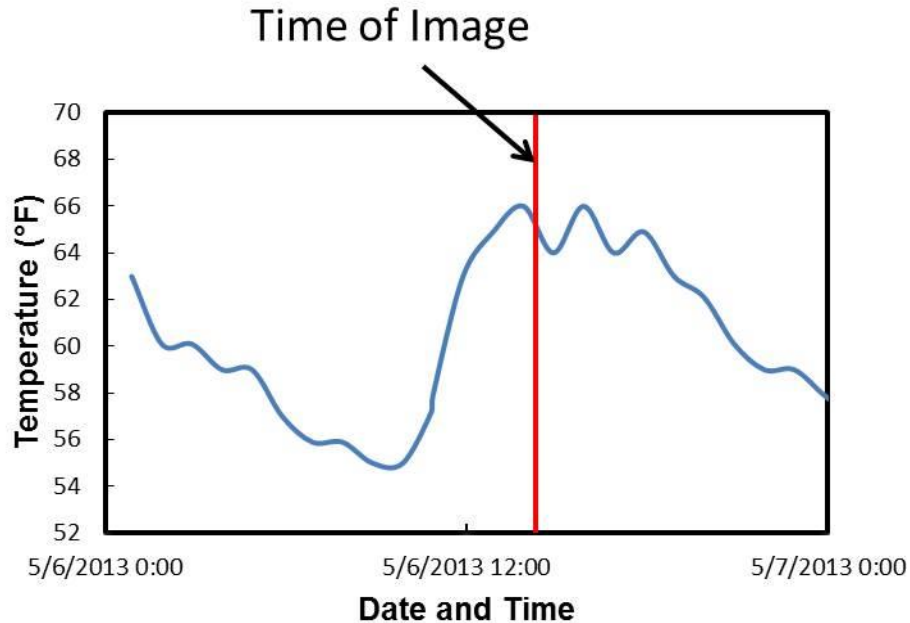


**Figure 3-2: Ambient temperature surrounding Figure 3-1 during Ohio training**

### 3.2 Kentucky

A training trip to Kentucky was completed July 31 – August 1, 2014. The training was conducted in Lexington at the Kentucky Transportation Center. After the half day classroom session, field testing was conducted on a bridge close to the University of Kentucky. Due to rain, this field inspection focused on the substructure. Delaminations were detected in the pier caps. Field testing on the second day was conducted in Louisville at a bridge on I-65, spanning the Ohio River. The main focus of this inspection was the columns. The columns were chosen because they had been inspected previously, and field testing at locations that have been previously inspected is a good way for trainees to observe how delaminations are supposed to look; this is because trainees have an idea of which

concrete areas are damaged and they know, generally, where to inspect. An image from the first day of training is shown in Figure 3-3 and the ambient temperature surrounding the testing is shown in Figure 3-4 (Wunderground 2013-2015).

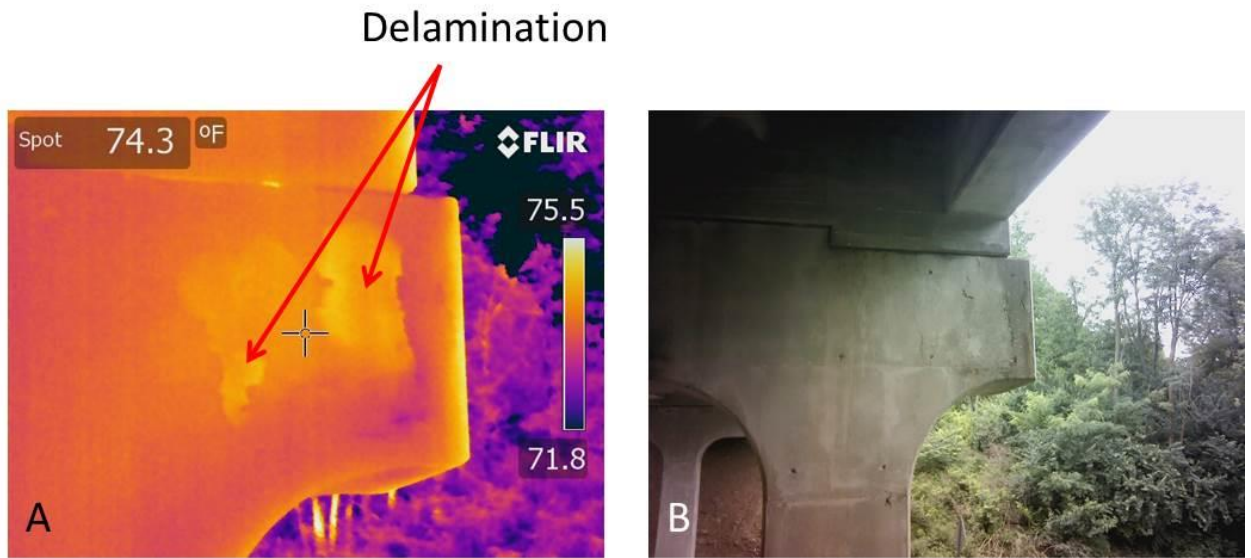


**Figure 3-3: IR (A) and digital (B) images of a pier cap delamination captured during Kentucky training**

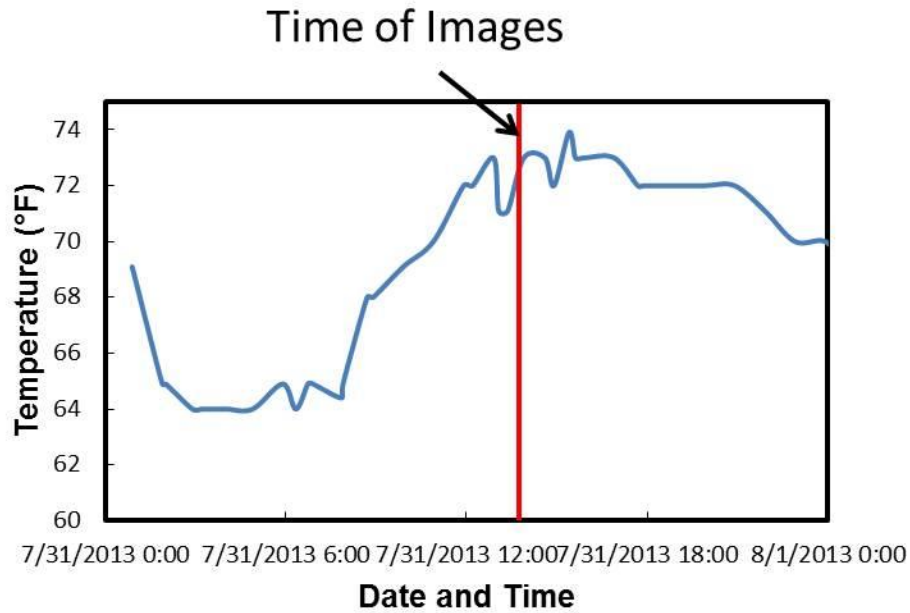


**Figure 3-4: Ambient temperature surrounding Figure 3-3 during Kentucky training**

### 3.3 Florida

Training was completed April 29-30, 2014 in Tampa, Florida. The classroom portion of the training was conducted at a DOT office in Brandon, FL. Field testing during the first day was unsuccessful due to the fact that the bridges that were inspected had no observable damage, although environmental conditions were conducive to IR inspection. Soffits were the focus of inspection due to high traffic volume on the highway bridges in the area. Field testing on the second day was conducted on the North Sunshine Skyway fishing pier. This pier was part of the original structure that spanned Tampa bay before the Sunshine Skyway Bridge was constructed. The testing was performed on the deck of the fishing pier. An example of a detected delamination is shown in Figure 3-5.



## Delamination

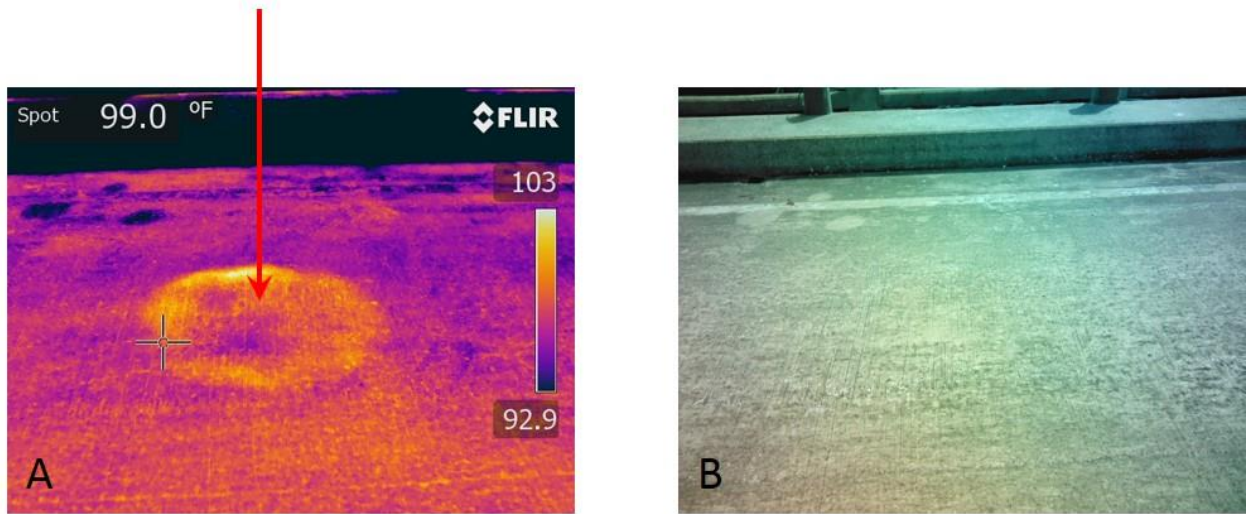


**Figure 3-5: Infrared (A) and digital (B) images of a deck delamination in Florida**

Given the temperature change and wind conditions, it was a good day for infrared thermography based on the inspection guidelines. The ambient temperature for the day is shown in Figure 3-6 below (Wunderground 2013-2015). The wind speed was 5-9 mph for most of the day. There were short periods of wind speeds at 13 mph. The ambient temperature change was greater than 15 degrees for the day and was also more than 10 degrees in the first six hours after sunrise.

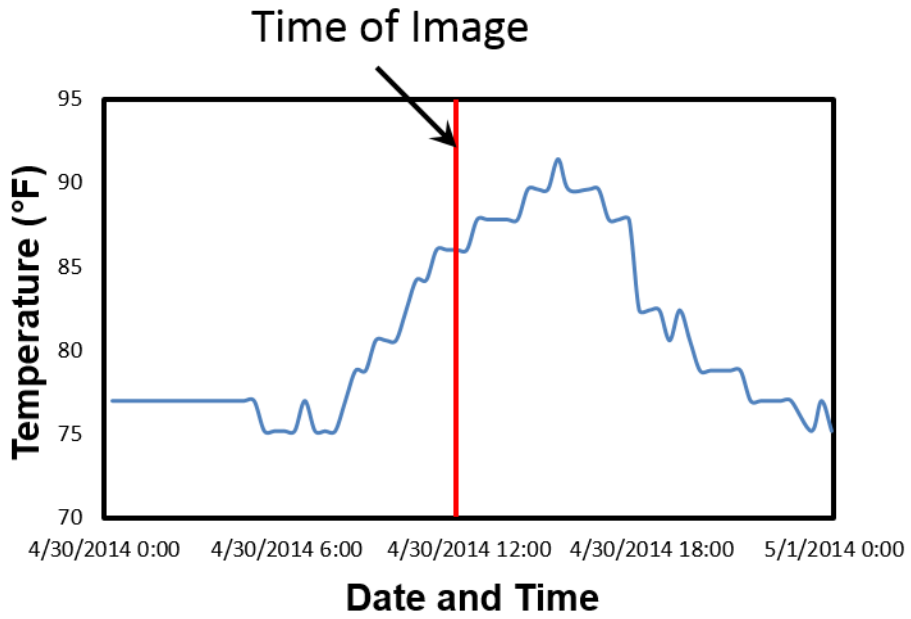


**Figure 3-6: Ambient temperature on April 30, 2014 for Tampa, FL**

## **4 HAND HELD VERIFICATION RESULTS**

Verification testing was planned to be conducted in each of the participating states. However, due to weather conditions and scheduling conflicts some trips were unable to be conducted to complete this portion of the research as planned. Verification testing was completed in all of the participating states with the exception of Wisconsin, Michigan, and Florida. The purpose of verification testing was to verify the thermographic inspection guidelines developed in Phase I of this project. Environmental conditions were compared to the guidelines for each verification inspection to determine that meeting the guidelines resulted in successful IR inspection. This analysis is shown in chapter 6. A comparison of infrared imaging to hammer sounding results was also performed and is shown in section 4.12. This analysis was performed to determine the accuracy of infrared imaging when measuring the area of damaged concrete.

### **4.1 Tools for Inspection**

#### **4.1.1 Lens Selection**

Tools for inspection and progressive improvements to the guidelines were also made during this portion of the project. The revised guidelines are provided as Appendix A of this paper. Guidance on lens selection was one of the additions to the guidelines. A field of view study was conducted with the wide (45°) and regular (25°) lenses. The T620 infrared camera has an array of 640 x 480 pixels. Identification of an object is based on its smallest, or critical, dimension that can

be resolved (Shirkey 2001). Equation 4-1 was used to determine critical dimension as a function of object distance from the lens.

$$\text{Critical Dimension} = N \left( \frac{\text{pixel pitch}}{\text{focal length}} \right) (\text{Target Distance})$$

#### **Equation 4-1**

Where:

Critical Dimension = Smallest dimension of target (ft)

N = Number of pixels occupied across critical dimension

Pixel pitch = length of pixel on camera sensor (m)

Focal Length = Distance from focus to center of lens (m)

Target Distance = Distance from lens to target (ft)

The number of pixels that must be occupied across the critical dimension for identification of an object is 12. Pixel pitch for the T620 infrared camera, provided in the specification, was 17 micrometers. Focal length varied based on what lens was used for inspection. Focal lengths of the regular (25°), wide (45°), and telephoto (15°) lenses were 24.6 mm, 13.1 mm, and 41.6mm, respectively. Although the telephoto lens was not utilized in the study, calculations for critical dimension were performed for the telephoto lens. Figure 4-1 shows a graph of critical dimension as a function of target distance.

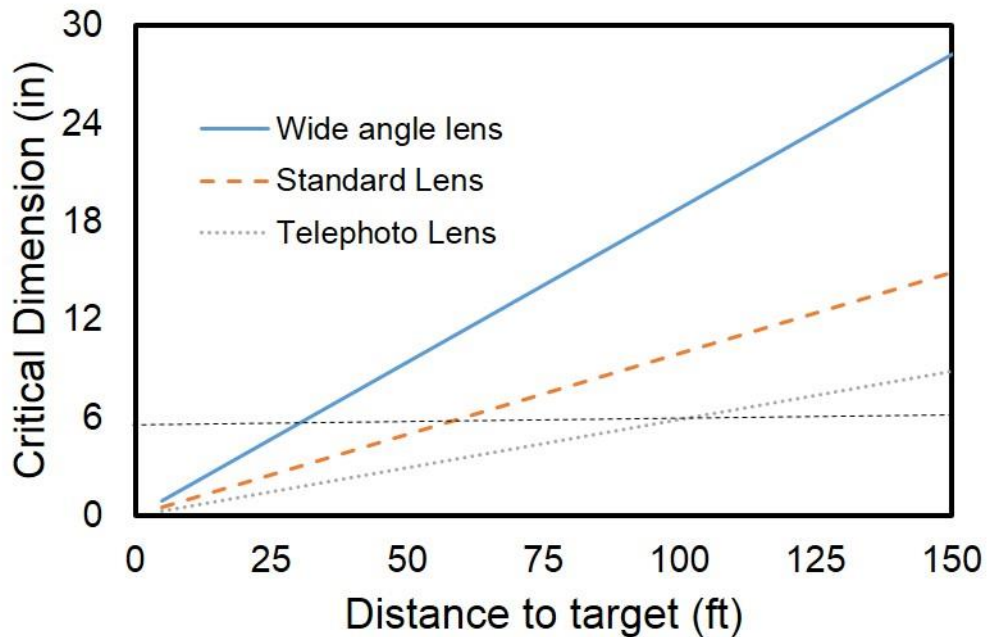


**Figure 4-1: Critical dimension as a function of target distance**

A study was conducted with the regular and wide angle lenses to verify the calculations. Three terracotta pots and a metal can, painted matt black, were utilized for the study. The small pot, medium pot, paint can, and large pot had critical dimensions of 3.5, 3.75, 4, and 4.5 inches, respectively. Pot names were determined based on critical dimension; the pot with the smallest critical dimension was called the small pot, and so forth. Terracotta pots were used because terracotta has a similar emissivity value, 0.95, to concrete. The painted can was used to achieve as close to a black body (emissivity of 1.0) as possible. The objects were filled with ice water to create a thermal contrast relative to the surrounding environment. Table 4-1 shows the maximum target distances for each object based on critical dimension.

**Table 4-1: Maximum identification distances for each object of the study**

Object	Critical Dimension (in)	Max Identification Distance (ft) 45° Lens	Max Identification Distance (ft) 25° Lens
Small Pot	3.5	18.7	35.2
Medium Pot	3.75	20.1	37.7
Paint Can	4	21.4	40.2
Large Pot	4.5	24.1	45.2

Infrared images of all four objects were captured at intervals of 5 ft from target distances of 5 feet to 60 feet. Figure 4-2 shows the setup of the objects. Images of the wide angle lens at a target distance of 25 feet (A) and the regular lens at a target distance of 50 feet (B) are shown in Figure 4-3.

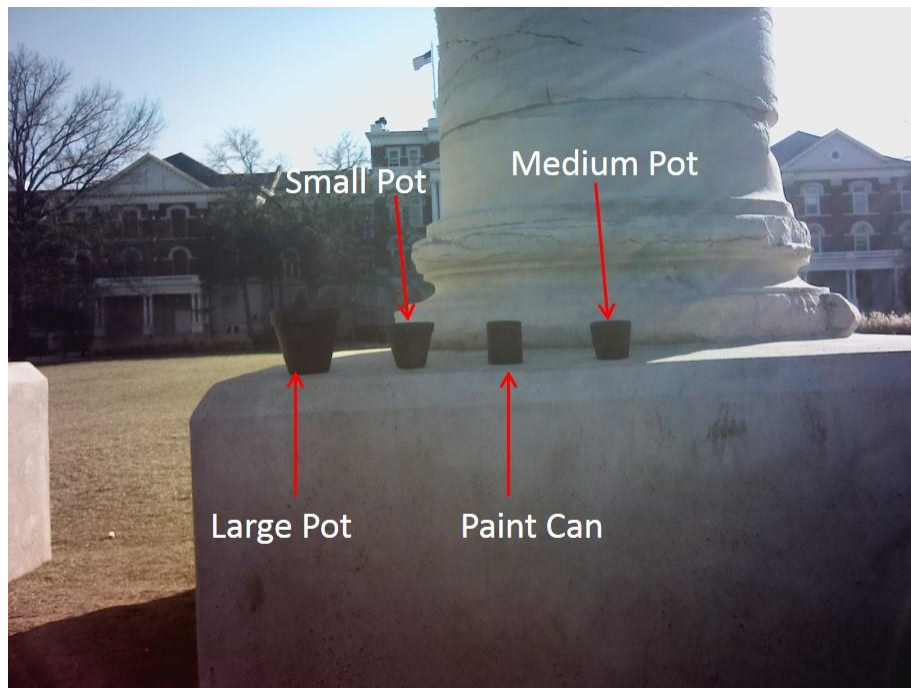


**Figure 4-2: Critical dimension study setup**

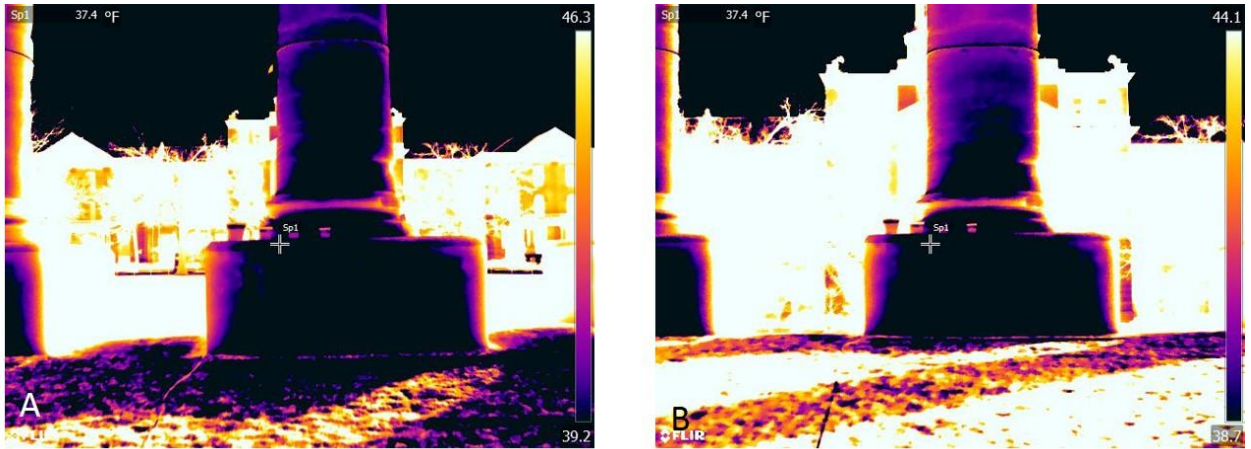


**Figure 4-3: Target distances of 25 ft with the wide lens (A) and 50 ft with the regular lens (B)**

Target distances of 25 feet for the wide lens and 50 feet for the regular lens were used because they were greater than the maximum distance for identification for the largest critical dimension in both cases. The pots are detectable in the images but an inspector with no knowledge of what the objects were would not be able to identify them as pots. A critical dimension for inspection was chosen as six inches to be conservative, although bridge delaminations are typically larger. An inspection threshold of 35 feet was determined based on the critical dimension calculations and target distance study.

#### **4.1.2 Wind Speed Analysis**

A wind speed analysis was conducted to correlate data collected during Phase I of the project to data provided by the National Weather Service (NWS). The measured wind speeds from Phase I were averaged over six hours during the second and third quarters of the day. It was determined in the original guidelines that a wind speed of 8 mph was detrimental to thermographic inspection.

However, the reported wind speed by the NWS is calculated differently than what was measured; it is taken as a two minute average once per hour. Correlation of the experimental data to the NWS data resulted in the inspection guideline being changed from 8 mph to 15 mph. Figure 4-4 shows a correlation of experimental data to data produced by the NWS. The graph shows that the NWS reported wind speeds were higher than what was measured during testing.

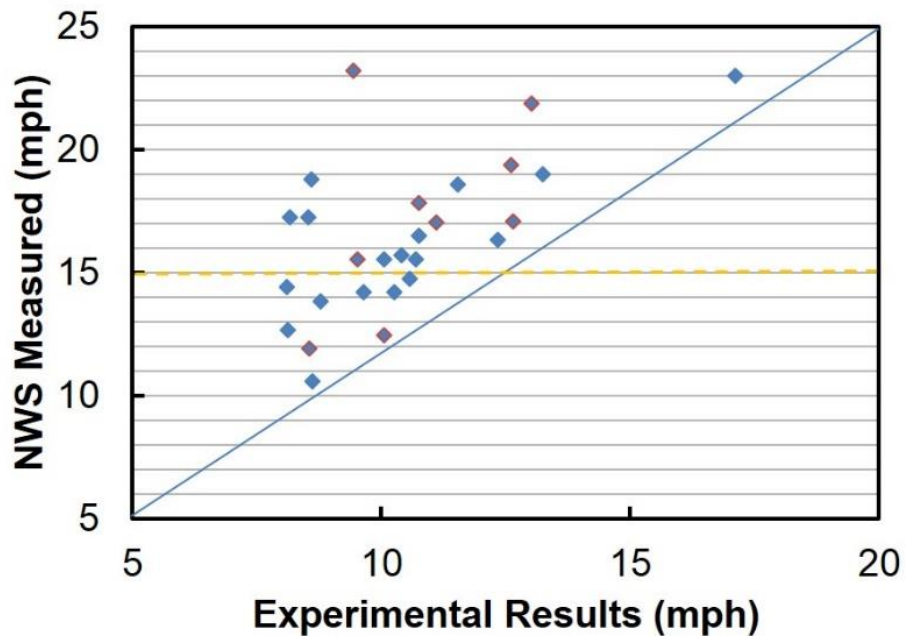


**Figure 4-4: Correlation of experimental wind data to NWS wind data**

#### **4.1.3 Shared Data Site**

A shared data site was created to help with the verification phase. The purpose of the shared data site was to create a database of images for future inspectors. Inspectors uploaded images to the site with corresponding information such as state, bridge ID, location, date and approximate time images were



captured. Weather data was taken from the closest weather station to the bridge's location and provided with the uploaded images. The images provide a reference for the way in which delaminations appear under different environmental conditions. Currently, there are approximately 100 entries, many containing multiple images.

#### **4.1.4 Weather Checker**

One useful tool for inspectors developed during Phase II was the weather checker. The weather checker uses the location of an inspector's phone or computer and determines, based on the inspection guidelines, if it is a good time to conduct thermographic inspection. The weather checker also gives predicted trends in temperature. If the current time is not conducive for inspection, the weather checker can be used to determine if conditions will be conducive at a later time.

## **4.2 Kansas City**

Due to the close proximity to the University of Missouri, testing in Missouri is ideal. Bridge A0295 in Kansas City was originally constructed in 1959 and never opened to traffic due to a change in the original plans. Since the bridge had no traffic volume, salt had never been applied to the bridge deck. This bridge was selected for research since it would provide a good baseline for the performance of similar bridge decks in the area; also, researchers hoped to demonstrate the impact of salt on the amount of delamination on a deck by comparing similar bridges exposed to traffic and salt to this bridge.

The verification testing was completed on this bridge on March 9, 2014. For future research purposes, only the North span of the bridge will be included in these results and will be referred to as the “open” span.

Testing on this bridge was conducted so that the results achieved with the infrared camera could be compared to chain drag results. An infrared camera located and captured the delaminations. Chain dragging was performed by the Missouri Department of Transportation to verify the infrared results. Each delamination identified with the infrared camera was verified by the results of the chain dragging. The results of the chain drag are shown in Figure 4-5 below. Figures 4-6 and 4-7 show infrared images of these delaminations.

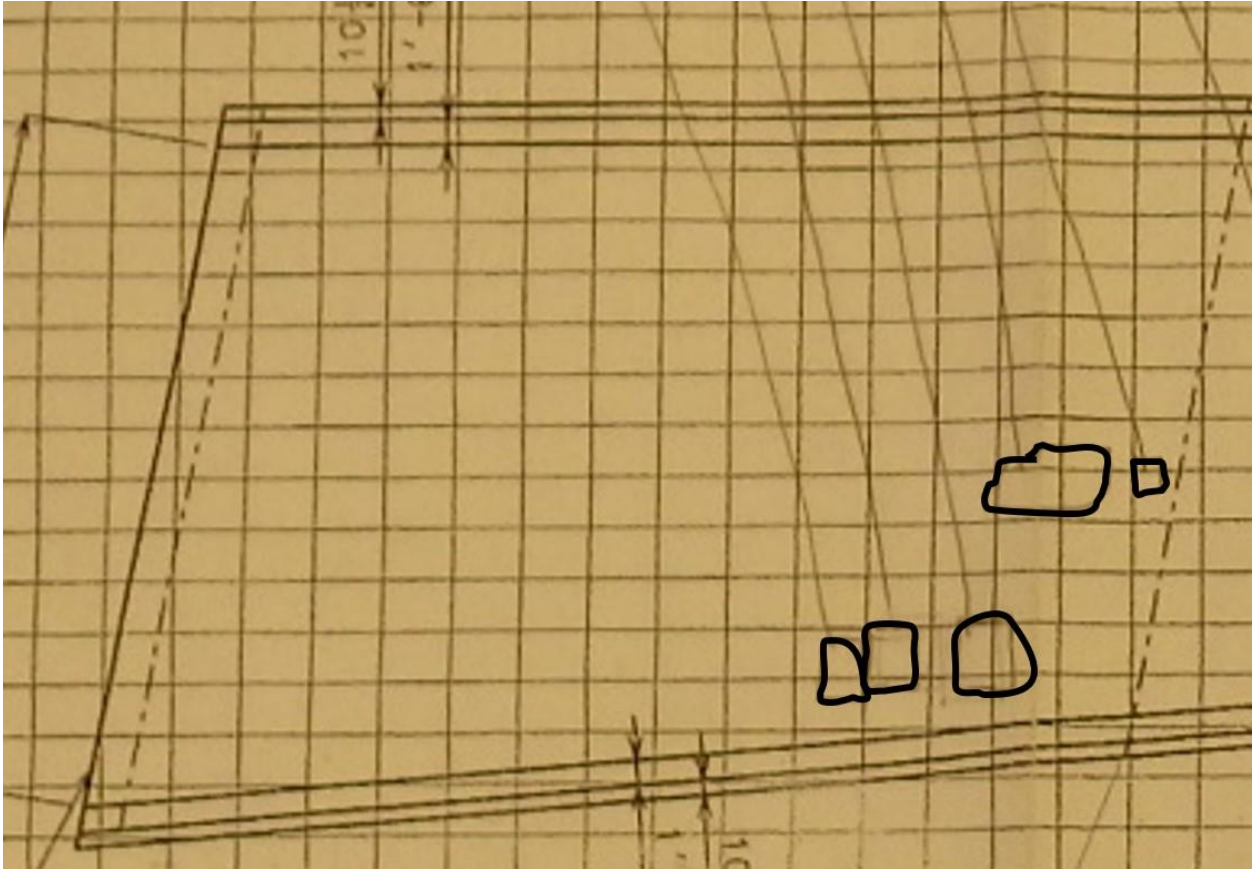


**Figure 4-5: Chain drag results for the North span of Bridge A0295**

The delamination edges for one delamination were sounded; the hammer sounding results were compared to the infrared images. The accuracy of the infrared images are shown in Figure 4-6 below. The hammer sounding results are shown in the digital image as a red outline. It is important to note that hammer sounding can be subjective and is dependent on inspector training and experience.

## Delamination

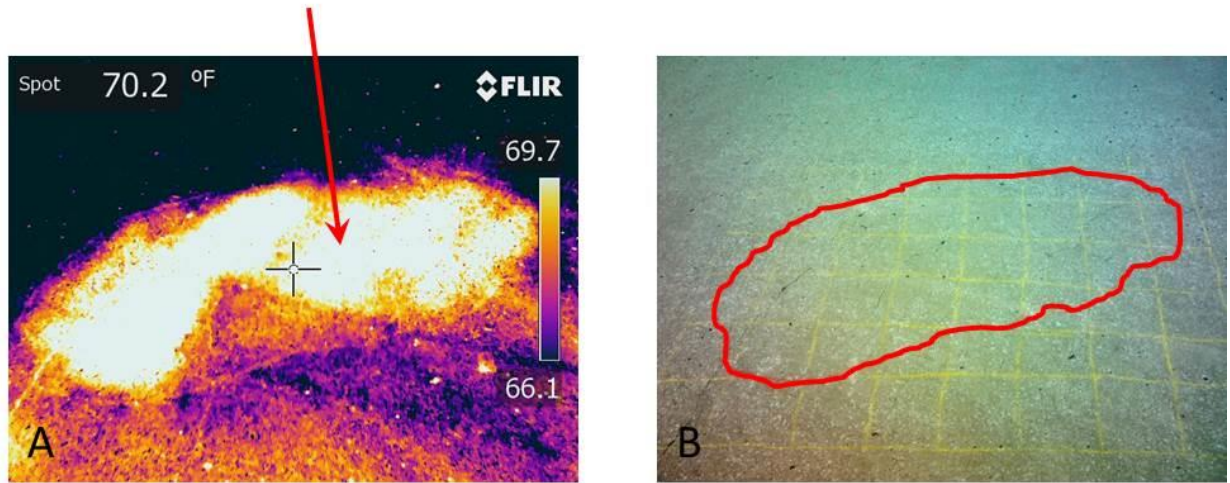


**Figure 4-6: Infrared (A) and digital (B) images of a deck delamination in Kansas City**

The two images demonstrate that the accuracy of the hand held infrared camera is very high. The red outline marking can be seen in the infrared image indicating how accurate the infrared camera and the hammer sounding results really were. Another group of delaminations are shown in Figure 4-7.

## Delaminations

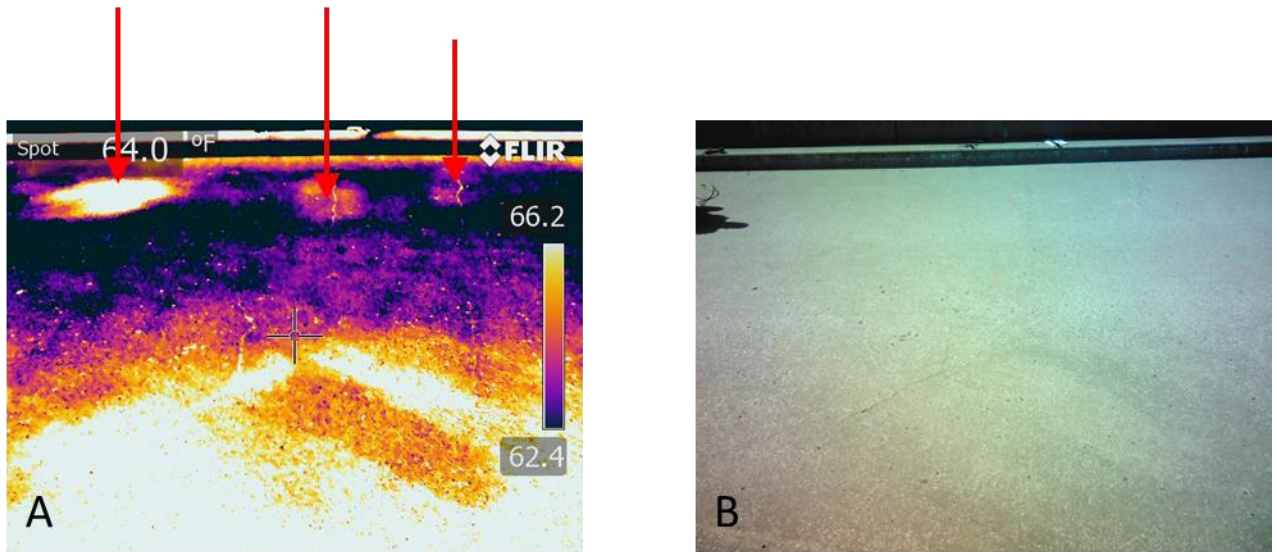


**Figure 4-7: Infrared (A) and Digital (B) images of a group of delaminations in Kansas City**

The guidelines for inspection suggest an ambient temperature change of 15°F with at least 10°F of that change occurring in the first six hours after sunrise. The weather conditions for the day were highly conducive for infrared thermography. The ambient temperature change was approximately 37 degrees over the span of the day with a change of 27 degrees in the first six hours after sunrise. The wind speed increased to 21.9 miles per hour, which is above the desired threshold for inspection (15 mph as stated in the guidelines); however, the high wind speeds were not enough to be detrimental to inspection due to the dramatic change in ambient temperature. The ambient temperature data for the day is shown in Figure 4-8 (Wunderground 2013-2015).

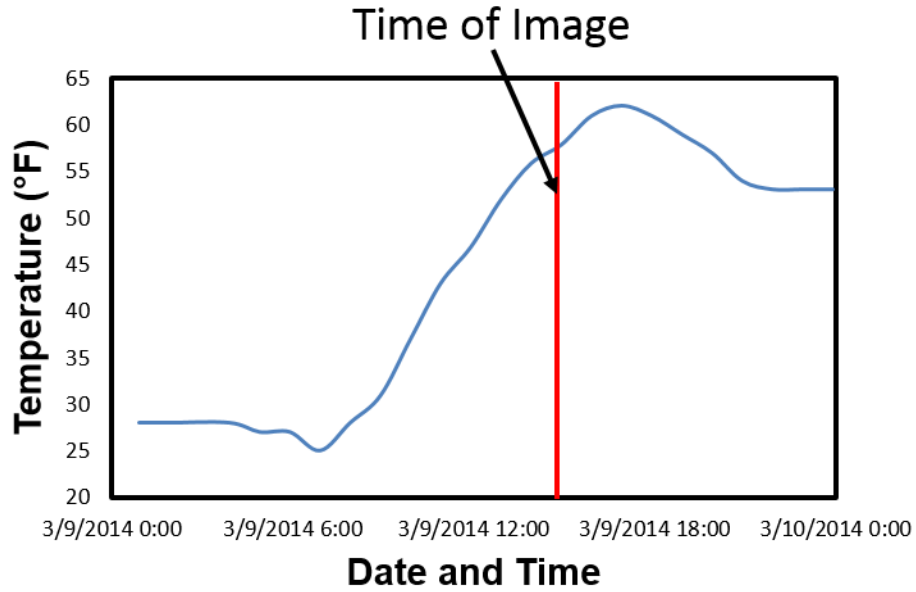


**Figure 4-8: Ambient Temperature for Kansas City, MO on March 9th, 2014**

### **4.3 Providence Road**

The Providence Road Bridge over Hinkson Creek in Columbia was tested on May 6, 2014. The testing was conducted on the northbound lanes of Providence Road. This bridge was chosen for testing because of its close proximity to the University of Missouri. Images were taken of the deck and soffit

of the bridge. Soffit images are shown on the pooled fund website. Delaminated areas are shown as “hot spots” in Figure 4-9.

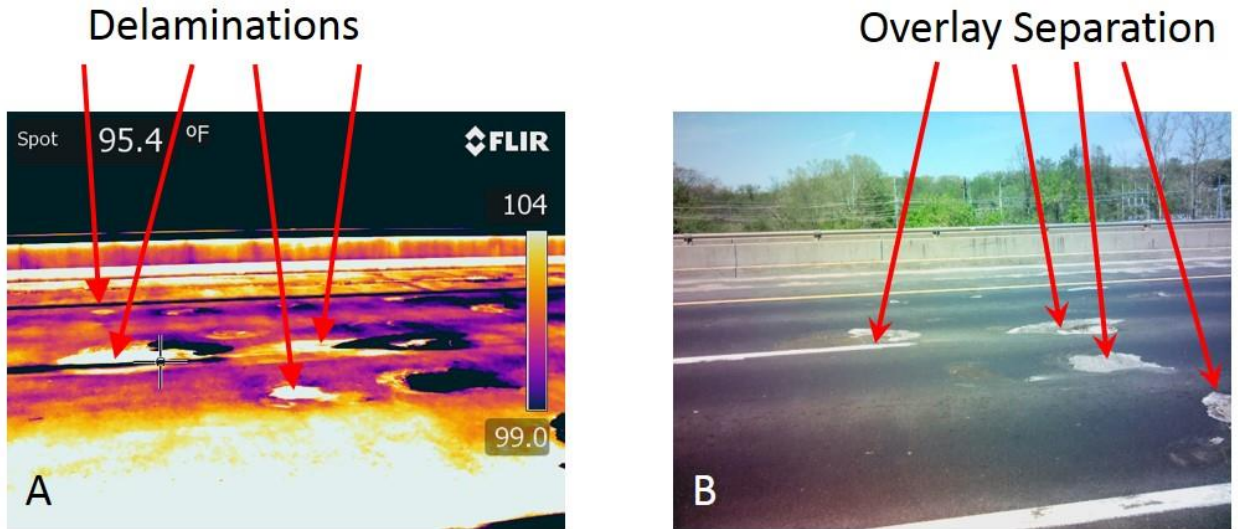


**Figure 4-9: Infrared (A) and Digital (B) images of Providence Rd. Bridge (northbound) over Hinkson Creek**

The conditions were excellent for inspection with infrared thermography. Figure 4-10 shows the ambient air temperature for the day of the test (Wunderground 2013-2015). As shown in the figure, the ambient temperature change is approximately 32 degrees with 23 degrees of change in the first six hours after sunrise. The wind speed reached approximately 22 mph. With a smaller difference in ambient temperature, a 22 mph wind speed would likely be detrimental to inspection. In this case, the amount of change in ambient temperature was sufficient to reduce the effects of cooling by the wind.

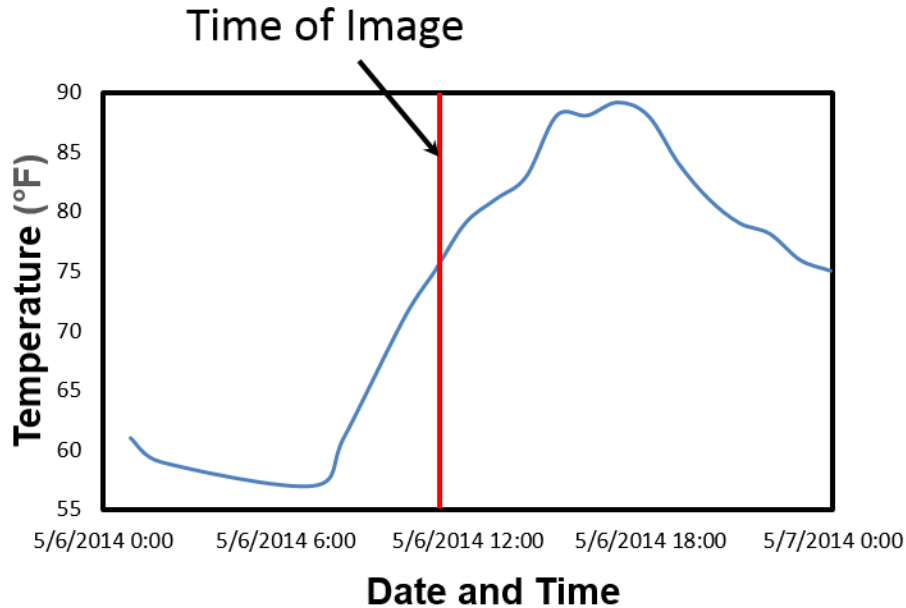


**Figure 4-10: Ambient temperature on May 6th, 2014 for Columbia, MO**

#### **4.4 Iowa**

A bridge in Iowa was inspected for the purpose of IR-UTD testing. The bridge was located on Highway 69 over I-35 in Lamoni, IA. This bridge's deck would be going through the repair process of injecting epoxy into delaminations. This is a method used by Iowa DOT to elongate the service life of the bridge deck. After epoxy is injected into a delamination, thermal contrast relative to the sound concrete around the delamination is lost (Nelson 2013). For that reason, images with the hand held camera were captured before the epoxy injection process.

The Iowa Department of Transportation hammer sounded the entire deck to locate the areas where epoxy injections were going to be necessary. Infrared images were taken at many of those locations; in addition, borescope measurements were taken at one of the larger delaminations. The borescope



allows for inspection of the interior of the structure by taking a small camera and inserting it into a drilled hole; in this way, an image of the delamination can be captured. Figure 4-11 below shows an image of a large deck delamination. The reason for hand held imaging and verification with hammer sounding and a borescope were to evaluate the area and depth. Hammer sounding was utilized to measure the area of the delamination and the borescope was used to measure its depth.

Images of the delamination in Figure 4-11 were also captured on the soffit. The soffit images are shown in Figure 4-12 below.

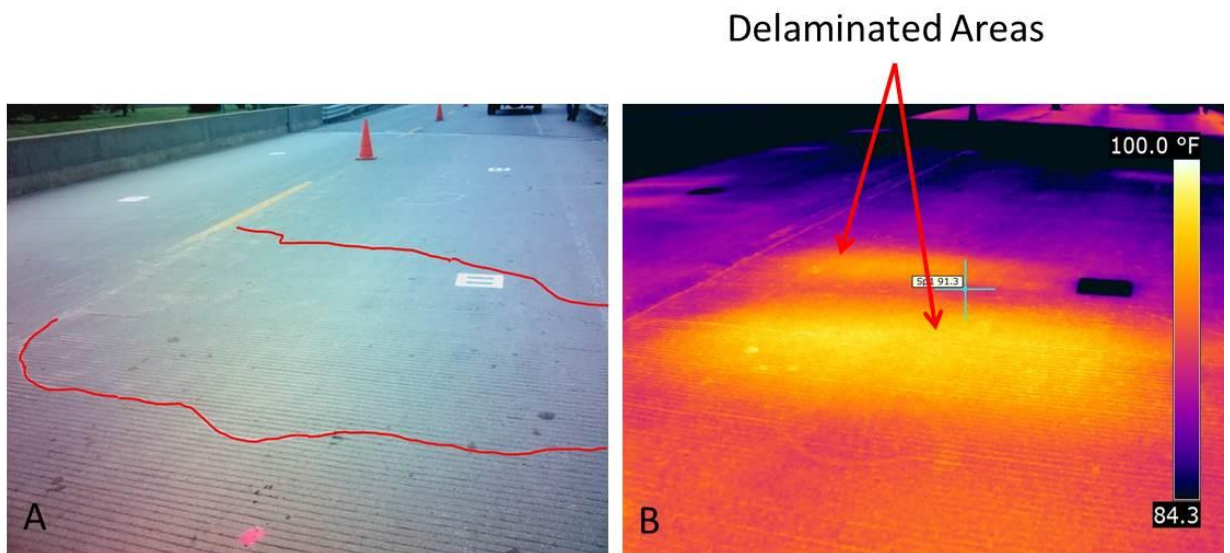


**Figure 4-11: Hammer sound result (A) and Infrared (B) images of a deck delamination in Lamoni, IA**

## Delamination

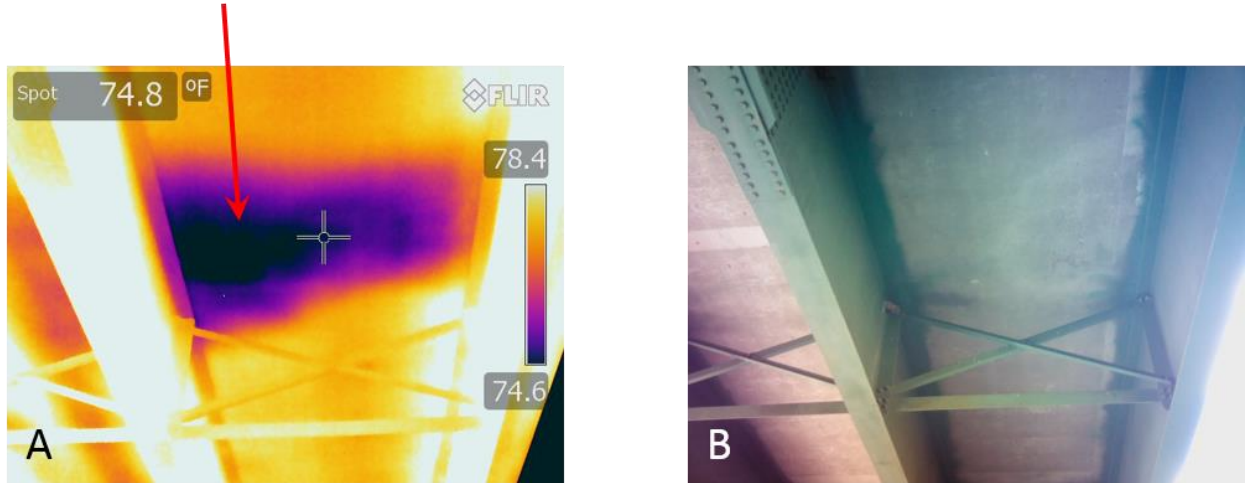


**Figure 4-12: Infrared (A) and Digital (B) images from the soffit of the delamination in Figure 4-11**

The images from Figure 4-12 were captured in the afternoon. Over the course of the project, it has been observed through the verification process that delaminations on the deck show up as “cold spots” on the soffit in the afternoon. The inability of the heat to transfer through the depth of the deck because of the air void is the cause of the “cold spots”.

The borescope was also used to verify the depth of the delamination. Sixteen locations throughout the area of the delamination were measured. The depths and locations of each measurement are shown in Figure 4-13 below.

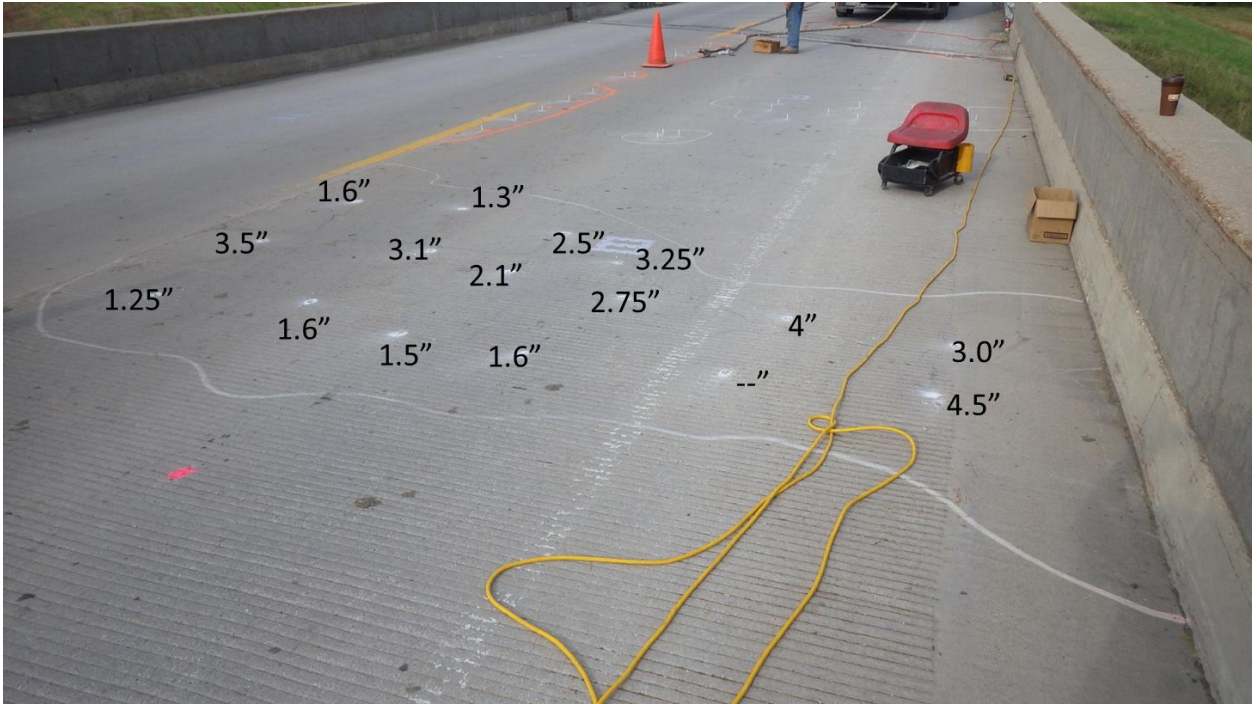


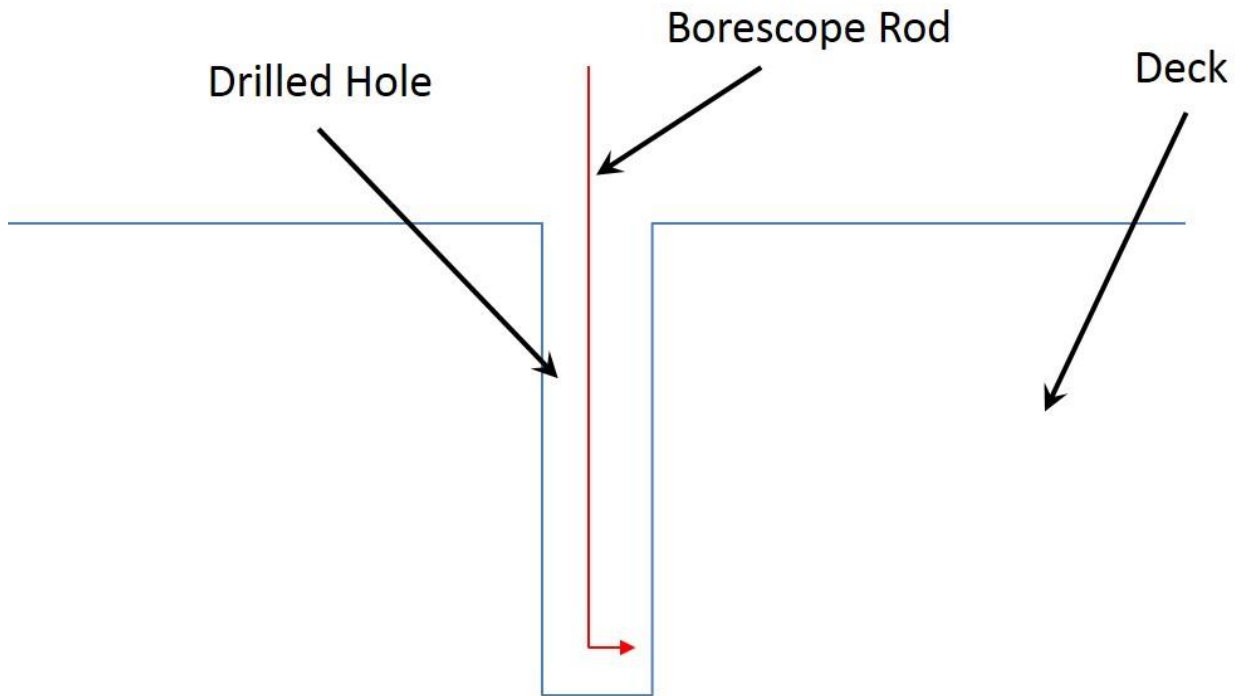
**Figure 4-13: Drilled hole locations for borescope measurements**

In order to measure the depth of the delaminations, the borescope was inserted into the hole to the point where the crack could be seen and these measurements were recorded. Figure 4-14 shows an image captured with the borescope. Figure 4-15 shows a schematic diagram of how the borescope is used for inspection.

Delamination



**Figure 4-14: Borescope image of a deck delamination**



---

**Figure 4-15: Schematic diagram of how the borescope is used for inspection**

Weather conditions for the day were conducive for inspection using infrared thermography. The wind speed was as high as 16 mph, but the speed was consistently between 6 and 9 mph for most of the day. The guideline suggests a threshold of 15 mph. In situations with higher ambient temperature change than is suggested by the guidelines, the amount of wind must also increase in order for the conditions to become detrimental to inspection. The ambient air temperature for the test is shown in Figure 4-16 below (Wunderground 2013-2015).

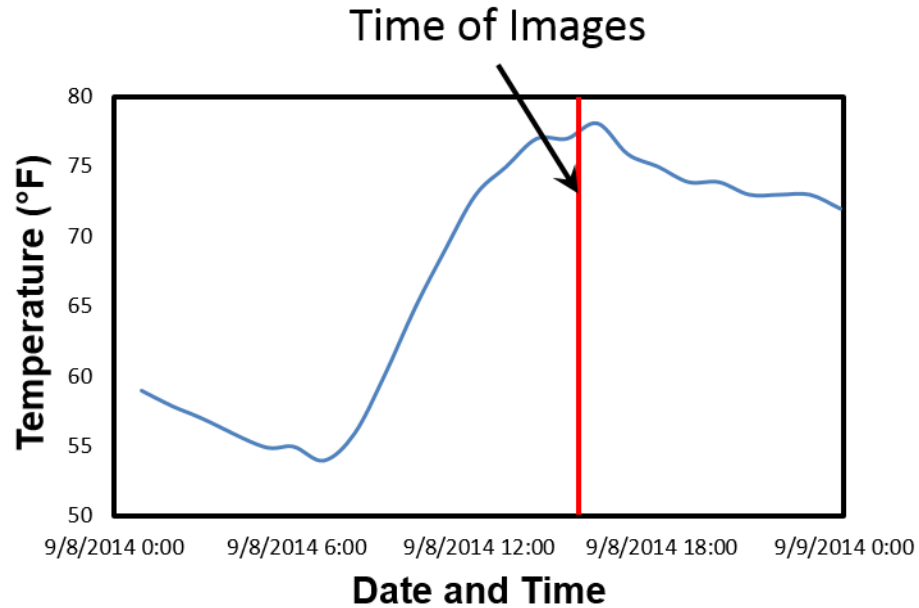


**Figure 4-16: Ambient temperature for verification in Lamoni, IA**

#### **4.5 Georgia**

The November 2012 trip to Atlanta yielded no results due to poor weather conditions; this trip was unsuccessful pertaining to verification. This was one of three state trips that was unsuccessful. There was rain and very little temperature change throughout both days of the trip; rain is completely detrimental to bridge deck inspection and no quality images could be taken for that reason. During this trip, the time was spent working with the inspectors to review the guidelines and the process of uploading images to the infrared thermography shared data website. A graph of the ambient temperature during the trip is shown in Figure 4-17 below (Wunderground 2013-2015).

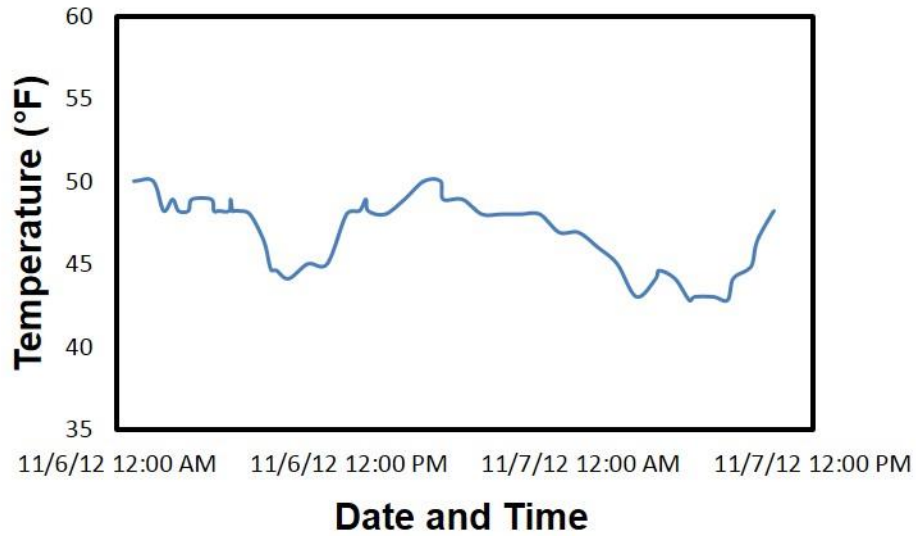


**Figure 4-17: Ambient air temperature for the verification trip to Georgia (2012)**

Three locations were tested on the return trip - Jonhstonville Rd. spanning I-75, Dames Ferry Bridge deck spanning a railroad track, and Dames Ferry Rd. Bridge spanning the Ocmulgee River. The trip was carried out May 28, 2014 near Forsyth.

The weather conditions for this trip were ideal for thermographic inspection since there was sufficient ambient temperature change and little to no wind. Figure 4-18 shows the ambient temperature for the day of inspection (Wunderground 2013-2015).

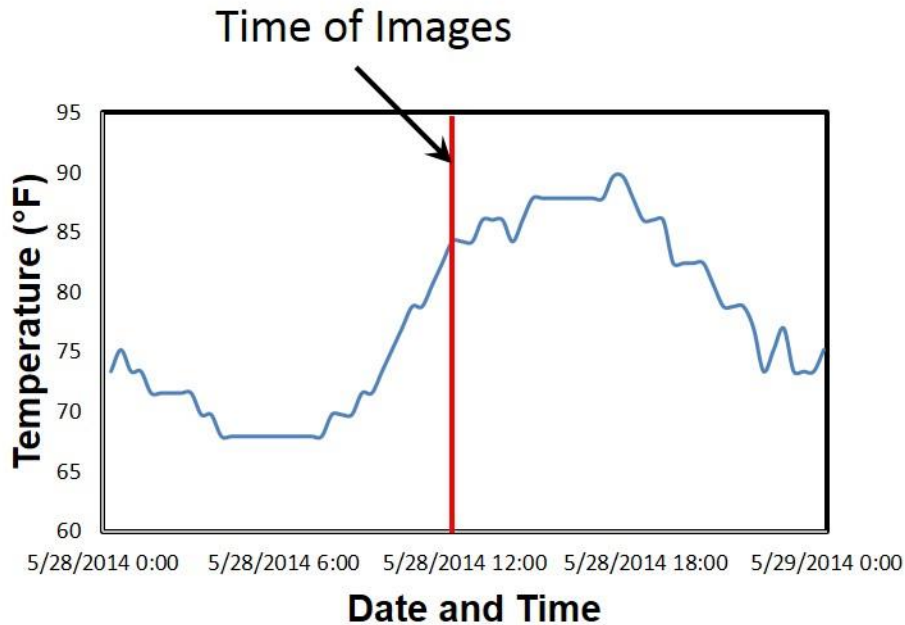


**Figure 4-18: Ambient air temperature for the verification trip to Georgia (2014)**

In order to verify the I-75 Bridge, GDOT workers hammer sounded the deck and marked delaminations with bright orange spray paint. Although the Georgia Bridges had been hammer sounded prior to this May 2014 trip, but the markings had washed away. After the initial assessment with hammer sounding, inspectors employed the infrared camera to detect delaminations. Since the IR inspection was performed in the ten o' clock hour, the deck had not experienced enough solar exposure to yield desirable results. To allow for a larger temperature change to occur, a return trip was made to the bridge at approximately 3 P.M. Figure 4-19 shows an example of the results for the Johnstonville Road Bridge spanning I-75.



## Delamination

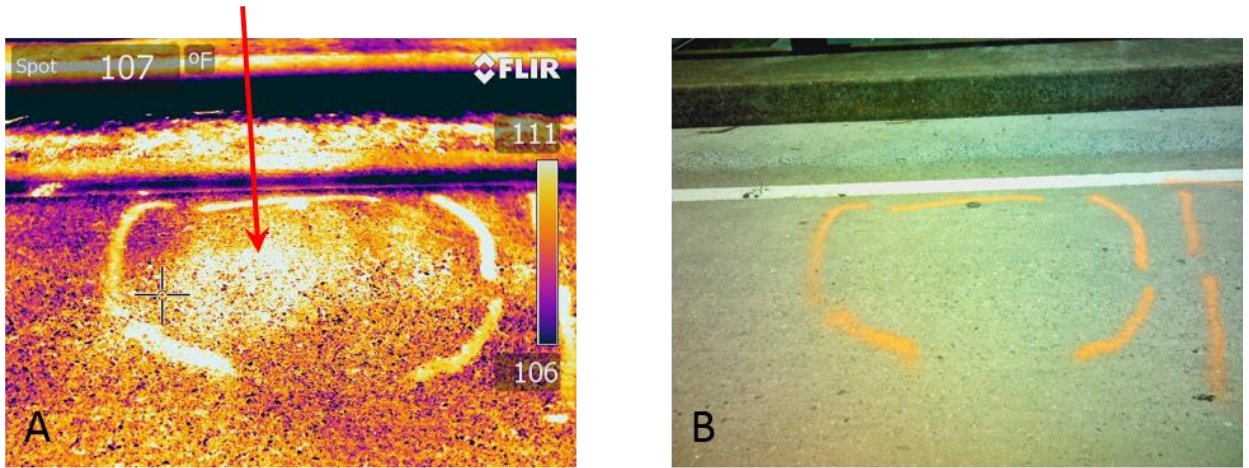


**Figure 4-19: IR (A) and digital (B) images of a deck delamination on Johnstonville Rd.**

The infrared camera was used as the initial inspection tool on both of the Dames Ferry Road bridge decks; verification was completed with hammer sounding. Due to ideal weather conditions and relatively shallow steel reinforcement, both bridge decks provided excellent results. Examples of delaminations from those bridge decks are shown in Figures 4-20 and 4-21.

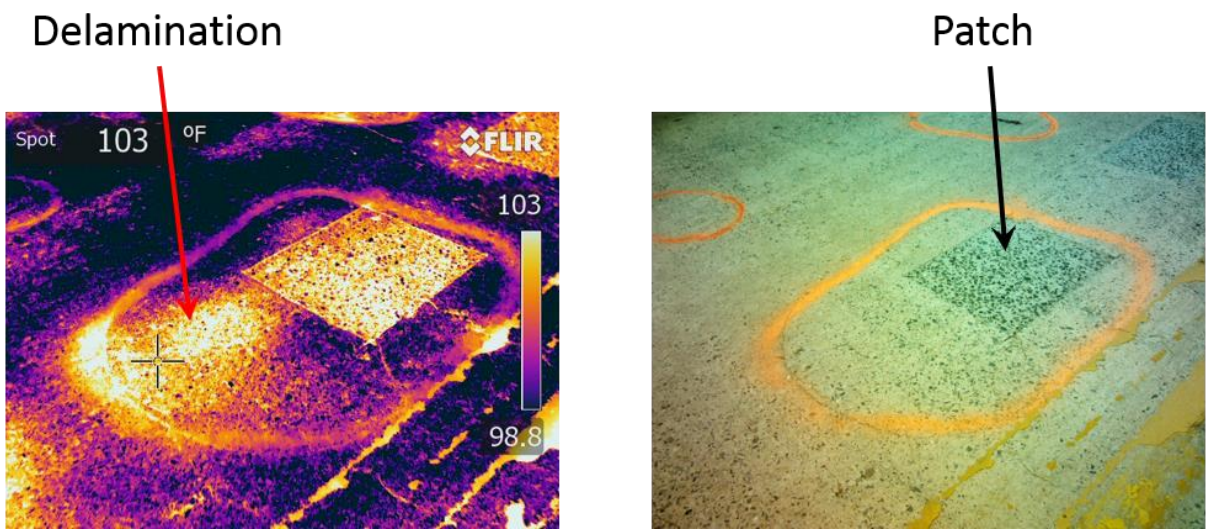


Figure 4-20: IR (A) and digital (B) images of a deck delamination over Ocmulgee River

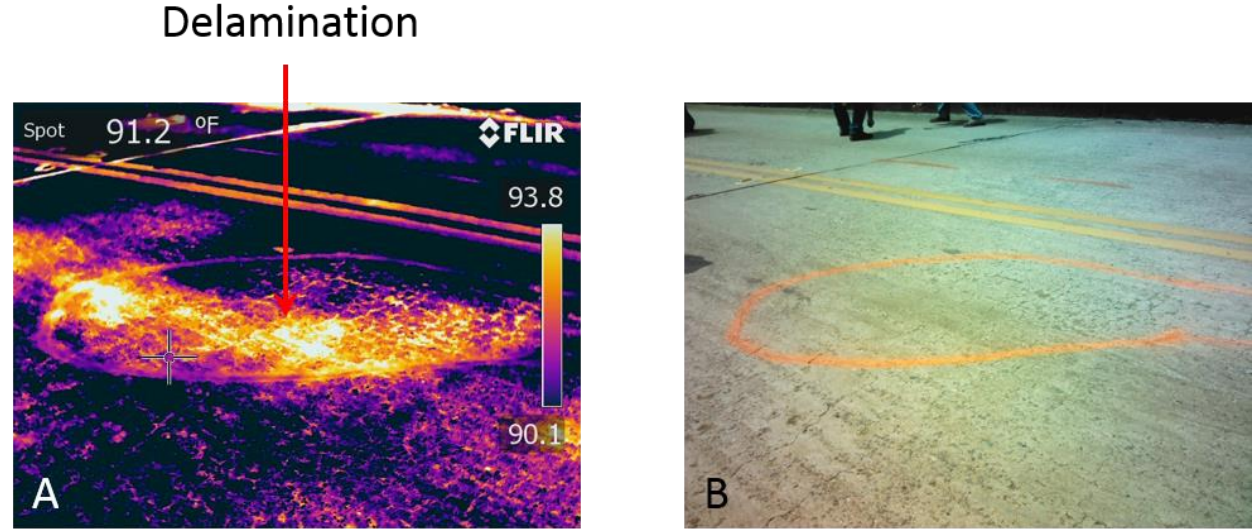
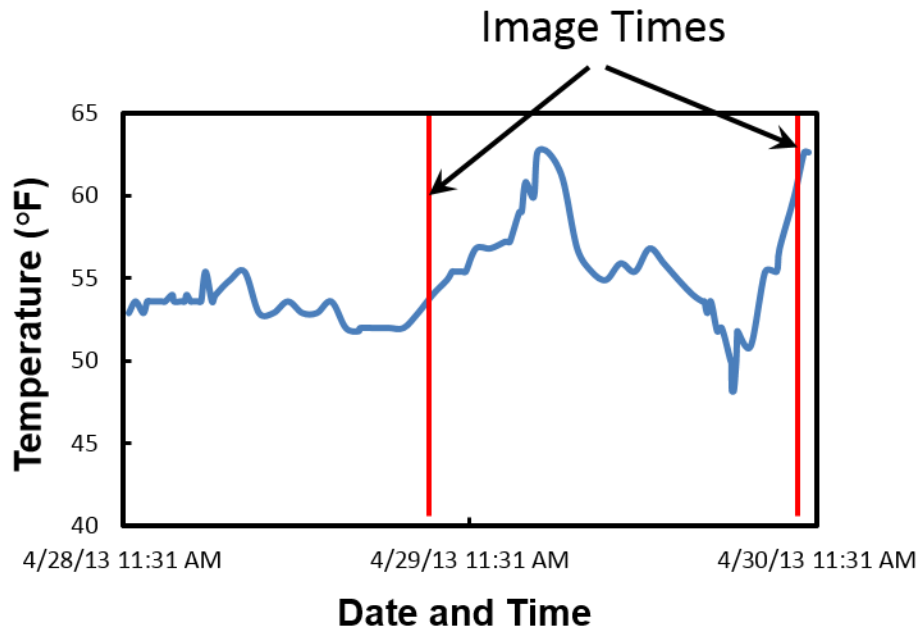


Figure 4-21: IR (A) and digital (B) images of a deck delamination over a railroad on Dames Ferry Rd.

Figure 4-20 illustrates a delamination near the edge of a patch in the deck, a common occurrence with patches that are not fully repaired.

## 4.6 Pennsylvania

A bridge on I-376 over the Shenango River was tested on April 29 and 30, 2013. The weather for the April 29<sup>th</sup> IR inspection of the bridge was not conducive to producing quality thermography images. The temperature at the time of inspection remained fairly constant although there was an 11 degree temperature change that occurred later in the day. The wind was calm, not measuring greater than 7 mph during inspection. Figure 4-22 provides a graph of the ambient temperature change for both days of the Pennsylvania bridge inspection (Wunderground 2013-2015).



**Figure 4-22: Ambient air temperature for the verification trip to Pennsylvania**

Scattered showers throughout the first day interfered with the deck inspection; therefore, the substructure was inspected instead. Although weather

conditions were less than ideal, delaminated areas could still be seen in one of the pier caps. A thermal and digital image of the delaminations are shown in Figure 4-23 below.

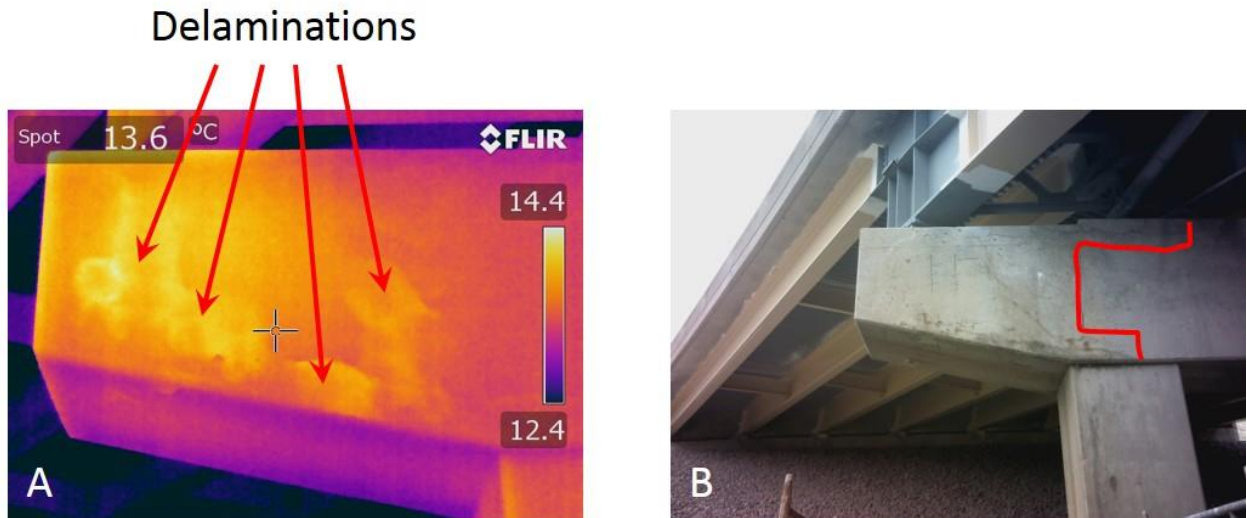


**Figure 4-23: Thermal image (A) and digital image (B) of a pier cap delamination**

The pier cap was hammer sounded and defected areas were marked. The edge of the marking is located above the left side of the column in the image above. It has been traced for clarity.

On the second day of testing, an early morning rain caused water to collect on the deck. However, by about 10:00 A.M. the deck started to dry and images were captured from the boom of a truck. The truck is shown in Figure 4-24. The change in temperature during the three hours of inspection time was 7°F. The temperature change allowed for enough thermal contrast to develop in the delaminated areas of the deck. The wind speed varied over the course of the inspection period but never exceeded 9 mph (Wunderground 2013-2015). An

image from the boom is shown in Figure 4-25 below. More examples can be viewed on the pooled fund shared data website.



**Figure 4-24: Boom truck utilized for imaging a bridge deck from an elevated location**

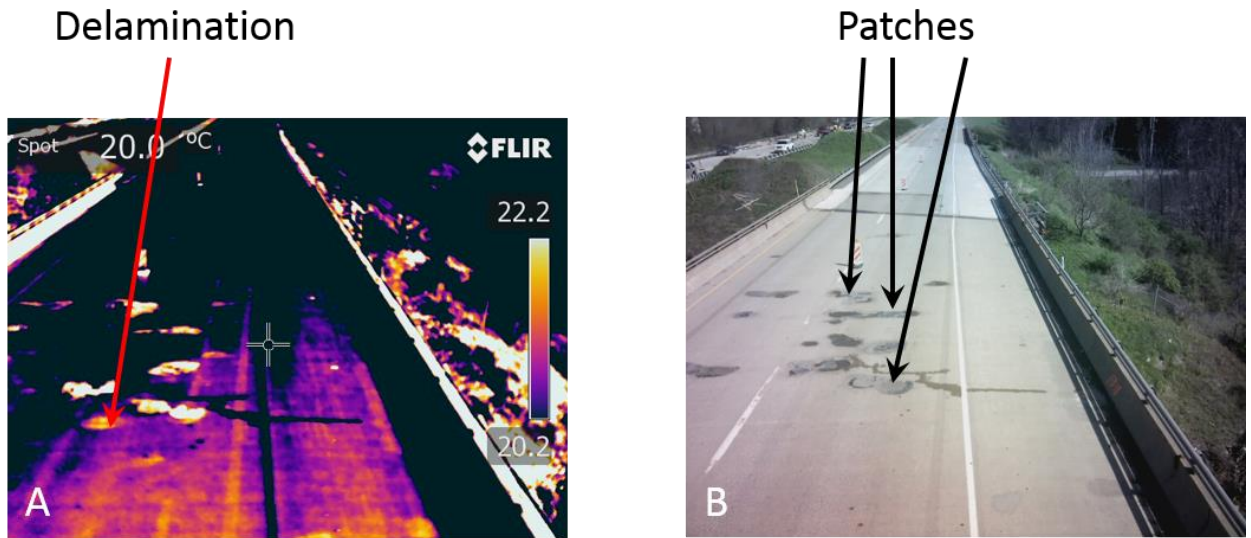


**Figure 4-25: IR (A) and digital (B) images from a boom of a deck in Pennsylvania**

Figure 4-25 illustrates the ability of infrared thermography to distinguish between delaminations and patches on the deck. Patches in the deck are easily identified in the digital image and can be paired with the infrared image. Delaminations are unlikely to be visible in the digital image.

#### **4.7 Texas**

Multiple bridges in Texas were inspected and verified on May 29 and 30, 2013. One bridge was of particular concern for Texas DOT since there was some transverse cracking in the deck. The concern was in regard to separation in the precast panels and cast in place concrete. The bridge deck consisted of a four inch thick cast in place concrete deck on four inch thick precast concrete panels. A delamination due to the separation of the deck from the precast panels would be

at a depth of approximately four inches. It was expected that detection would be difficult even under the most ideal weather conditions for infrared thermography.

Due to less than ideal weather conditions for thermographic inspection, the trip was unsuccessful. On May 29<sup>th</sup>, the change in temperature was 15°F with a wind speed of 14-18 mph and cloudy conditions during the time of inspection (Wunderground). It is preferred, for deck inspections, to have clear, sunny skies to allow for maximum solar loading. In addition, the temperature and wind parameters were also at the edge of the guideline threshold for successful inspection. The figure below shows a graph of the ambient temperature during the testing period (Wunderground 2013-2015).

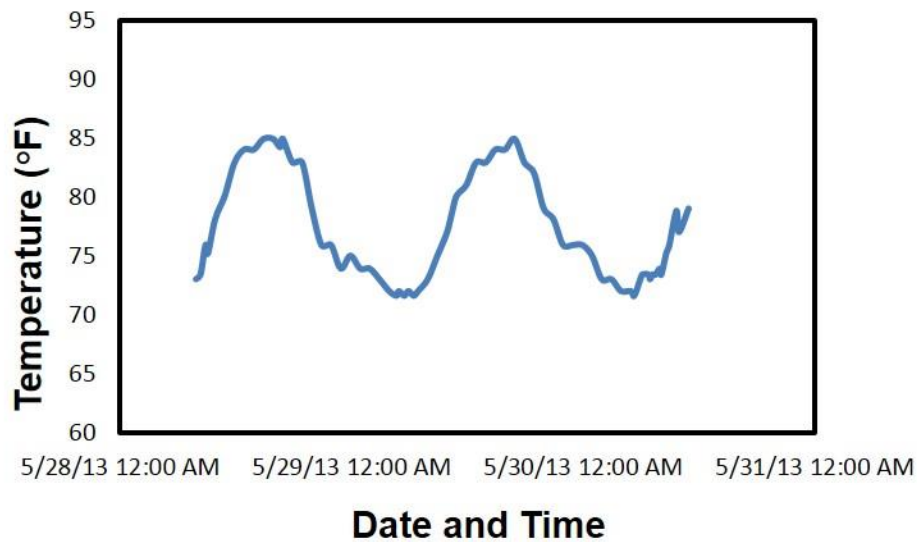


**Figure 4-26: Ambient temperature for the verification trip to Texas**

The weather conditions on May 30<sup>th</sup> were similar to May 29<sup>th</sup> with the exception of the temperature change during the time of inspection. With the

combination of the depth of possible delaminations and less than ideal weather conditions, no quality thermal images could be taken.

#### **4.8 Oregon**

The Oregon bridge chosen for verification testing was located at Crosby Rd. over I-5, north of Woodburn. Testing was accomplished on August 8, 2013. The Oregon Department of Transportation had performed a previous inspection with the report completed by Wiss, Janney, Eistner Associates Inc.; this inspection included findings of delaminations in the soffit and Reinforced Concrete Bridge Girder (RCBG) in the middle bent of the bridge (Simonen 2013).

The weather for the day was ideal for infrared thermography. The weather conditions included an ambient temperature change of 27°F, wind speeds of 5 mph, and no precipitation. Sunrise occurred at 6:04 A.M. with a temperature of 57°F. The temperature at 12:04 P.M. was just above 71°F allowing for a temperature change of 14°F in the first six hours after sunrise. A graph of the ambient temperature is shown in the figure below (Wunderground 2013-2015).



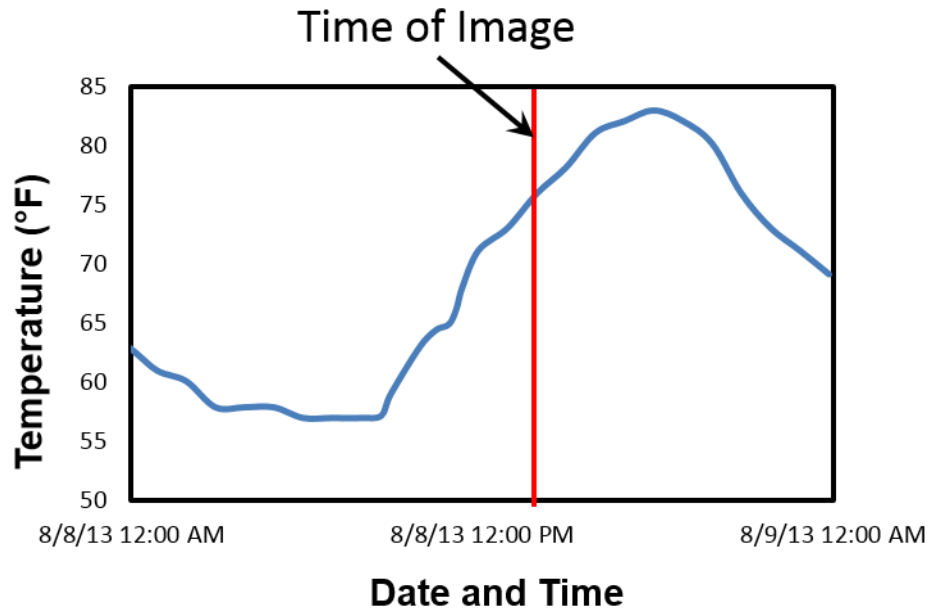


**Figure 4-27: Ambient temperature for the verification trip to Oregon**

An image of the sounding results from the report along with the corresponding delamination near one of the drains are shown in Figures 4-28 and 4-29 below. The sounding results are outlined for clarity.

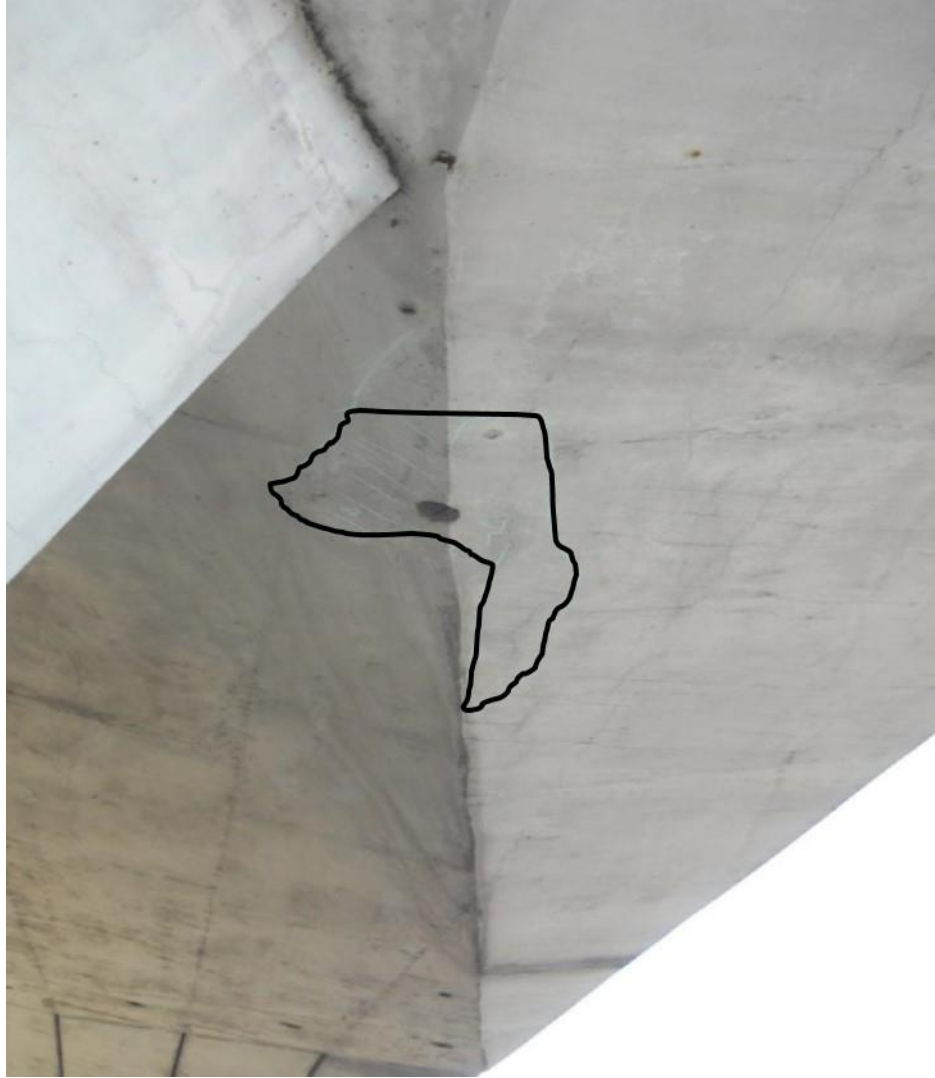


**Figure 4-28: Hammer sounding results of a drain delamination from the WJE report**

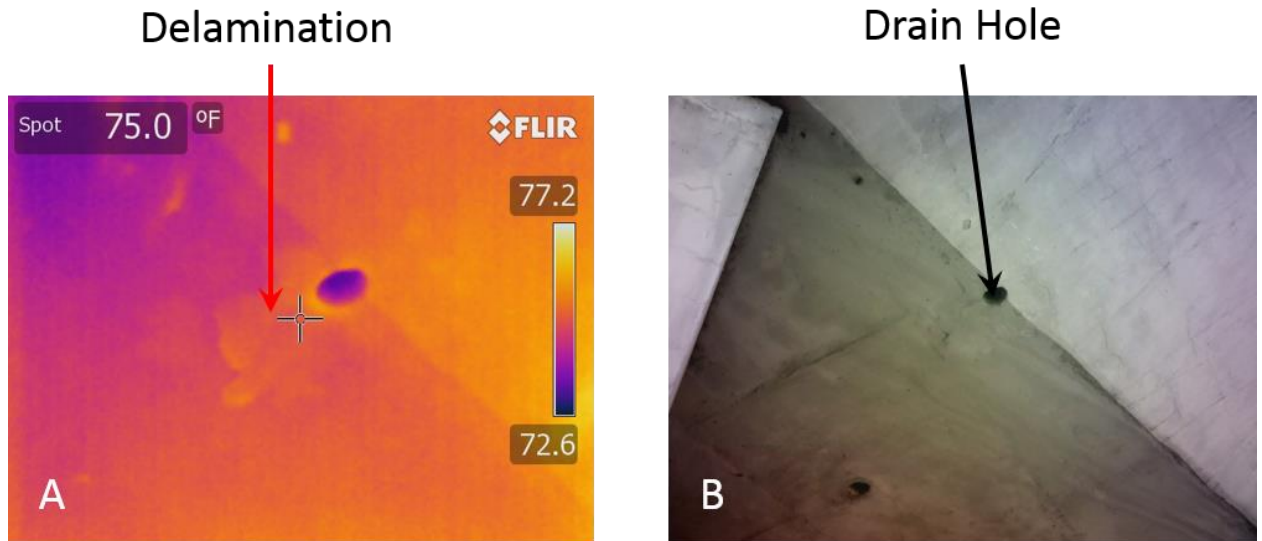


**Figure 4-29: Thermal image (A) and digital image (B) of a drain delamination**

Figure 4-29 was captured at approximately 2:30 in the afternoon when the temperature was approximately 77 °F (Wunderground 2013-2015). The temperature in the day had changed 20 degrees and should have been sufficient to capture a quality image. The image shows little thermal contrast between the delaminated area and the undamaged concrete with the smallest span possible for the camera. Higher thermal contrast between the delamination and sound concrete was expected with the weather conditions that were experienced.

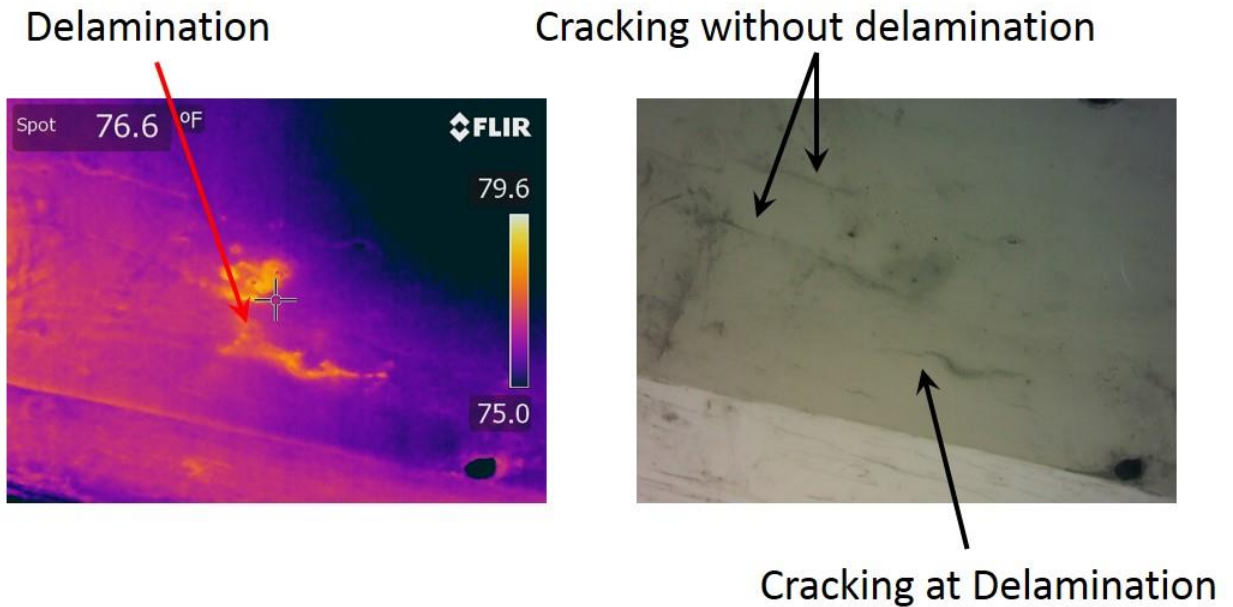


**Figure 4-30: IR (A) and digital (B) image of a possible parge coat delamination**

Figure 4-30 illustrates a possible delamination in the parge coating. There are other cracks similar to the area in question that show no evidence of thermal contrast. The fact that there is no thermal contrast in other areas would indicate that this is a delamination in the parge coating, not in the concrete.

The goal of the inspection for this bridge was to capture quality thermal images of delaminations that had been previously detected with hammer sounding by the Oregon Department of Transportation. The weather conditions for the day were conducive for quality images to be captured. However, the images captured did not show the expected results with positive weather conditions. Delaminations detected in the concrete showed subtle thermal contrasts, though the contrast is typically larger with the experienced weather conditions.

A possible cause for the lack of quality images could be due to the fact there was a parge coating applied to the bridge (Simonen 2013). The irregularities in the coating compared to the concrete underneath it may have caused poor results.

The verification trip can still be considered a success because of the lack of prior knowledge or experience with parge coatings and their effect on thermal imaging. Normally, images are captured on the deck where parge coats are not applied. It is now known that, even in ideal weather conditions, parge coatings can affect the way a delamination will appear in a thermal image.

#### **4.9 Kentucky**

The Kentucky verification trip was completed August 26, 2013 in Louisville. The bridge chosen crossed over Kentucky St. on I-265. A large abutment wall, piers, and pier caps were tested. Those three components were sounded and the areas designated for repair were marked. Example images are shown in Figures 4-31 and 4-32 below.

## Delaminations

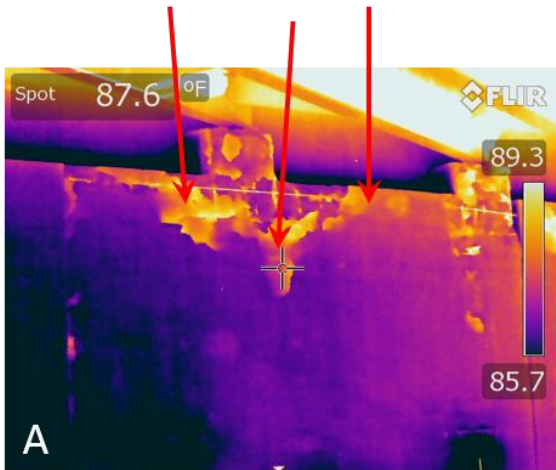
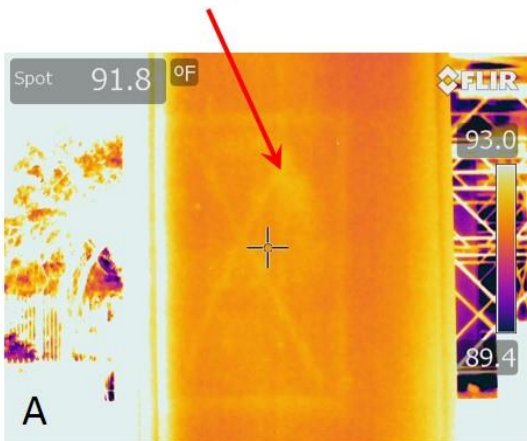


**Figure 4-31: Thermal (A) and Digital (B) images of a delaminated abutment wall under I-265**

## Area in question



## Hammer Sounding Result



**Figure 4-32: IR (A) and digital (B) images of hammer sounding results on a pier in Kentucky**

The comparison of the thermal and digital images show that some of the areas the inspectors did not mark are delaminated; this is consistent with additional images on the pooled fund shared data website. Since replacing

concrete is typically done on per a square foot basis, minimizing the amount that needs to be replaced and ensuring that all the delaminated concrete is removed is a primary objective of repair. The infrared results and the hammer sounding may not always match. Hammer sounding is a subjective approach to inspection and may vary by inspector. The infrared camera has the capability to optimize the process and can be completed more efficiently. Instead of sounding the entire abutment wall, the camera can identify the areas of concern and sounding, along with other methods, can be used to verify delaminations.

There was also a case where the inspectors hammer sounded a delamination that the infrared camera did not identify. Further analysis of the image was completed using a computer program called FLIR tools. The analysis showed that a 0.5° F contrast existed between the area in question and the surrounding concrete. It was determined that the delamination in question went undetected because a thermal contrast that small would not be readily apparent in the field.

Conditions of the day were conducive to inspection using infrared thermography. The weather conditions included a temperature change of 19°F with approximately 13°F of that occurring in the first six hours after sunrise. The wind speed for the day reached as high as 12 mph, but was 5 mph at the time of the inspection. A graph of the ambient temperature is shown in the figure below (Wunderground 2013-2015).

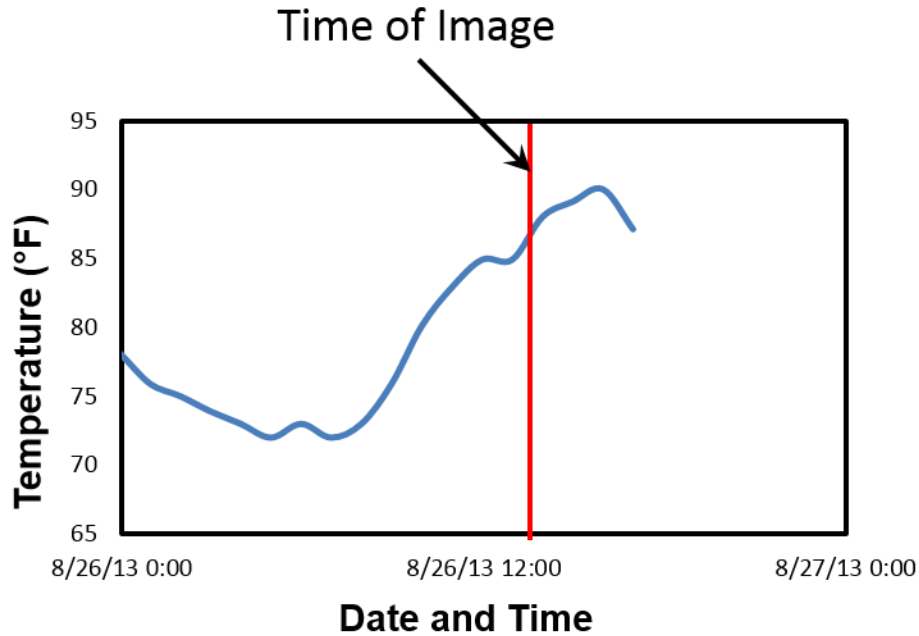


**Figure 4-33: Ambient temperature for the verification trip to Kentucky**

#### **4.10 New York**

The New York verification testing was conducted on a pair of bridges at Albany Shaker Rd. under I-87 and was completed November 20, 2013. The bridges were built in 1959. A previous inspection from November 2012 had been completed and shared by the New York Department of Transportation. The NYDOT inspection included findings of delaminations detected by hammer sounding in the pier columns and caps.

Figure 4-30 shows the ambient temperature change. This image is taken from the weather checker on the pooled fund shared data website. It displays both the previously recorded ambient temperature data along with the forecasted data.



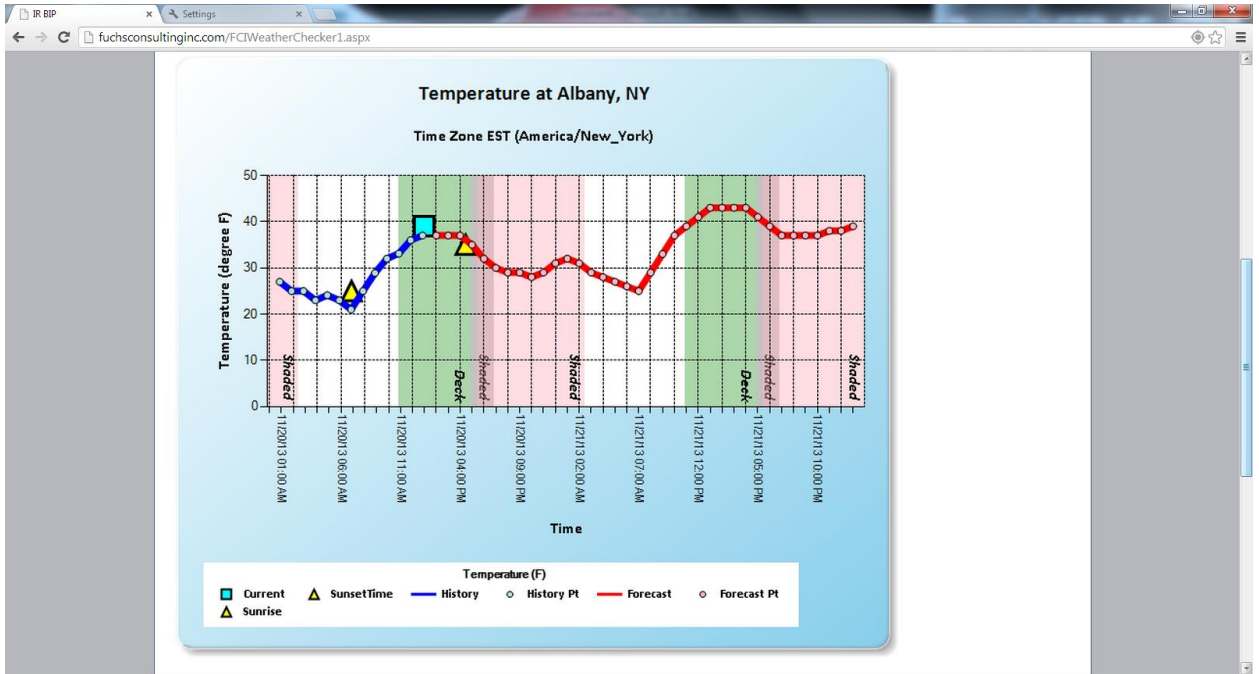


**Figure 4-34: Previous and forecasted weather conditions of Albany, NY provided by the weather checker**

Three sets of images were taken on the New York verification trip. The images were captured at approximately 8:00 A.M, 11:00 A.M. and 2:00 P.M. The decrease in light in the late afternoon and the high traffic volume in the area of inspection would have made it dangerous for a night inspection. An image of a pier column is shown in Figure 4-35 and more images are available on the pooled fund shared data website.

## Delamination

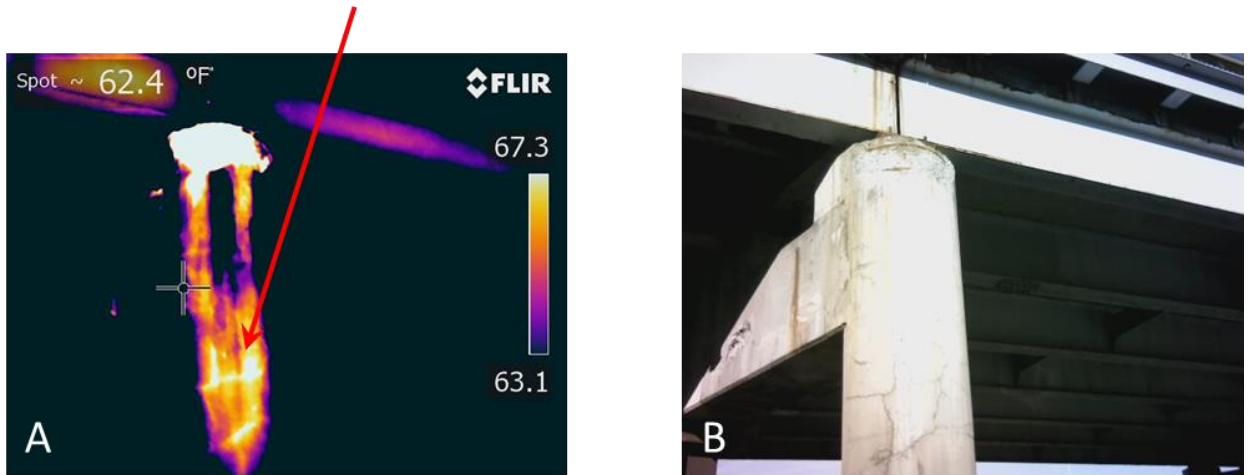


**Figure 4-35: IR (A) and digital (B) images of a delaminated column on Pier 1 of South Bridge**

An extreme thermal gradient is evident in the figure. The digital image shows that the sunlight is directly hitting the delaminated area; this direct sunlight provided better thermal imaging results. The delaminated area can be seen as the “hot spot” in the picture. A report provided by NYDOT lists this particular column as having map cracks with rust stains. It is possible that the previously identified cracks may have propagated in the time since the report to form these identified delaminations.

To further demonstrate the effect of a thermal gradient on an IR image, Figure 4-36 shows four of the same image with four separate temperature spans: 10°F (A), 20°F (B), 30°F (C) and 45°F (D). A typical span for capturing a good image in the field is approximately 4-8°F. For this example, a span of 40° F is required for everything in the infrared image to be visible.

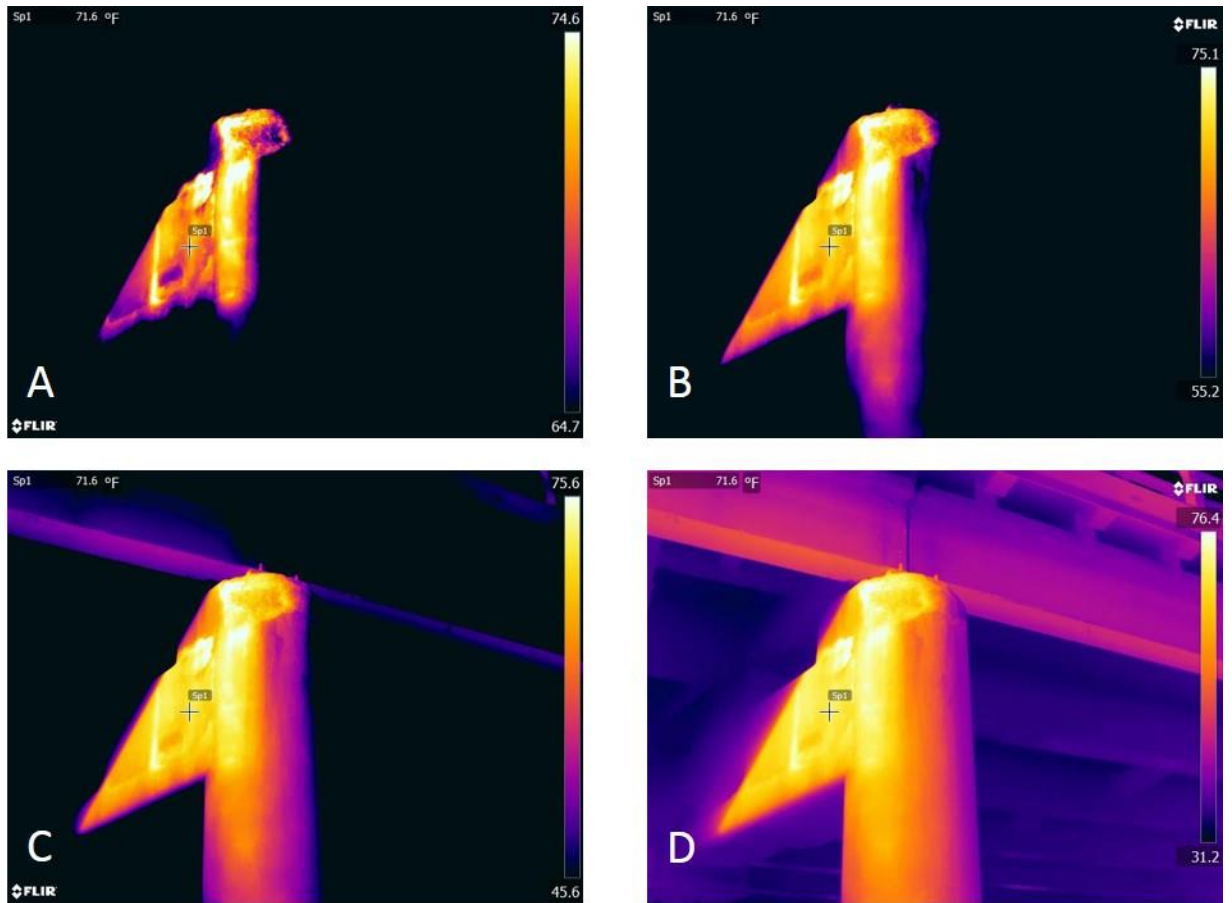


**Figure 4-36: Illustration of how thermal gradient can affect an image**

The goal of the inspection for this bridge was to capture quality thermal images of delaminations that had been previously detected by the New York State Department of Transportation. The weather conditions for the day were sufficient enough for quality images to be captured. The thermal gradient of the transition from sun affected areas to non-sun affected made it difficult to capture quality images in some areas. However, there was a greater temperature contrast in the areas that the sun was affecting. An effective solution to the thermal gradient issue would be to capture images at night when there is no exposure to sunlight.

## 4.11 Ohio

A wide bridge located at I-70 over Glenwood Avenue was inspected June 23, 2014 in Columbus. Members of Ohio Department of Transportation had been having some issues with getting useful infrared results on a wide bridge (greater than 100 ft). This was the first time this issue had been identified. The Glenwood Avenue Bridge was selected as a testing site to determine if wide bridges could provide enough ambient temperature change underneath to allow for good infrared inspection results. Two other bridges were also inspected on the Ohio trip; these images can be seen on the pooled fund shared data website.

. Images from the Glenwood Avenue Bridge were captured in the morning and the afternoon. The morning images were captured between 7:30 A.M. and 8:15 A.M. The thermal contrast began to disappear toward the end of that inspection interval. The afternoon images were captured between 2:45 P.M. and 3:00 P.M. By capturing images in both the morning and afternoon, it shows that delaminations appear differently during different times of the day. An example of the difference in thermal images is shown in the two figures below. The images are not in the same location but Figure 4-38 shows images located near the center of the width.

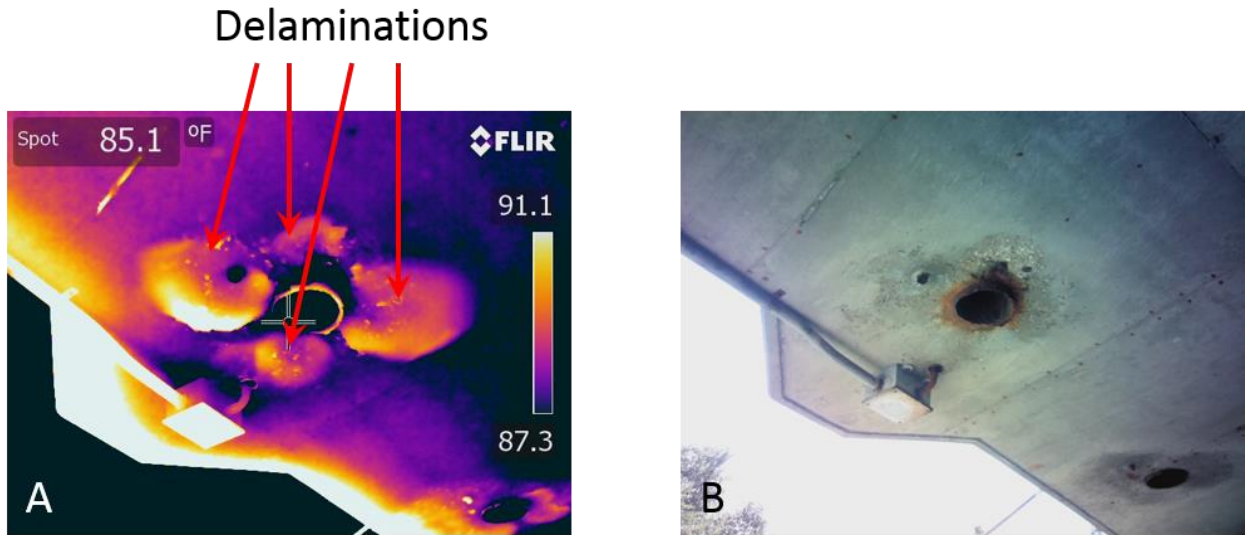


**Figure 4-37: Afternoon infrared (A) and digital (B) images of a soffit delamination in Columbus, Ohio**

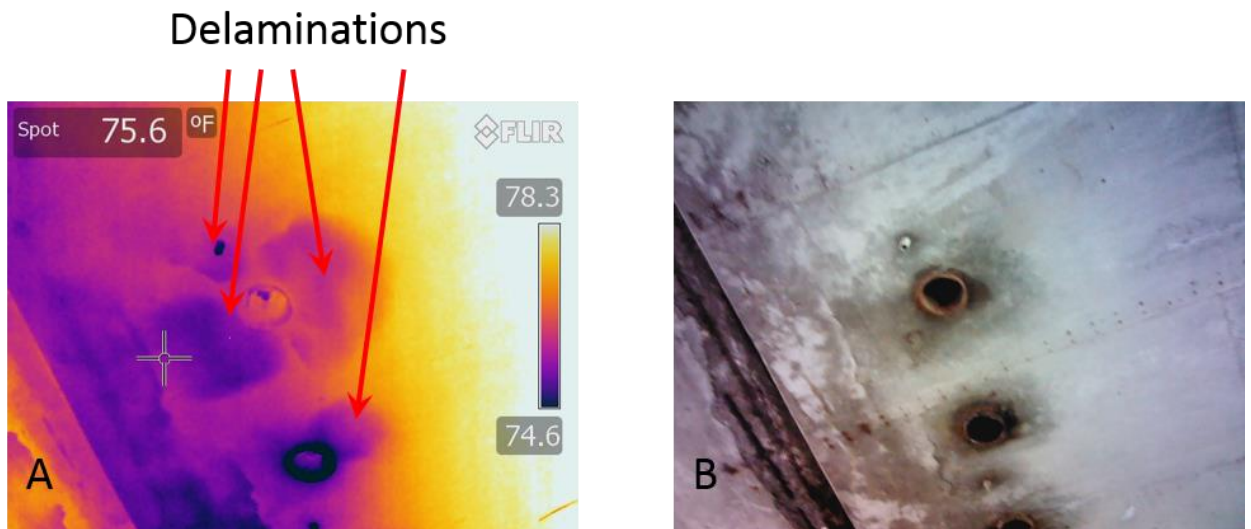


**Figure 4-38: Morning infrared (A) and digital (B) images of a soffit delamination in Columbus, Ohio**

Another example in Figure 4-39 shows delaminations surrounding a scupper in the soffit of the bridge. The figure shows the same area of the bridge

during the morning and afternoon. As shown in the images, the delaminations appear as cold spots during the morning hours and as hot spots during the afternoon.

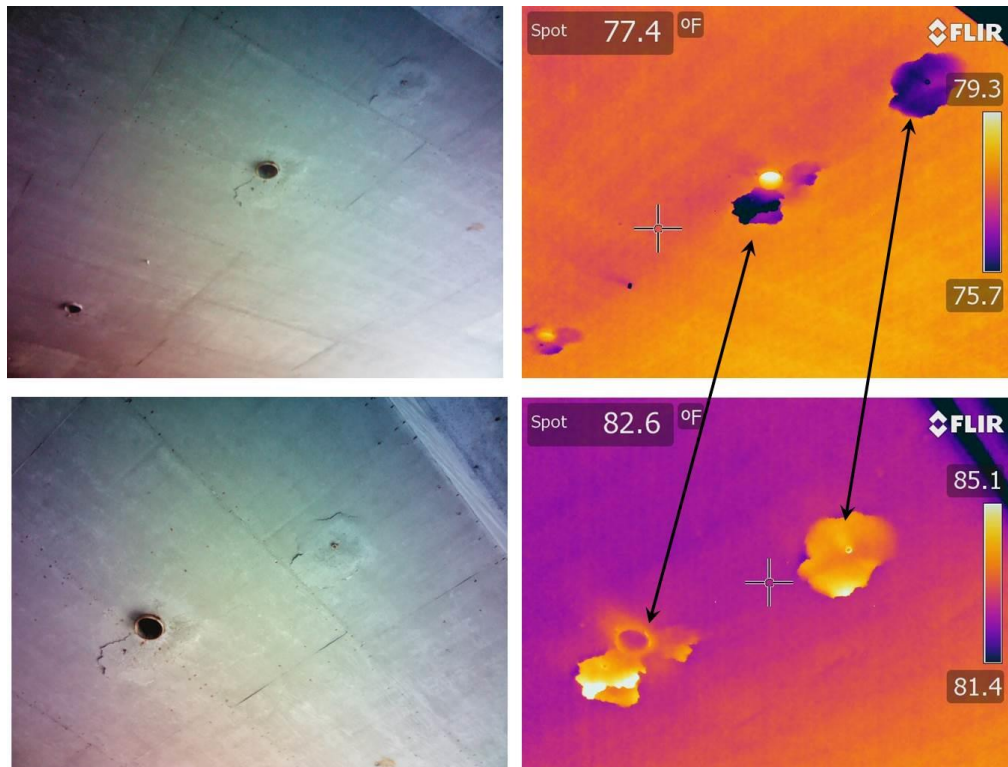


**Figure 4-39: Thermal images of delaminations in the soffit of a wide slab bridge, showing morning (top) and afternoon (bottom) results**

Images were also captured which showed damage surrounding a longitudinal joint at the center of the bridge. Again, images are included from the morning and the afternoon. As shown in these figures, damage surrounding the longitudinal joint could be imaged both in the morning and in the afternoon.



**Figure 4-40: Thermal images showing damage along a longitudinal joint in a 159 ft wide slab bridge**

The experienced weather conditions indicated a successful day for infrared inspection. The ambient temperature for the day is shown in Figure 4-41 below (Wunderground 2013-2015). The times marked on the graph indicate the times of day that the images from Figures 4-38, 4-39, and 4-40 were captured. The wind speed was consistently below the 15 mph threshold provided in the guidelines.

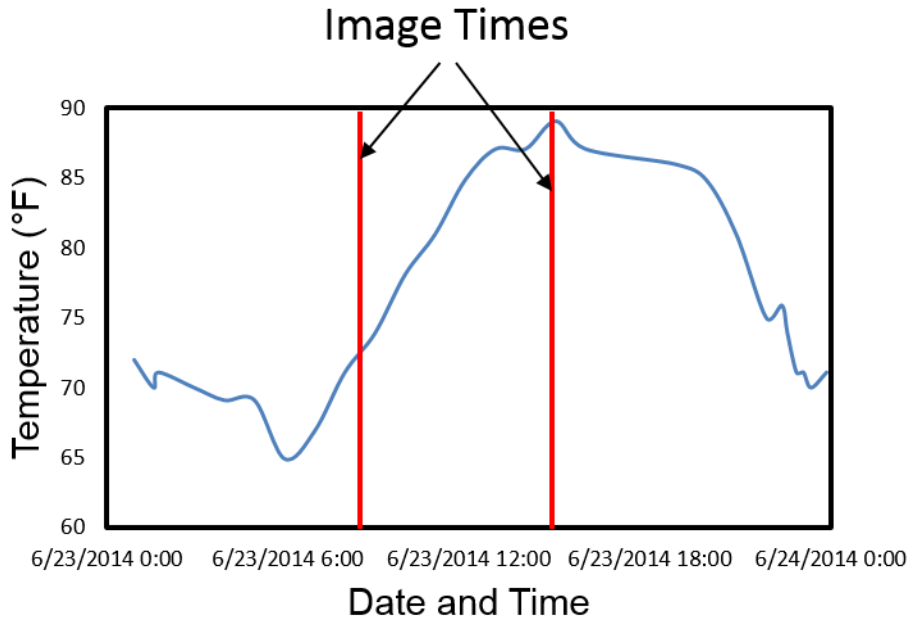


**Figure 4-41: Ambient temperature for June 23, 2014 in Columbus Ohio**

It was concluded that, with sufficient weather conditions, the width of a bridge would not be a concern for inspection using infrared thermography. These conclusions were drawn from the image quality obtained from both the morning and afternoon images. The images were comparable to soffit images from other bridges under similar weather conditions.

#### **4.12 Comparison of Results**

Results achieved with the hand held infrared camera are difficult to quantify. There is no way to determine the area or depth of damage without further physical inspection. This section will provide a partial quantitative comparison of handheld infrared data and corresponding hammer sounding results for various inspection cases.



Infrared images and images of hammer sounding results were analyzed utilizing a computer program that calculates the partial area of an image using a drawing tool. An exact area of delamination could be calculated using this technology with a correct scale relating the size of an object in the image to the drawing tool area. For example, a line one inch in length corresponding to a 20 inch line in the image would have a scale of 1:20. This analysis was a relative comparison between two results, IR imaging and hammer sounding, to determine the accuracy of the hand held camera. Therefore, the scale was not necessary to determine the exact areas of delamination for each case.

Thirty delaminations including both infrared and hammer sounding results were included in the analysis. The delaminations from this chapter included in the analysis were from Figures 4-6, 4-11, 4-19, 4-20, 4-21, and 4-31. Delaminations not included in this paper, from the same inspections as the figures listed, were also included in the analysis. Statistics of the analysis are included in Table 4-2. The calculated values are based on the infrared areas relative to the hammer sounding areas. A value larger than 1 indicates that the infrared results occupied a larger area than the hammer sounding results.

**Table 4-2: Results of the comparison between IR and hammer sounding results**

<b>Statistic</b>	<b>Relative comparison of IR area to hammer sounding area</b>
Average	0.909
Maximum	1.497
Minimum	0.560
Standard Deviation	0.242

It was determined from the results of the analysis that infrared results occupy less area than a typical hammer sounding result. This is due to the fact that, during a hammer sounding inspection, inspectors tend to mark damaged areas conservatively. Inspectors would prefer to mark an area that is larger than the damaged area to avoid an incomplete repair of the damaged area.

## **5 IR-UTD VERIFICATION**

Further verification was performed with another system that had been developed as part of the pooled fund project. The Infrared Ultra Time Domain (IR-UTD) system is an inspection tool that utilizes infrared imaging over an extended period of time rather than capturing a single image for analysis like with the hand held camera. The IR-UTD system consists of a camera head with both infrared and digital imaging capability, an enclosure including a computer and internal battery, a monitor for controlling the system, cables to connect the camera and monitor to the computer enclosure, a battery charger, and a wireless keyboard. The system was built by Dr. Paul Fuchs from Fuchs Consulting Inc. in Leesburg, VA. An image of the main system components are shown in Figure 5-1.

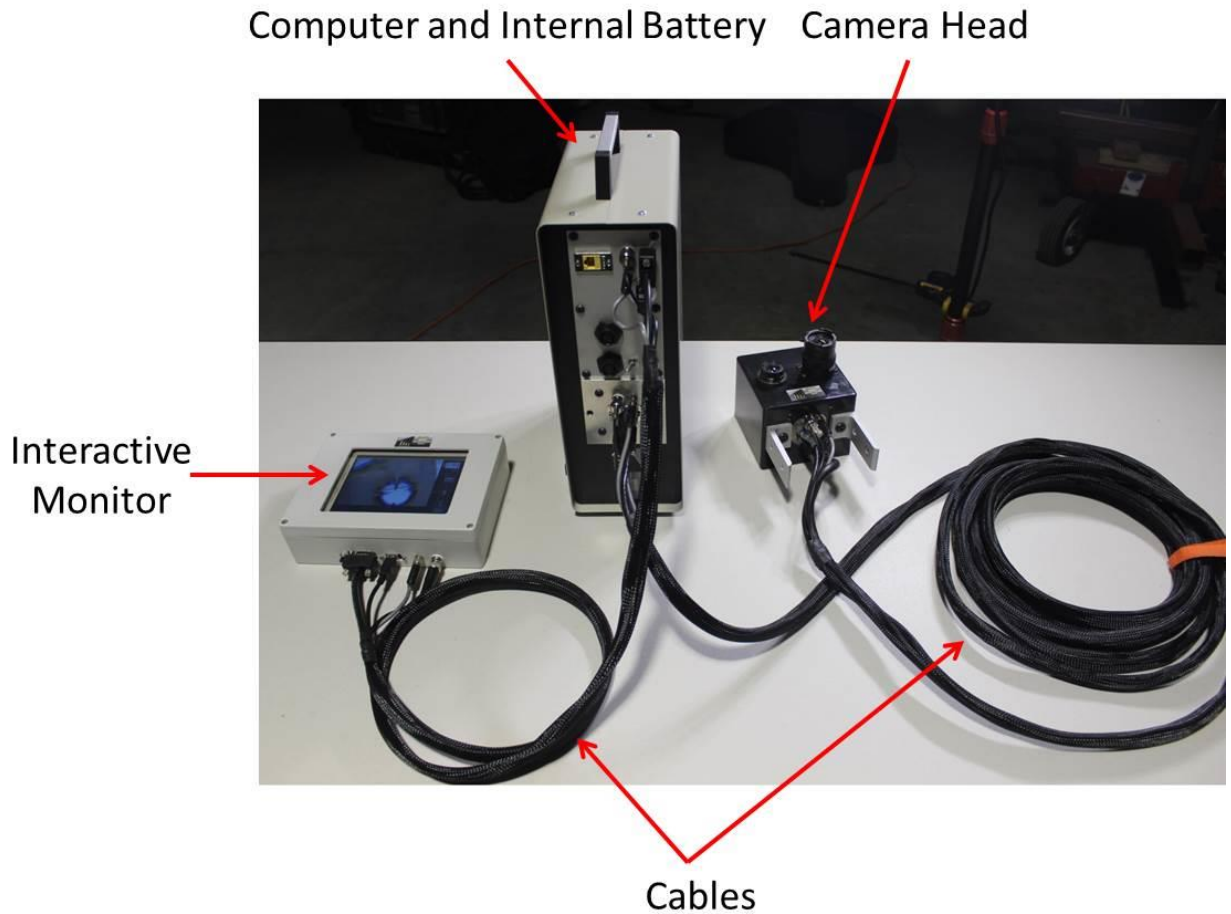


**Figure 5-1: Components of the IR-UTD system**

The concept of the IR-UTD system is that it can be mounted on a mast, pole, light trailer, or other similar structures on the side of a bridge and capture images at an interval and time duration of the inspectors choosing. The parameters of the test are set using the interactive monitor which can be controlled using either its touch screen or a wireless keyboard. Data can then be retrieved from the system during testing or at its completion using a variety of methods, including a USB drive, crossover cable, or a wireless router connected to the

system. The data are then inputted along with corresponding temperature data into a MATLAB program that produces multiple processed images for analysis.

There are many advantages to the IR-UTD system. The most significant advantage is the ability of the system to capture images with no inspector present after its operation is initiated. This allows inspectors to capture a full work day of infrared data and reallocate the amount of time that would have to be spent at the bridge if the same data were collected with a hand held camera. Another important advantage of this system is that it relies less on environmental conditions than a typical hand held IR inspection. While ambient temperature change is still necessary for successful testing, the amount needed is smaller due to the post-processing abilities of the technology. The rate of change of infrared radiation can be analyzed with the processing ability of the IR-UTD system rather than analyzing an image based on one infrared radiation reading as with the hand held camera. Other advantages of the IR-UTD system include the ability to inspect large areas at a time, collected data can be post-processed for enhanced results that are quantitative and reproducible, and there are a variety of ways to mount the camera head. In addition, direct access to the inspection area is not needed, which reduces the need for lane closure.

The IR-UTD system does have some disadvantages. This type of system is unique as it was custom made and built by hand. For that reason, it is expensive relative to other NDE technologies. Although the IR-UTD system does not depend as heavily on environmental conditions as traditional IR inspection, ambient temperature change and lack of precipitation are still necessary for successful

inspection. A less significant disadvantage of the IR-UTD system is the setup time. Currently, there is no way to adjust the angle of the camera head after it has been deployed. For that reason, it may take multiple attempts to obtain the correct configuration of the camera head. This requires a separate deployment of the mast and light tower with each attempt.

The IR-UTD system provides an alternative method of producing infrared results. Traditional IR inspection measures the amount of infrared radiation at a single point in time. The IR-UTD system increases the effectiveness of infrared technology for inspection by measuring the rate of change of IR radiation. Measuring that rate of change does not require as significant of an ambient temperature change as needed with the hand held camera.

## **5.1 Test Blocks**

### **5.1.1 Lab Test Block**

Initial testing of the IR-UTD system was performed in the lab to gain familiarity with setting parameters and determining field of view capabilities of the camera lenses. The testing was performed on a fabricated concrete slab, measuring 48" x 31" x 4", that contained targets of different size embedded at depths of two inches. The targets were embedded to simulate an air void in a concrete bridge deck.

The test setup consisted of the IR-UTD system, the test block, infrared heat lamps, a stand constructed of 80/20 aluminum framing material, and a temperature data logger with attached thermocouple. The camera head was mounted to the

80/20 material through a series of aluminum plates. Two infrared heaters were suspended from the ceiling to create a temperature change in the test block. The thermocouple for the temperature data logger was taped to the surface of the concrete block and set to take measurements every five minutes. Figure 5-2 shows an image of the test setup.

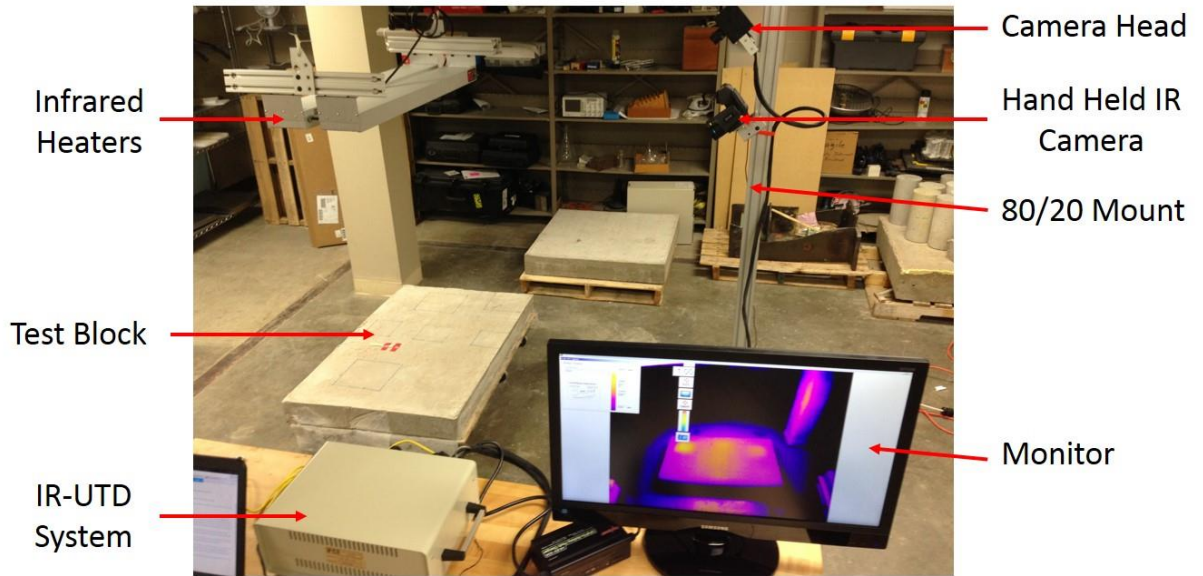


**Figure 5-2: Lab test block setup**

The parameters of the test were set to capture images every five minutes over a span of 12 hours. The heaters were turned on for two hours, shut off for four hours, turned on for two more hours, and shut off for the last four hours of the test. The reason for running the heat intermittently during the test was to simulate the trend in temperature that a bridge would experience. In a typical day, there is an increasing temperature trend early in the day when the sun rises, a peak is reached, and then a cooling trend occurs as the sun is going down and through the night. This test simulated two cycles of heating and cooling trends that would

be encountered during a bridge deck test. At the conclusion of testing, data was collected from the system for post-processing. Figure 5-3 shows the results of testing.

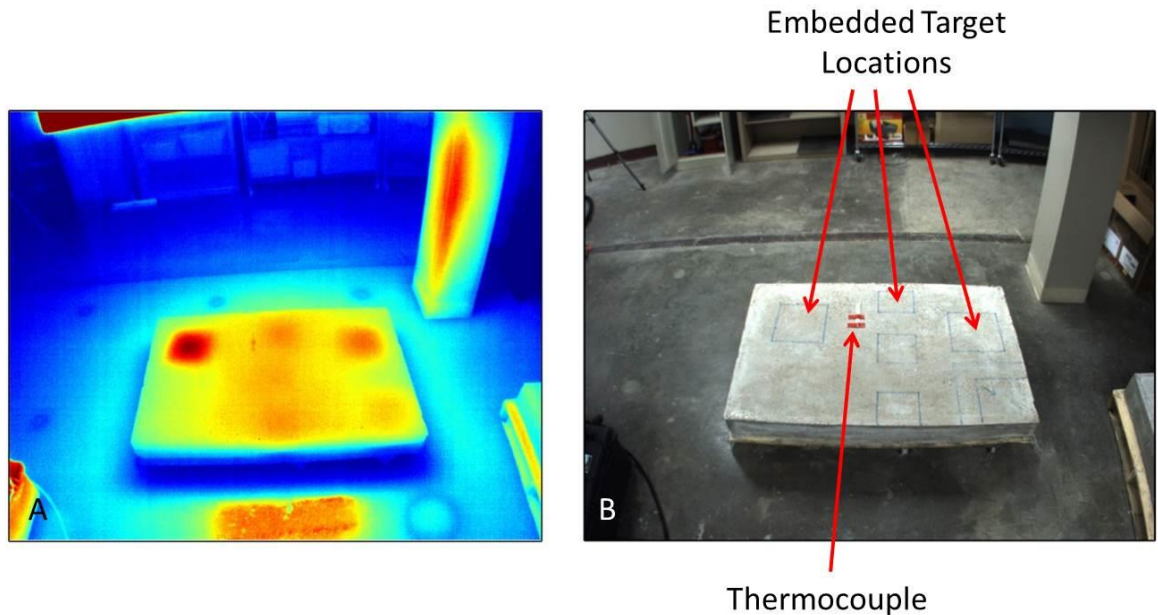


**Figure 5-3: Post-processed infrared (A) and digital (B) images of a lab IR-UTD test**

### 5.1.2 RTF Test Block

Testing was completed on a test block located at the University of Missouri's Engineering Research Test Facility (RTF) on September 4, 2014. The purpose of the test was to demonstrate the resolution of the IR-UTD camera. The test block was constructed to test multiple nondestructive evaluation technologies, including IR thermography, impact echo, and ground penetrating radar. Targets measuring 6" x 6", 1' x 1', 1.5' x 1.5', and 2' x 2' were embedded throughout the test block at a depth of two and a half inches.



A similar test setup to the one described in Section 5.2 was utilized for the test due to minimal setup time. Minor changes in setup were the use of a pan and tilt mount rather than aluminum plates and a battery in place of the generator. Parameters of the test were set to capture images every two and a half minutes for seven hours starting at 3:34 P.M. Images of the test setup and test block are shown in Figures 5-4 and 5-5.

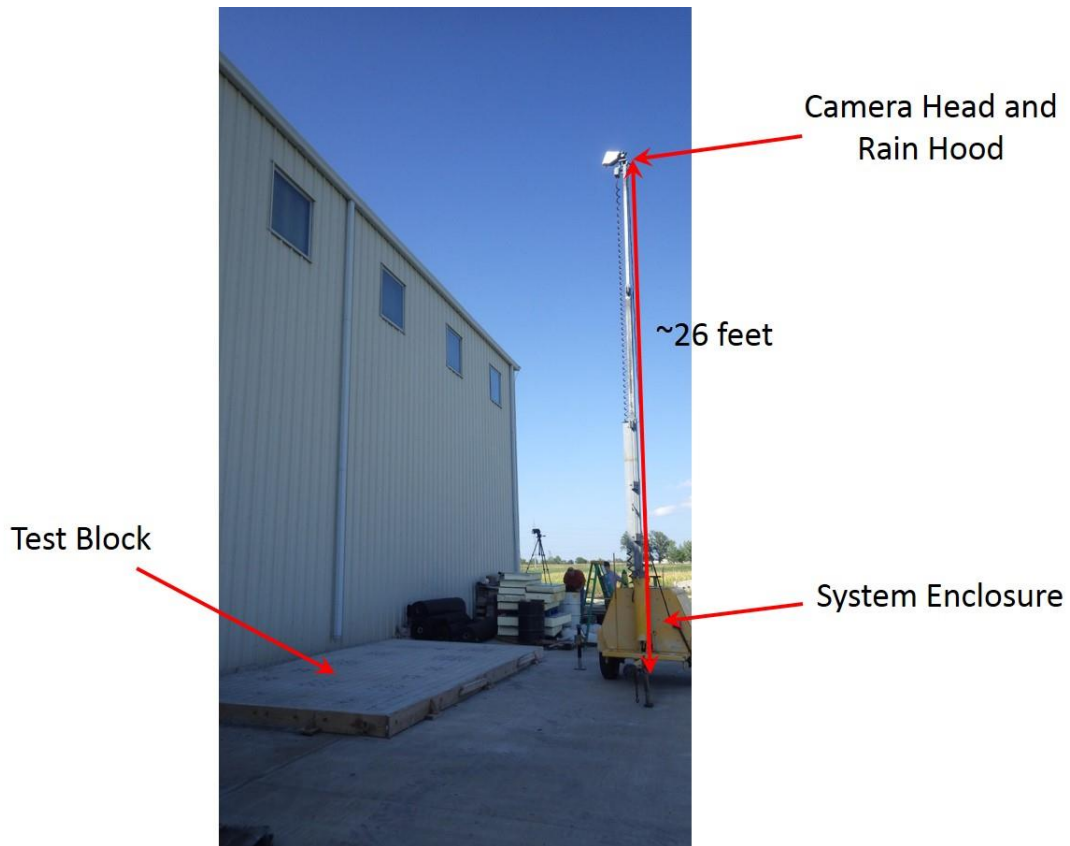


**Figure 5-4: Test setup for the IR-UTD test conducted at the University of Missouri**

**RTF**



**Figure 5-5: Concrete block constructed for testing nondestructive evaluation technologies**

Environmental conditions for the test included an ambient temperature change of 11°F and an average wind speed of approximately 10 mph (Wunderground 2013-2015). Figure 5-6 shows an image of the results and Figure 5-7 shows the four 6" x 6" targets enlarged to demonstrate the spatial resolution of the camera.

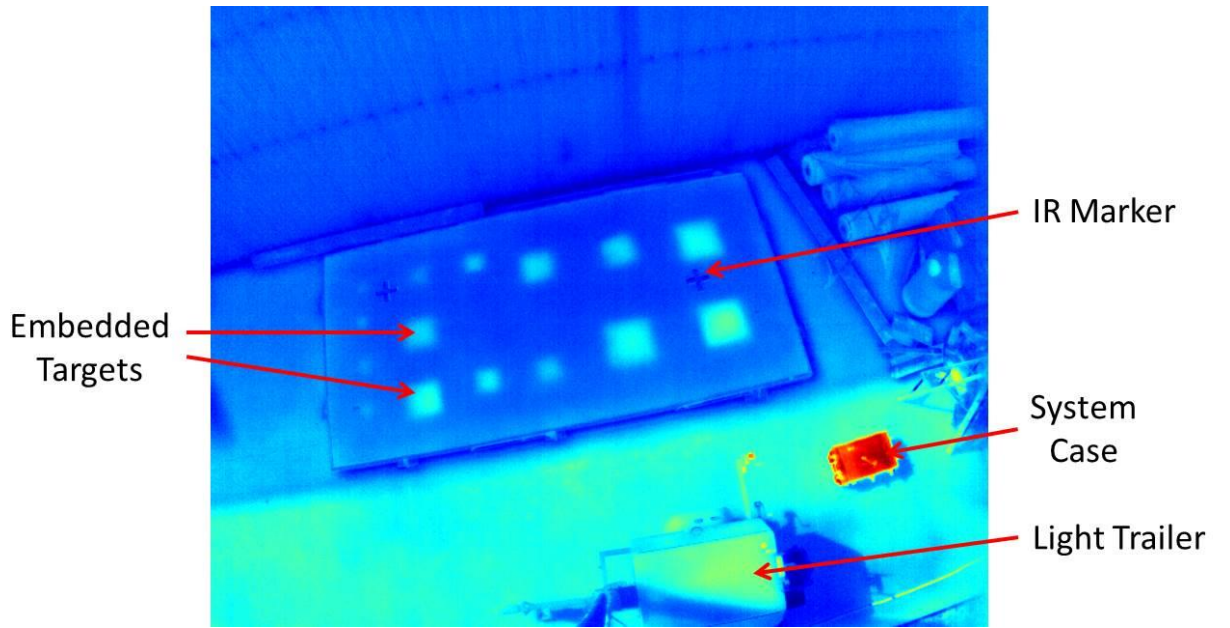


**Figure 5-6: Processed results of IR-UTD test conducted on September 4, 2014**

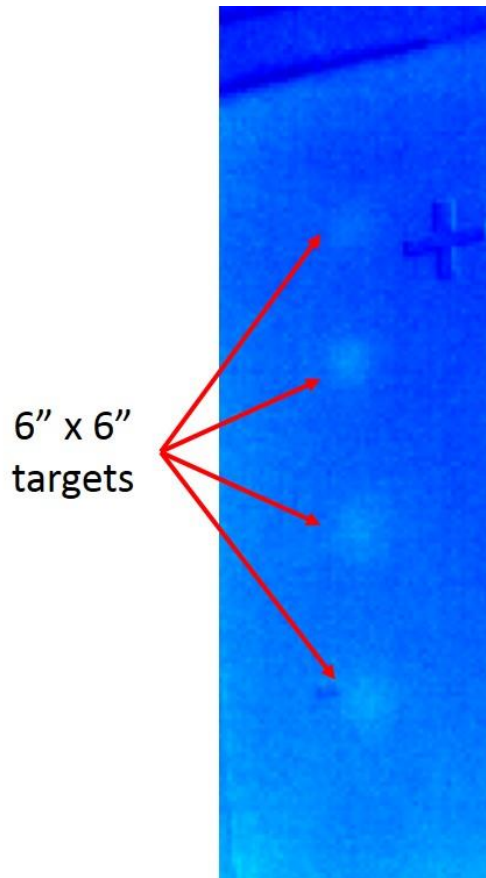


**Figure 5-7: Demonstration of IR-UTD spatial resolution**

## **5.2 Providence Road**

The first field test of the IR-UTD system was performed on a bridge deck on Providence Road over Hinkson Creek in Columbia, MO on May 6, 2014. In addition to the IR-UTD system, hand held verification was conducted (Section 4.2). This bridge was chosen for testing due to its close proximity to the University of Missouri. This was a two lane bridge with a shoulder, 207 feet long, and had an asphalt overlay containing multiple areas of deterioration.

A light trailer was used to house the system, and the camera head was mounted on the trailer's deployable mast. The cable connecting the camera head

to the system was fed through a hole for electrical cords in the front of the trailer. The system was powered with a generator. The trailer was placed at the north end of the bridge on the east side of the roadway. It was placed the afternoon before the test to allow for a faster setup. The location was chosen to achieve an optimum camera angle to the bridge deck. An angle as normal to the bridge deck as possible is optimum to reduce distortion along the edges of an image. The bridge elevation was higher at the south end than at the north end and would have created a flatter angle from the camera head to the deck. No traffic control was necessary for the setup; however, cones were placed near it to make motorists aware of the trailer's location. Figure 5-8 shows an image of the test setup.

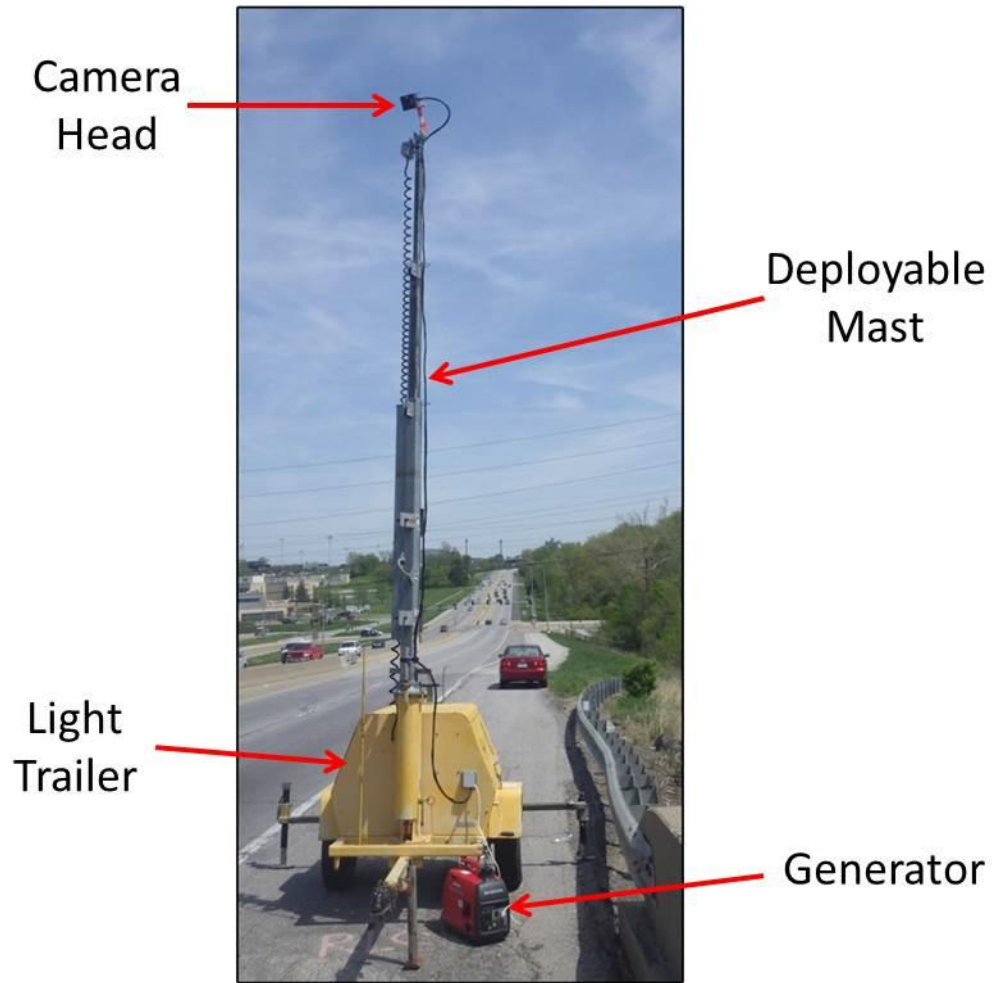


**Figure 5-8: Test setup for IR-UTD test of Providence Road bridge**

The test parameters were set in order to capture images every two and a half minutes from 6:30 A.M. to 9:00 P.M. This testing duration allowed the technology to capture both a heating and cooling trend of the day. Weather conditions for the test included an ambient temperature change of 32°F for the first ten and a half hours and 11°F for the last four hours (Wunderground 2013-2015). Figure 5-9 shows the results of the test. The main areas of concern are those located inside the boxes.

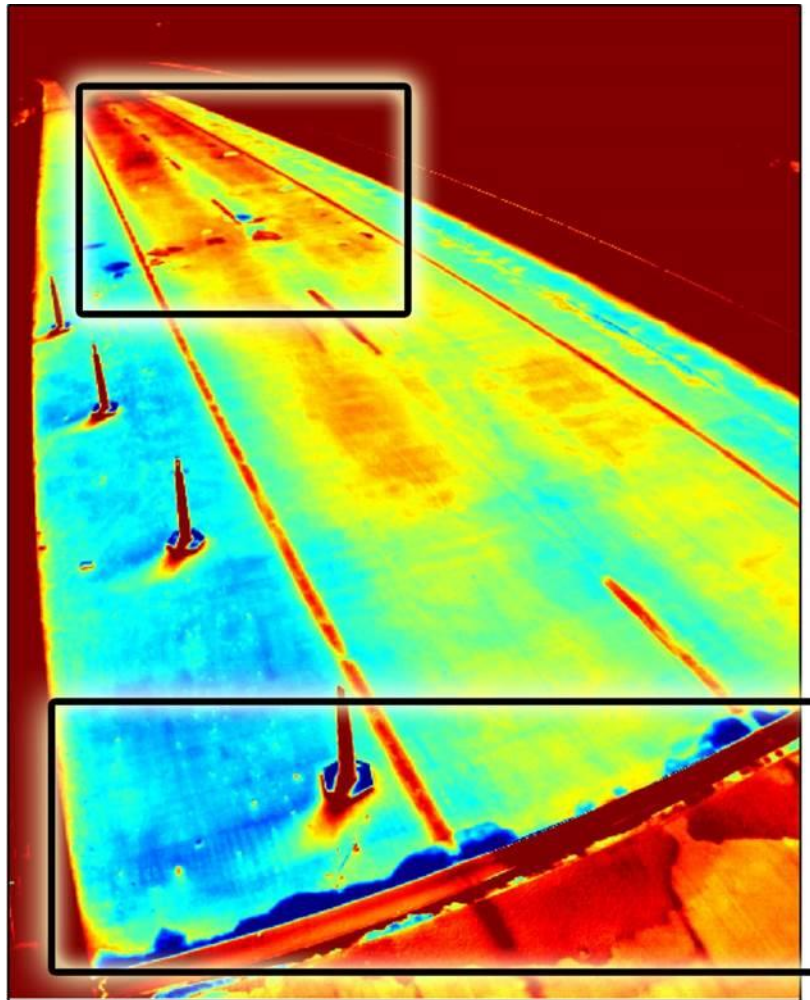


**Figure 5-9: Processed results of Providence Road test conducted on May 6,  
2014**

The area of deck captured in this image is significantly more than those of later tests. However, it is difficult to determine accurately any delaminations on the far side of the image. As a result, a change was made after this test to orient the camera head so that the field of view was more normal to the deck surface.

### **5.3 Kansas City, MO**

The test specimen in Kansas City, MO, as mentioned in the hand held verification section, has been closed to traffic since its construction in 1959. That is an ideal situation because no traffic control is needed during testing or the setup process. The bridge has a concrete deck 212 feet in length and a tapered width ranging from approximately 22 feet at the south end and 40 feet at the north end.

#### **5.3.1 Test One**

Two verification tests were conducted with the IR-UTD system on this bridge. The first test occurred on June 5, 2014. The light trailer that had been used for the Providence Road test was also used for this test. The camera head was mounted so that the infrared and digital lenses were in a horizontal alignment. A similar test setup was utilized including the trailer acting as an enclosure for the system. The system was powered by a generator and deck temperatures were collected with the thermocouple and attached data logger. An image of the test setup is shown in Figure 5-10. The goal of the inspection was to capture infrared data of the previously discussed “open” span of the bridge for comparison to hand held and chain drag results. The hand held and chain drag results are shown in Section 4.2 of this paper.



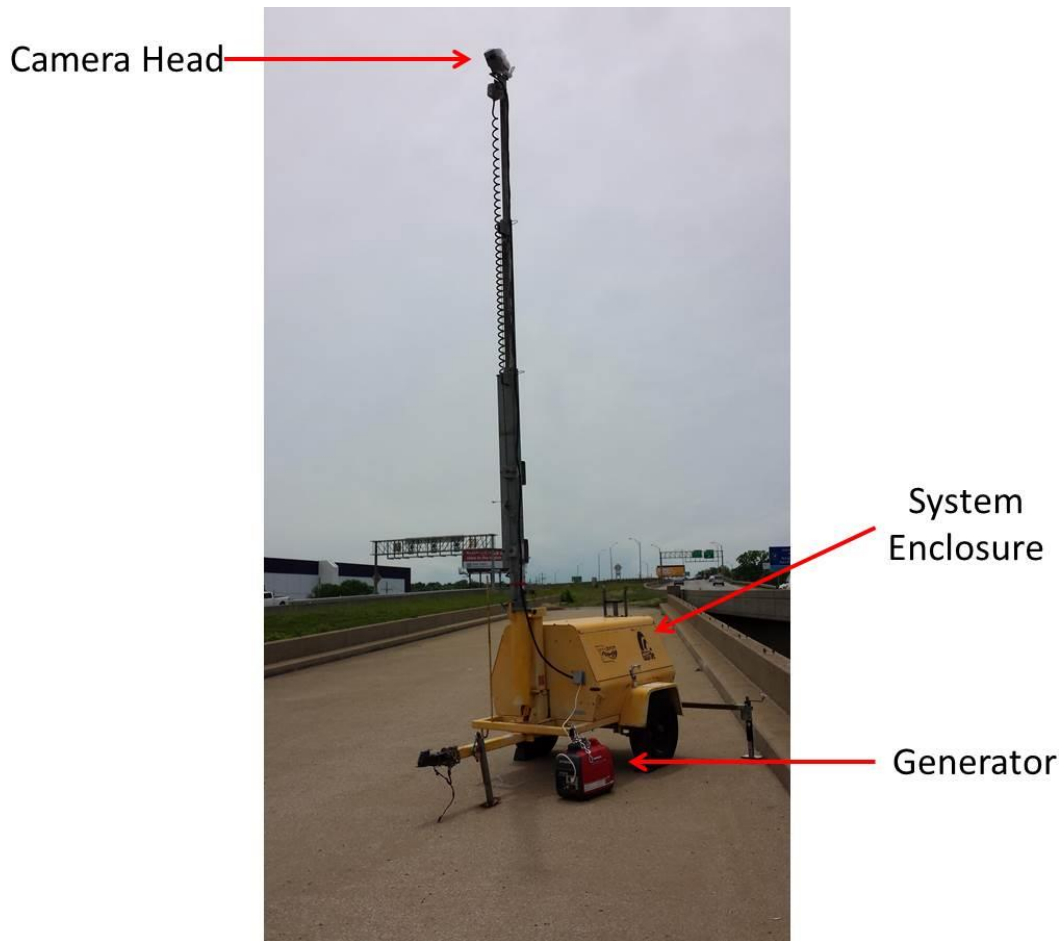


**Figure 5-10: Setup for IR-UTD test in Kansas City**

The parameters of the test were set to capture images every two and a half minutes for a duration of approximately six hours. An image of processed data from the test is shown in Figure 5-11 below. The image captures approximately 75 feet of the bridge deck length.

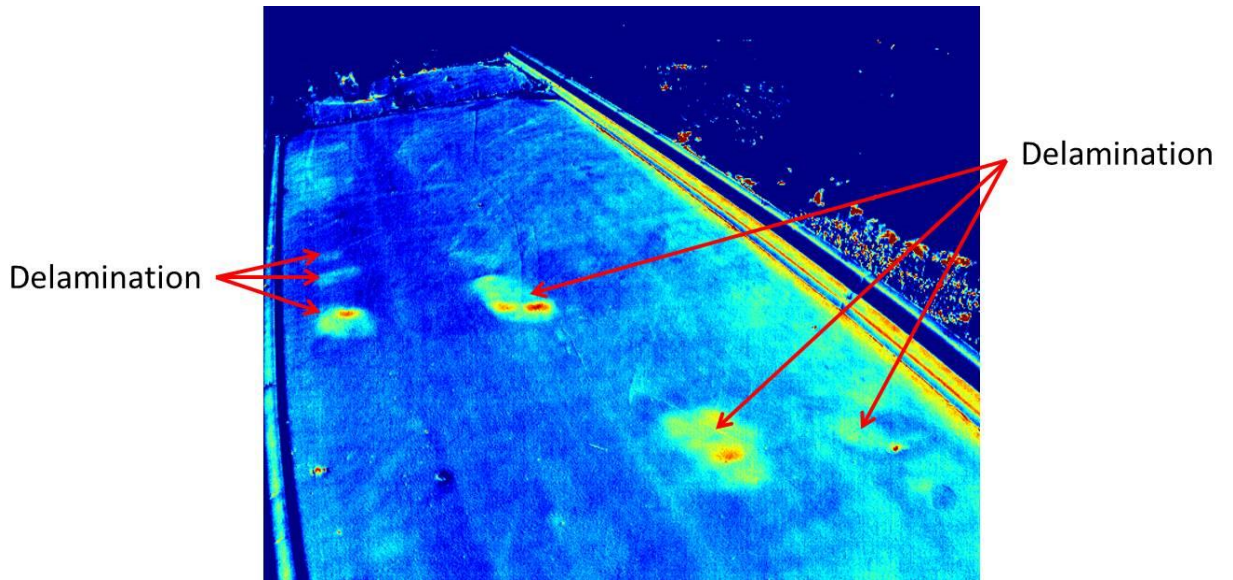


**Figure 5-11: Processed results of IR-UTD test conducted on June 5, 2014**

The weather conditions during the test included an ambient temperature change of 7°F during the first three hours of the test, 3°F during the last three hours, and an average wind speed of 7 mph (Wunderground 2013-2015). Figure 5-12 shows a graph of the deck temperature used for processing.

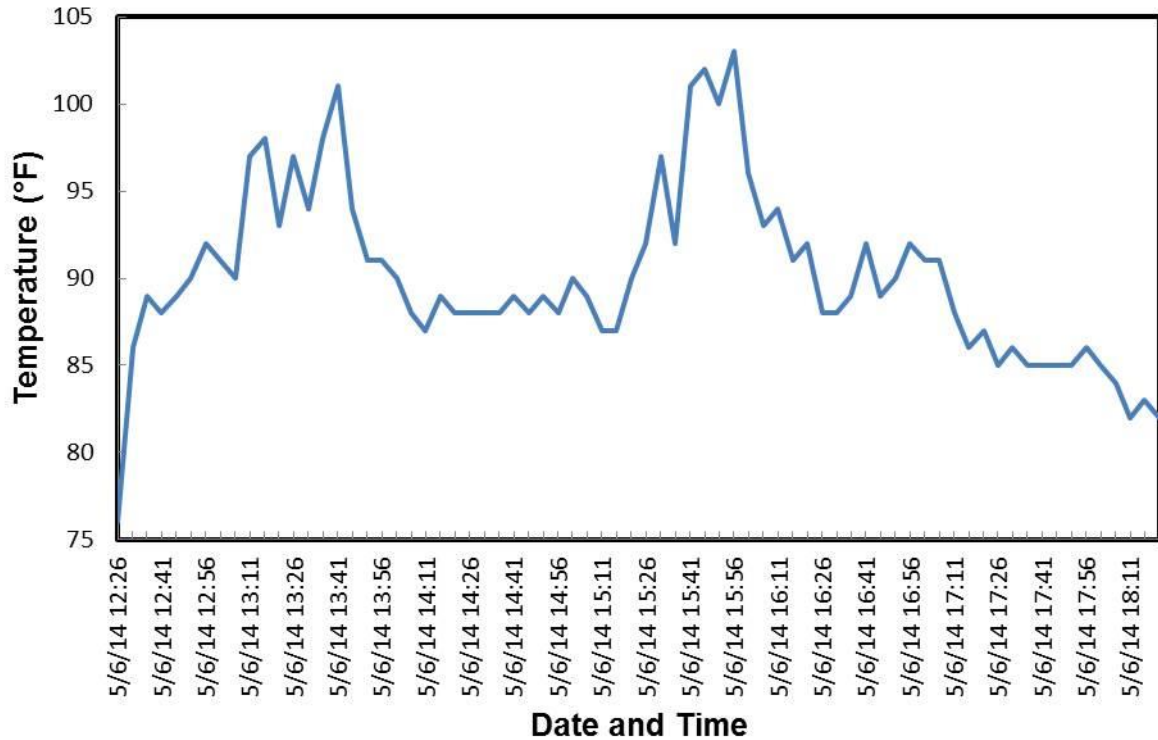


**Figure 5-12: Deck temperature of June 5, 2014 test measured with a data logger and thermocouple**

### 5.3.2 Test Two

A second test was performed on this same Kansas City, MO bridge deck on August 20, 2014. The same setup was used for this test as the one conducted on June 5. A larger area of bridge deck was inspected during this test. The light trailer was used to house the system and mount the camera head. The orientation of the camera head was changed as a result of test one. The camera head was mounted so that the infrared and digital lenses were in a vertical alignment. Figure 5-13 shows the mounted camera head orientation. Aligning the lenses in a vertical orientation allows images of greater length and less width to be captured because

of the lens angles. The objective of the test was to show the reproducibility of results using the IR-UTD system.



**Figure 5-13: Camera head with lenses positioned in a vertical orientation**

The parameters of the test were set to capture images every two and a half minutes for a duration of 12 hours. Figure 5-14 shows a side-by-side comparison of the processed images from the two tests. The image on the left is the result of the June 5<sup>th</sup> test and the image on the right is the result of the August 20<sup>th</sup> test.

The left image was the result of a horizontal camera lens alignment while the image on the right is the result of a vertical lens alignment. It is clear that more of the bridge deck is visible in the image on the right. This shows that using a vertical alignment of the lenses is more useful for testing on narrow bridges (2-3 lanes wide). Edges of the bridge would not be visible if a vertical lens alignment were used on a wider bridge deck. Although the position and alignment of the camera head were different, the same delaminations can be observed in both images. Figure 5-14 shows that the delaminations are also consistent with the chain drag results produced by MoDOT inspectors.

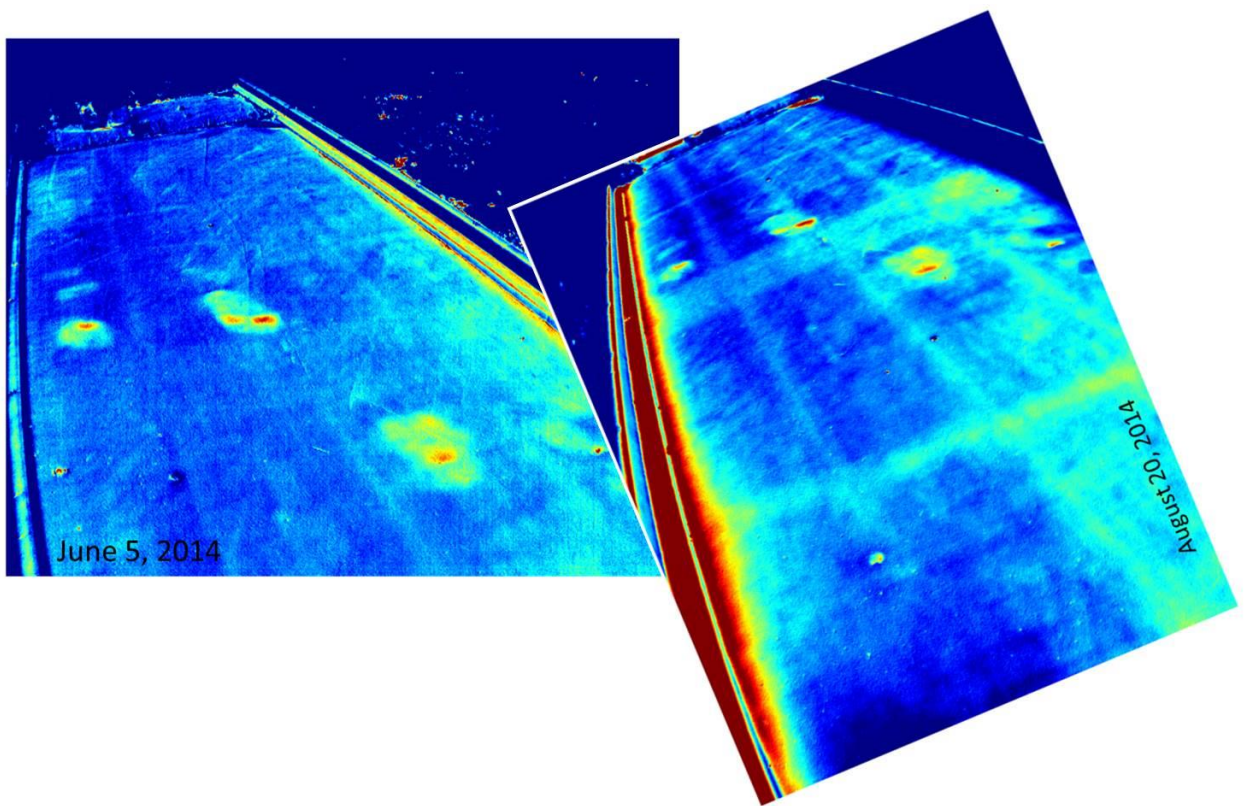


**Figure 5-14: Processed IR-UTD results of the June 5, 2014 (left) and August 20, 2014 (right) tests**

The weather conditions during the test included an ambient temperature change of 19°F during the first ten hours of the test, 4°F during the last two hours and an average wind speed of 11 mph (Wunderground 2013-2015).

#### **5.4 Lamoni, IA**

The Iowa bridge used for IR-UTD testing was the same bridge used for the verification of the hand held infrared camera. The testing was performed in Lamoni, IA on highway 69 over I-35. This bridge was chosen for testing because it was scheduled to have epoxy injected into the delaminated areas of the deck. Two tests were performed on the bridge deck. The pretest was completed over the course of 3 hours and the actual test took place over the span of four days. The inspected area was approximately 3200 square feet. Chain dragging was performed by members of Iowa DOT for comparison to the infrared results.

It was determined that a concrete blister, previously used for a light pole, on the outside of the bridge parapet would be the location to mount a hydraulic mast. The camera head was mounted at the top of the mast with a machined aluminum plate and four thumb screws. The mast was raised with a foot pump in four sections using collar locks between each section. A custom steel structure was fabricated to deploy the mast on the concrete blister. The main components of the steel structure included a strong back (1.5" x 1.5" x 1/4" tube) to support the mast, a 1/2" thick base plate with four thru-holes and a welded tube, and perforated tubes. Four 1.25" threaded rods protruding from the blister were used to attach the baseplate. The strong back was mounted on the baseplate by a tube welded to

the baseplate. The mast was connected to the strong back with ¼” plates attached to a mast collar and base. The perforated tubes accomplished two purposes. They were used as lateral supports anchored into the parapet and connected to the mast with angles and they were able to be attached to the strong back with U-bolts to support the IR-UTD system enclosure. Figure 5-15 shows an image of the assembled structure.

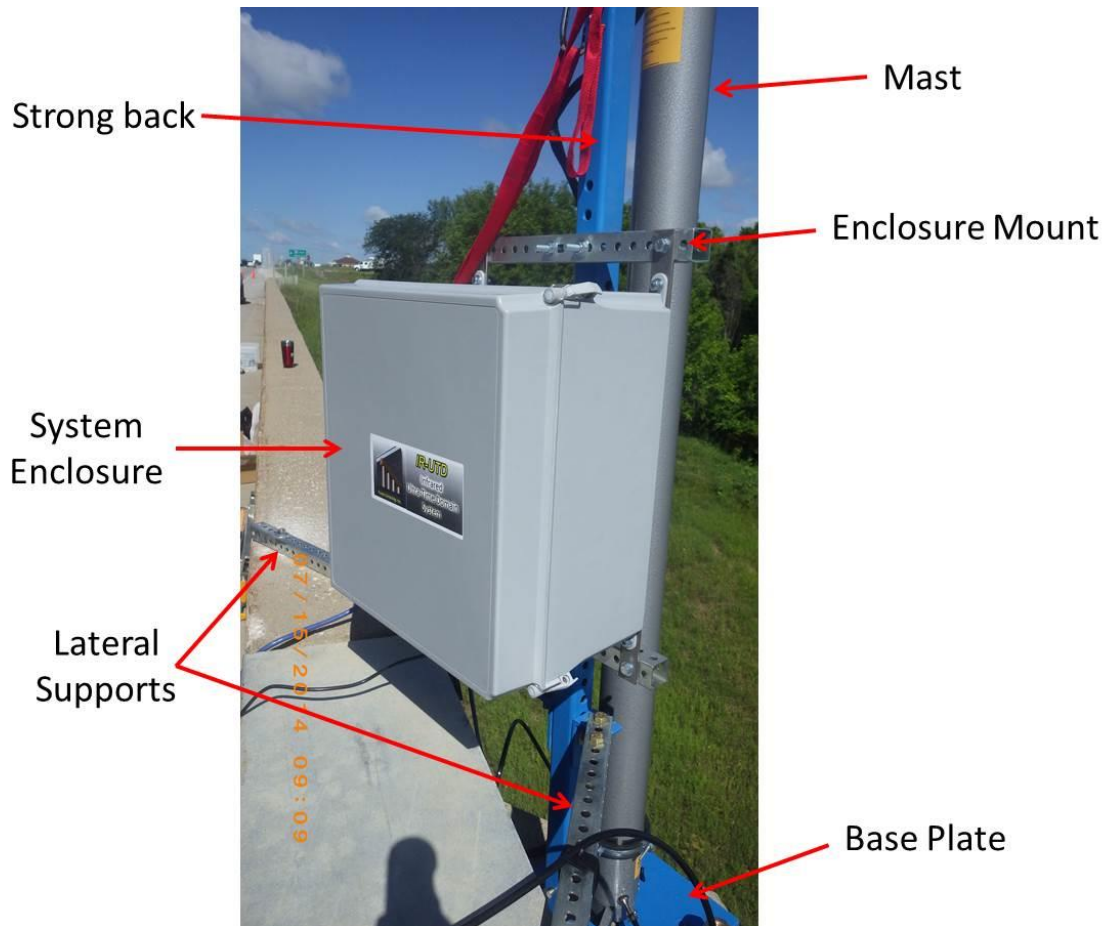


**Figure 5-15: Components of the IR-UTD test setup for Lamoni, IA**

#### **5.4.1 Epoxy Injection Pretest**

The pretest occurred on July 15, 2014. The reason for the pretest was to identify any potential complications that could occur during the full test. The pretest was also performed to ensure that the area of bridge deck to be inspected during the full test had a sufficient amount of delamination.

Iowa DOT members assisted with the test setup upon their arrival at approximately 7:30 A.M. It was discovered that the dimensions of the protruding threaded rods were not the same as the drawings provided by Iowa DOT. Also, the large hole in the center of the plate for clearing electrical connections was not large enough. For those reasons, only one of the four thru-holes in the base plate was used for the pretest. The strong back was then slotted onto the tube welded to the base plate and fastened with hardware. Lateral supports were connected to the strong back and anchored to the parapet. The mast was set into place and fastened in with the accompanying collar. The camera head was mounted to the top of the mast with the previously mentioned aluminum plate. For this test, a series of 80/20 plates were used to connect the camera head to the aluminum plate. The last attachment before deploying the mast was the enclosure for the IR-UTD system. After all parts were in place, the mast was deployed in four separate sections. The first section was unlocked by loosening a knob at its collar. A foot pump was used to deploy the first section. When fully deployed, the first section would then be locked into place with the same knob used to unlock it. A velcro strap was used to secure the cable connecting the camera head and system



to the mast. The second, third, and fourth sections were deployed in the same manner as the first. The figures below show the images of the test setup.

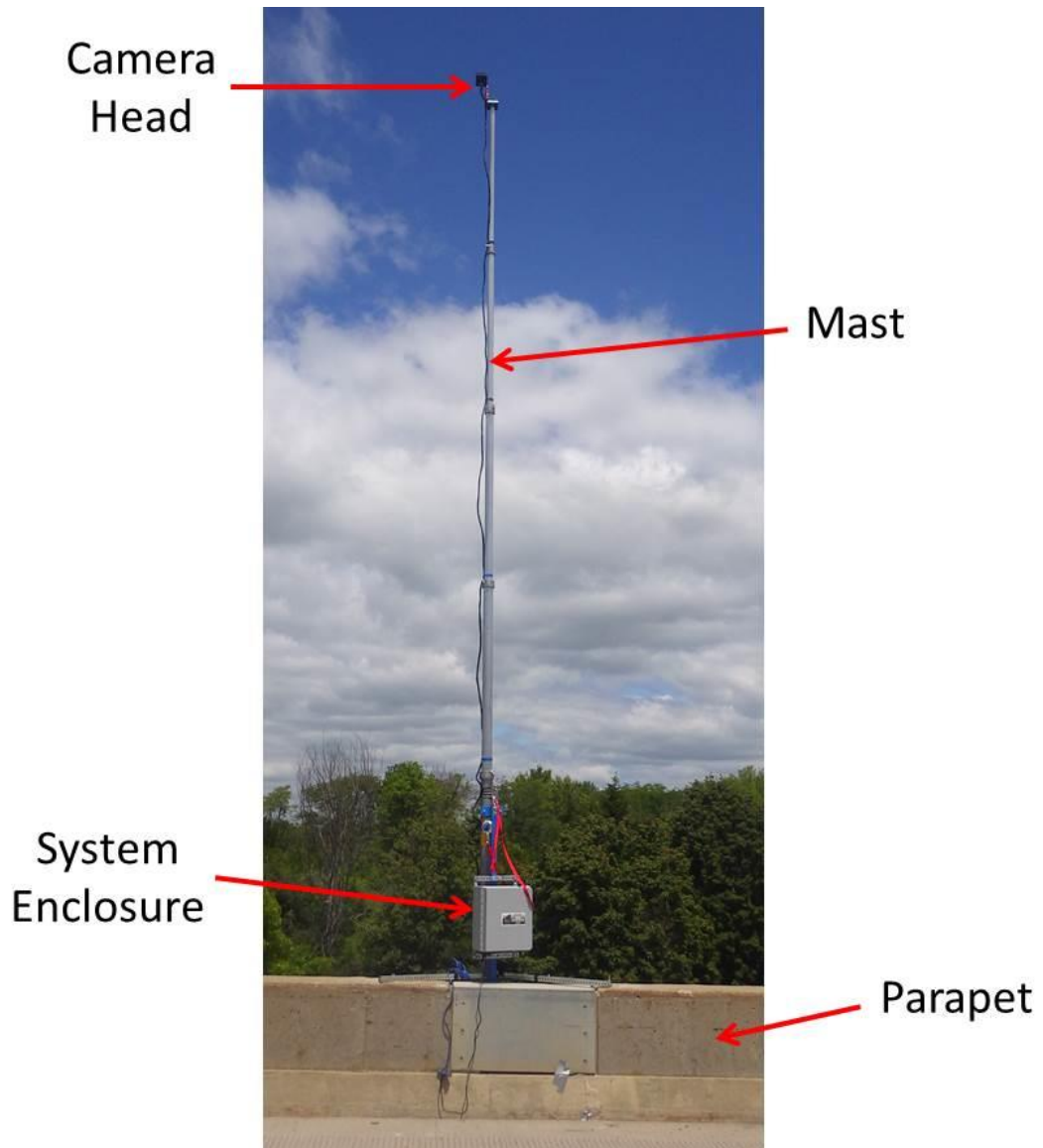


**Figure 5-16: Full view of the Lamoni, IA IR-UTD pretest setup**



**Figure 5-17: Close-up of the plate series used for mounting the camera head**



**Figure 5-18: Generator used to power the IR-UTD system during the pretest**

The IR-UTD system was powered using a generator located at the base of the bridge columns. The reason for this was to keep all components of the test off the bridge deck to allow access for traffic. The parameters of the test were set to capture images every two and a half minutes and for a period of approximately three hours. A thermocouple and accompanying data logger were placed on the deck to collect surface temperatures during the test. Hammer sounding was performed on the deck by Iowa DOT inspectors while the system was capturing images. No viable processed results could be produced due to the fact that a parked truck in the testing area prior to the test. Although the truck was moved for the test, the heat signature remained and affected the results. The results from the chain drag showed that a significant amount of delamination existed in the deck. Therefore, it was determined the deck would be a good candidate for testing. Plans were made to return and conduct a test over four days. The setup was disassembled in a similar manner to its assembly, in reverse order, at the conclusion of testing.

#### **5.4.2 Epoxy Injection Test**

Testing on the previously mentioned bridge in Lamoni, IA was performed over four days from September 8-11, 2014. The deck of the bridge was scheduled to be injected with epoxy at locations where delaminations were detected with hammer sounding. The hammer sounding results would also be used to verify the infrared results. The objective of the test was to capture infrared images before and after the epoxy injection to show its effect on infrared thermography.

There were some improvements made to the pretest setup so as to optimize results. The base plate of the steel structure was machined so that the rods protruding from the blister and the electrical connections would properly fit. A three dimensional pan-and-tilt head was purchased and utilized to mount the camera head at the top of the mast. The new mount allowed for a larger field of view because of its ability to tilt side to side rather than exclusively forward and backward as with the series of plates in the pretest. An aluminum hood was constructed for the camera head to protect it from periods of light rain. The IR-UTD system was powered using a battery connected by weather-proof tubing that was stored in a chest at the base of the columns below the bridge. A battery was a better option for power than a generator due to the length of testing. A router was also stored in the battery chest and connected to the system through the weather-proof tubing. The router allowed for data collection from the system without direct access during testing. Data was collected multiple times to observe results of each portion of testing. All of these changes were integral parts of optimizing the test as much as possible. Figures 5-19 through 5-21 show images of the test setup.

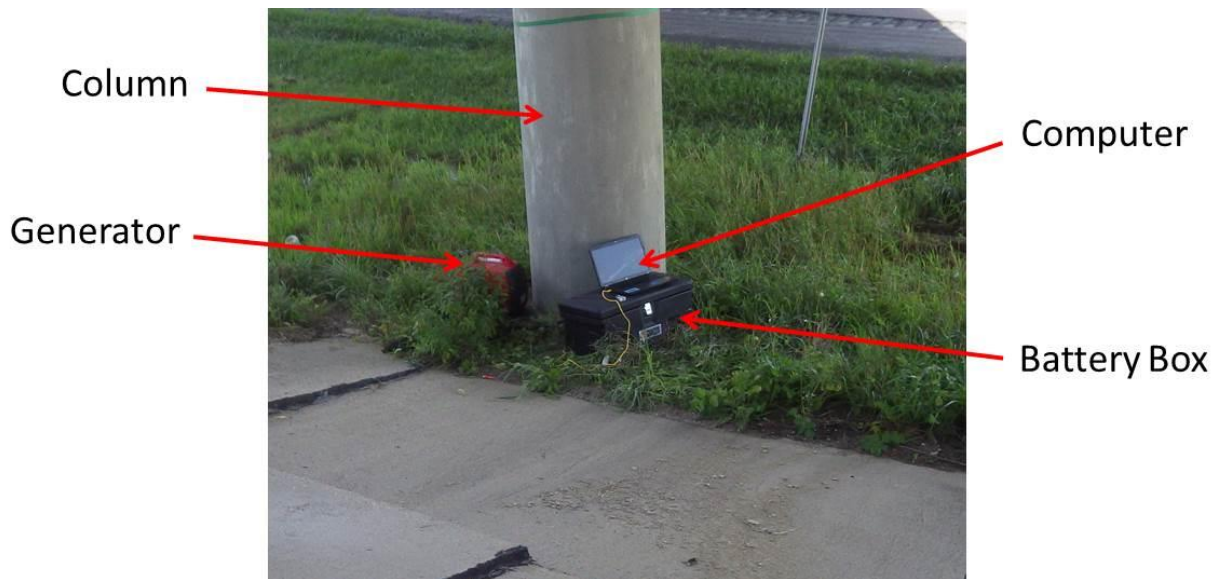


Camera Head  
and Rain Hood

Pan and Tilt  
Mount

Mast

**Figure 5-19: Close up of the pan and tilt mount and rain hood**



Column

Computer

Generator

Battery Box

**Figure 5-20: Battery box used to power the IR-UTD system during the epoxy injection test**

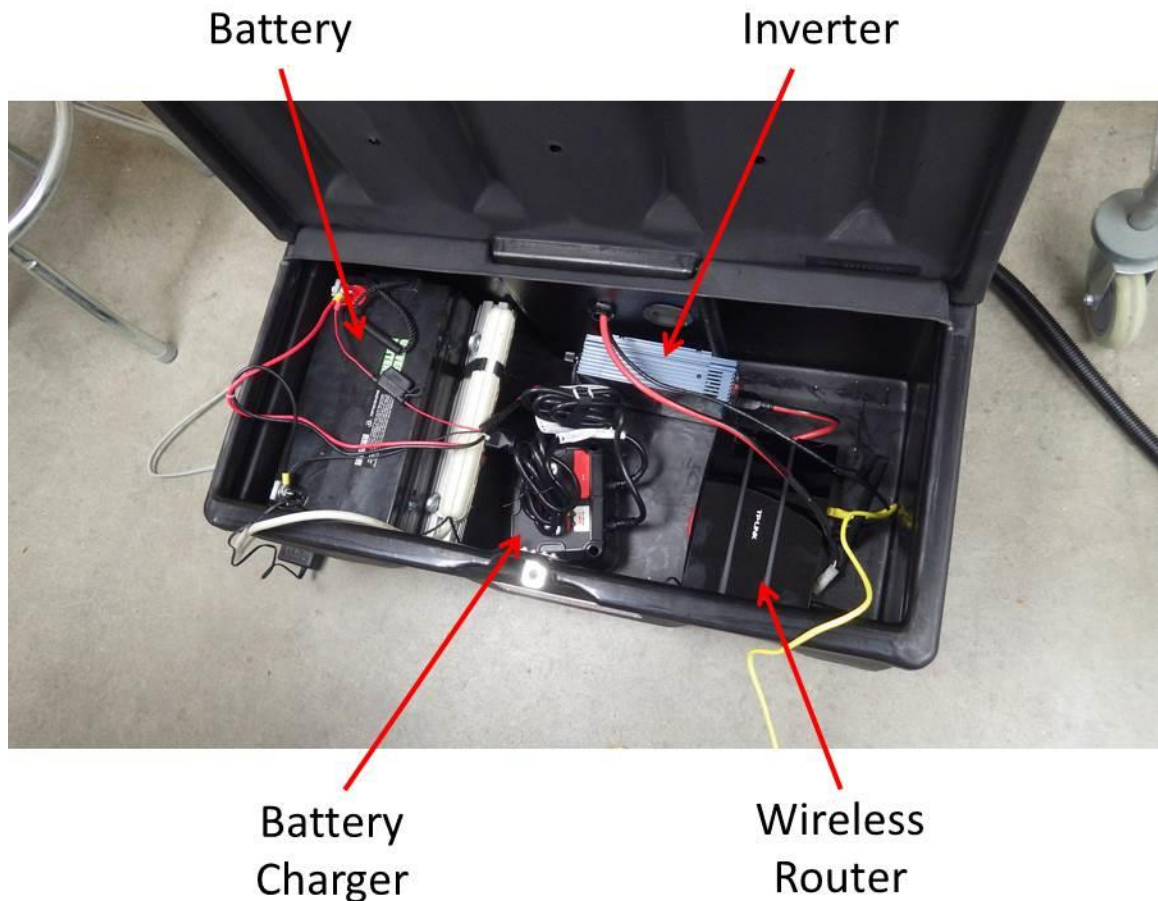


**Figure 5-21: Contents of the battery box**

The first day of testing was September 8<sup>th</sup>. This testing day would be used to gather data before the epoxy injection. Setup of the steel structure and IR-UTD system began upon arrival at the bridge at approximately 8:00 A.M. The setup process was similar to that of the pretest. However, this setup took longer because of multiple deployments of the mast in order to optimize the image field of view on the new pan and tilt head. Spray paint from a previous chain drag result were still visible on the deck to provide an estimate of where some of the delaminations were located. One foot squares of reflective tape were placed every twenty feet along

the length of the deck in both lanes. The squares were used as reference points throughout the testing process. When the optimal camera head orientation was achieved, the parameters of the test were set and the test was initiated. The parameters of the test were set to capture images every two and a half minutes and were collected for 26 hours beginning at 11:56 A.M. Weather conditions for the first day included a maximum ambient temperature change of 24°F and an average wind speed of 9 mph (Wunderground 2013-2015).

Hammer sounding was conducted in the test area by Iowa DOT inspectors on the morning of September 9<sup>th</sup>. The area was prepared for epoxy injection by drilling holes in the deck where delaminations had been located. Prior to initiating the epoxy injections, a borescope was used to determine the depths of delamination specifically at one location. The epoxy was pumped into the delamination until the delamination filled. It took most of the day to fill the delaminations in the accessible test area due to the amount of damage in the bridge deck. A routine check on the system revealed that the rain hood protecting the camera head was slightly interfering with the capture of the infrared image. A grinder was used to reduce the edge of the hood so that it would no longer interfere with the capture of the image. Weather for the day included an ambient temperature change of 6 degrees and an average wind speed of 9 mph (Wunderground 2013-2015). Light rain fell at approximately 2:00 P.M., but the light rain did not interrupt the test because the amount of rainfall was not enough to affect the thermal image of the bridge deck. Due to incoming storms, the testing was stopped and the camera head was taken down at 3:00 P.M. The pan and tilt

head, steel structure, and mast were left in place to allow for further testing with an identical setup and camera orientation. The enclosure for the battery at the base of the columns was moved to higher ground as a precaution.

The camera head was reinstalled and the test resumed on the morning of September 10<sup>th</sup>. The parameters of the test were set to collect images every two and half minutes to stay consistent with previous data. Data was collected throughout the day. While checking the system on the morning of September 11<sup>th</sup>, it was noticed that data had stopped collecting at 7:26 A.M. It was discovered that the battery had not been able to fully charge and ran out of energy during testing. Therefore, the system was powered by the generator for the conclusion of testing. Another set of data was collected from 10:30 A.M. to 1:30 P.M. with images captured at 30 second intervals. These images were collected to gather clearer digital images of the deck and to observe the effect of epoxy on the delaminated areas. At the completion of testing, the setup was broken down in reverse order of its assembly. Figures 5-22 and 5-23 show an image of the results and deck temperature data, including corresponding chain drag results.



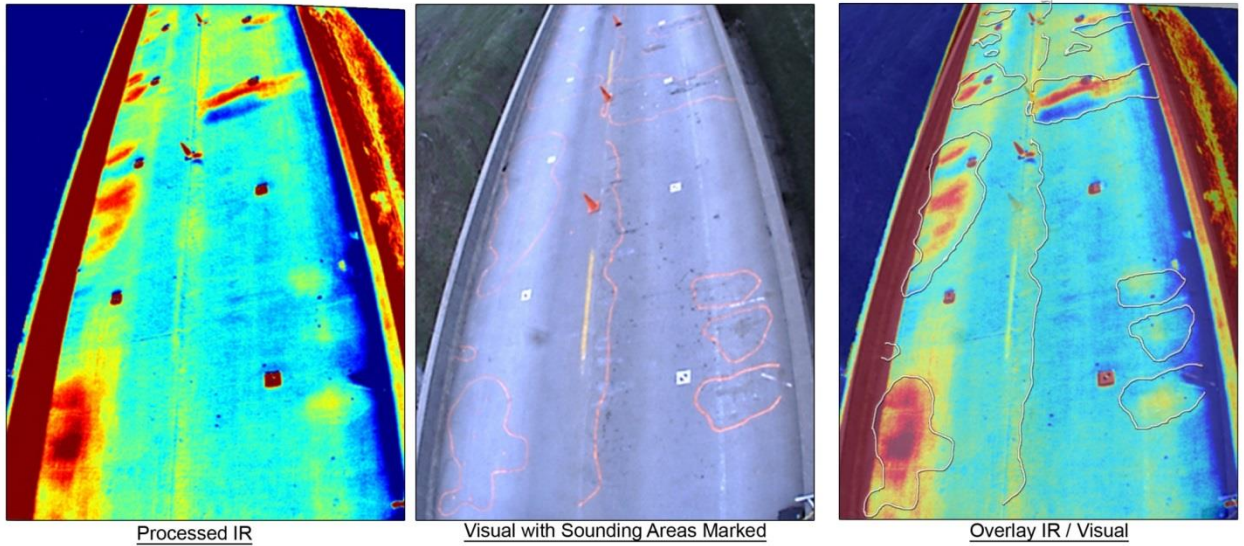


**Figure 5-22: Processed IR-UTD results (left), hammer sounding results (middle) and overlay of the two (right) of the epoxy injection test**

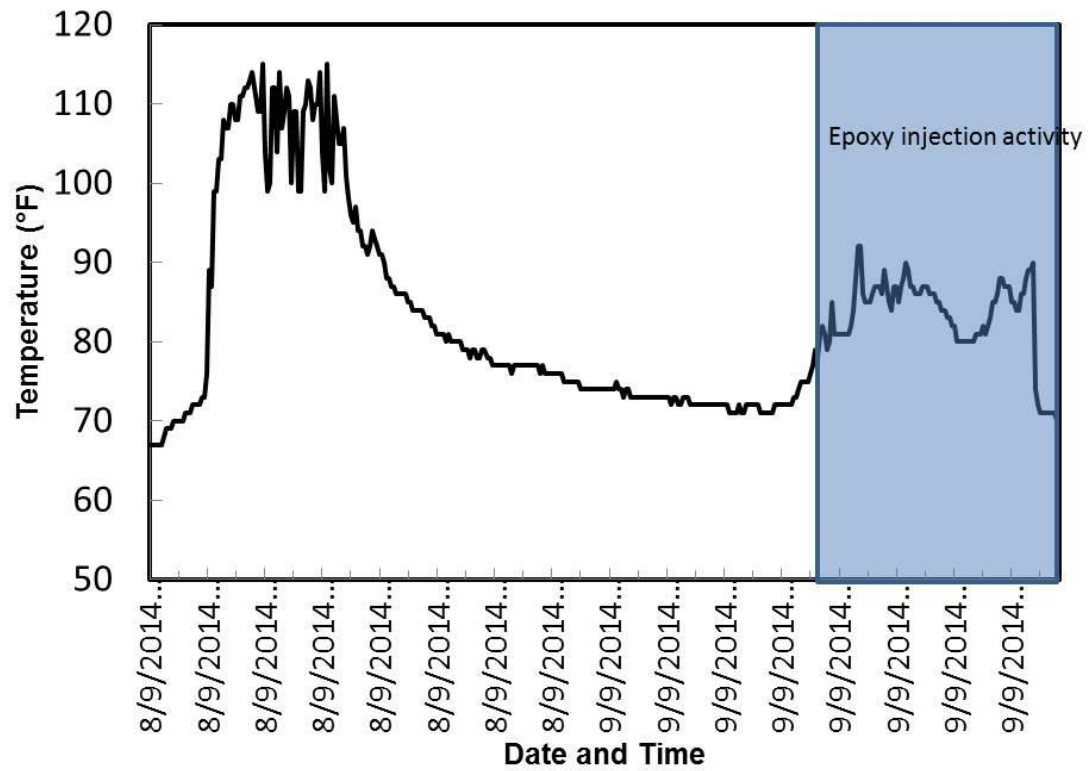


**Figure 5-23: Deck temperatures of the first two days of the epoxy injection test**

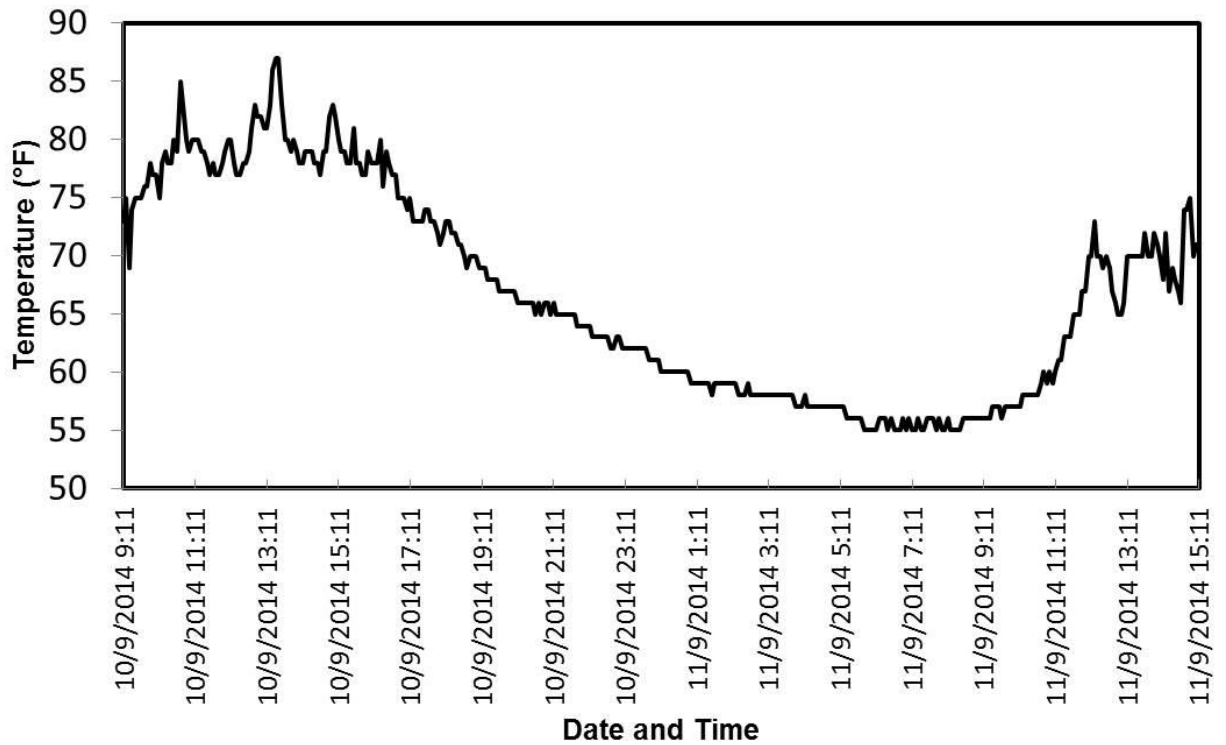


**Figure 5-24: Deck temperatures of the last two days of the epoxy injection test**

The accuracy of the technology is clear. The image showing the overlay of the IR and hammer sounding results depicts how well the results of each inspection coincide. Delaminated areas in the IR image can also be determined to be relatively deep or shallow. Determining relative depth of delamination will be further discussed in the analysis portion of this paper.

### 5.5 University of Missouri-Columbia Columns

The columns located on Francis Quadrangle at the University of Missouri-Columbia are the traditional symbol for the university. The columns were once a part of Academic Hall on the university campus. A fire destroyed Academic Hall

on January 9, 1892, and the columns were the only thing left standing (UMC 2015). However, the fire caused damage to the south face of the limestone columns. Infrared testing was performed on both faces of the columns to detect the extent and location of the damage.

### **5.5.1 South Face**

Testing on the south faces of the columns was conducted on December 12, 2014. The camera head did not need to be elevated for this test, so it was mounted on a tripod with the same pan and tilt head used for the IOWA epoxy injection test. The system was enclosed in the same case used for mounting on the steel structure during the IOWA tests. It was powered by a generator. The enclosure and generator were located at the base of the tripod. The setup was located approximately 75 feet from the faces of the columns to provide an optimum field of view. Figure 5-25 shows an image of the setup.



**Figure 5-25: Test Setup for the Columns test on the south face**

Parameters of the test were set to capture images every minute from its initiation at 9:25 A.M. to conclusion of the testing at 4:21 P.M. An image of the results is shown in Figure 5-26 below. Weather for the duration of the test included an ambient temperature change of 13°F for the first five hours, 2°F for the last two hours, and an average wind speed of 6 mph (Wunderground 2013-2015).

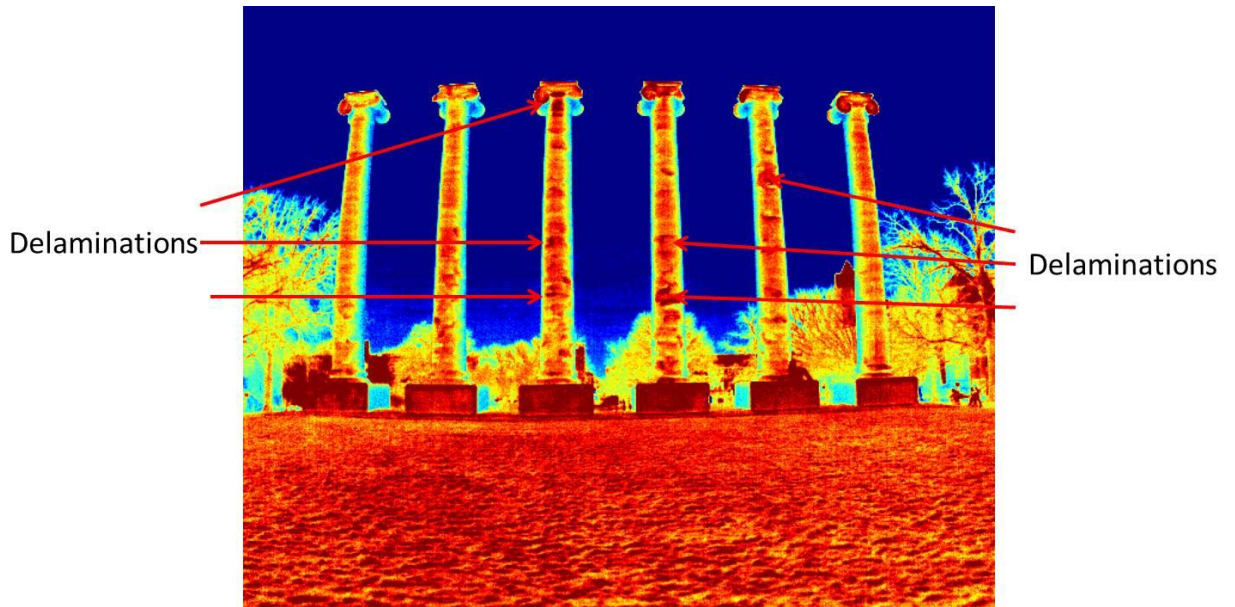


**Figure 5-26: Processed results of the IR-UTD test on the south face of the Mizzou columns**

Many areas on the south face of the columns were determined to be delaminated. Some of the heavily delaminated areas are indicated by arrows in the image above. There are more delaminated areas in the interior columns than the exterior columns; this was expected since the interior columns were exposed to a higher intensity of fire and the interior columns were located directly in front of the building center.

### **5.5.2 North Face**

A similar test of the south face was performed on the north face of the columns. The setup was approximately 75 feet from the faces of the columns. A tripod was used to mount the camera head and the same enclosure as the south face test was used to protect the system. The only difference between the north

and south face testing was that the system for the north face test was powered with the battery used during the Iowa tests.

Parameters of the test were set to capture images every minute from 9:07 A.M. to 4:30 P.M. An image of the results is shown in Figure 5-27 below. Weather for the duration of the test included an ambient temperature change of 8°F for the first five and a half hours, 1°F for the last two hours, and an average wind speed of 5 mph (Wunderground 2013-2015).

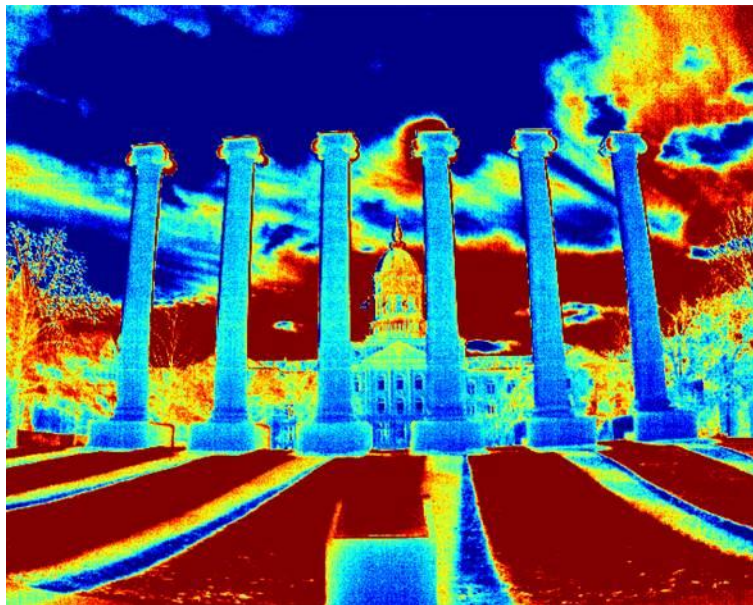


**Figure 5-27: Processed results of the IR-UTD test on the north face of the Mizzou columns**

No delaminated areas were detected on the north face of the columns, contrary to the delaminated areas detected on the south face. This result was expected due to the fact it was not exposed to fire. The image seems to be skewed a small amount. This is apparent with distinct difference along the left and right edges of the columns. It is assumed that the camera head may have been moved

slightly after the initiation of the test. Post-processing measures the change in infrared radiation of the pixel array. Moving the camera head resulted in pixels occupying different areas than they had previous to the movement. For that reason, the camera head should be kept stationary during testing.

## **5.6 West Boulevard**

A bridge located on I-70 over West Boulevard in Columbia, MO was tested utilizing the IR-UTD system on January 16, 2015. The bridge was selected because of its close proximity to the University of Missouri campus. The equipment could be transported to the site, set up, taken down, and returned to campus in the same day while still allowing for a full data set to be captured. All of the previous tests had been performed on bridge decks exposed to solar loading. The purpose of this test was to collect data and determine how effectively the IR-UTD system can perform when imaging bridge components without exposure to solar loading.

The test was set up upon arrival to the bridge at 8:00 A.M. The test setup was very similar to the one ran on the north face of the columns as described in Section 5.5.2. The camera head was mounted on a tripod and lowered as close to the ground as possible. It was mounted low to the ground to capture as much of the bridge soffit as possible. Figure 5-28 shows an image of the test setup.



**Figure 5-28: Setup for West Blvd. under I-70 in Columbia, MO**

Parameters of the test were set to capture images every minute from initiation at 8:55 A.M. to 4:31 P.M. Figure 5-29 shows an image of the results. Weather for the duration of the test included an ambient temperature change of 27°F during the first six hours, 7°F during the final two hours, and an average wind speed of 9 mph (Wunderground 2013-2015).



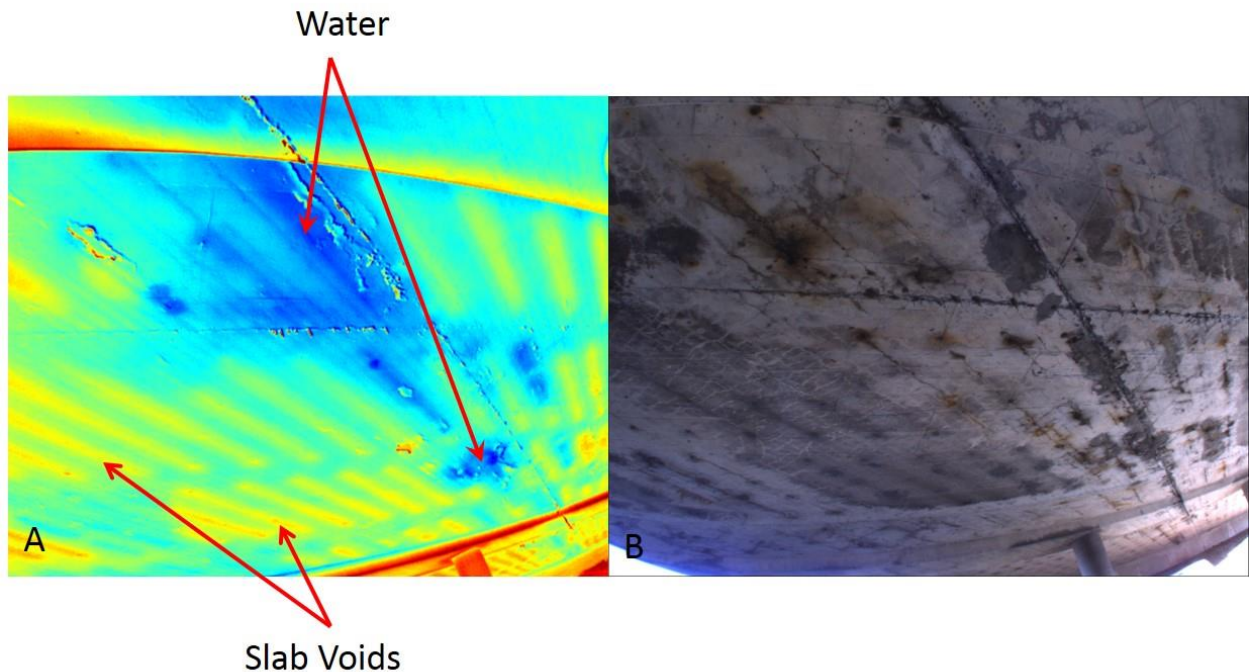


**Figure 5-29: Result for West Blvd. soffit test**

The slab voids are apparent in the processed results in image A. The slab voids heat up faster than the concrete around them because they act as an air void. However, the area in the center of the image appears to heat up at a slower rate than the sound concrete. Delaminations were expected to appear at higher rates of change of infrared radiation than the slab voids. Therefore, it was determined that the large, cool area in the center of the image was likely water from rain on a previous day.

## 6 ANALYSIS

Two systems were used for verification of infrared technology as a bridge inspection. Verification trips using the hand held camera were used to validate the thermographic inspection guidelines developed in Phase I of the project. Quantification of infrared data is currently being explored using the UTD system. Early results have shown that this technology can approximate areas and determine relative depth of delamination. This section will cover the success rate of verification trips utilizing the hand held camera, comparisons of images between the hand held camera and UTD system, the ability of the UTD system to quantify results, and the test repeatability of the UTD system.

Verification and training trips were considered successful if delaminations were detected with the hand held infrared camera. The inspection guidelines state that an ambient temperature change of at least 15°F should occur during the day, a temperature change of at least 10°F should occur in the first six hours of sunrise, and wind speeds should not exceed 15 mph. Table 6-1 shows a comparison of environmental conditions during testing to conditions deemed conducive by the inspection guidelines.

**Table 6-1: Environmental conditions for training and verification testing**

<b>Inspection</b>	<b>Ambient Temperature Change (°F)</b>	<b>Amb. Temp. change in first 6 hours (°F)</b>	<b>Wind Speed (mph)</b>	<b>Guidelines Met? Y/N</b>
Ohio Training	11	8	6	No
Kentucky Training	10	8	5	No
Florida Training	16	13	9	Yes
KC Verification	37	28	14	Yes
Providence Rd. Ver.	33	23	13	Yes
Iowa Verification	24	21	9	Yes
Georgia Verification (2012)	6	4	4	No
Georgia Verification (2014)	21	18	3	Yes
Pennsylvania Verification	24	15	3	Yes
Texas Verification	15	9	16	No
Oregon Verification	27	14	5	Yes
Kentucky Verification	21	16	7	Yes
New York Verification	17	16	3	Yes
Ohio Verification	26	20	6	Yes

Testing was successful in all cases where environmental conditions met the requirements of the inspection guidelines and in two cases when they were not. The two successful cases where environmental conditions did not meet the inspection guidelines were the training inspections for Ohio and Kentucky. Although environmental conditions for those inspections did not meet the guidelines, delaminations were still detected. Therefore, it was determined that the guidelines were conservative.

Data was collected with both the hand held camera and IR-UTD system on multiple occasions. Both systems have advantages, but the UTD system is able

to detect delamination under environmental conditions that may not be conducive to testing with the hand held camera. The UTD system is also able to detect more subtle thermal contrasts, which allows for the detection of deeper defects. Images using both systems were captured of the test block utilized for collecting data in Phase I of the project. The embedded targets are at depths of 1 in. (top right), 2 in. (bottom left), 3 in. (bottom right), and 5 in. (top right). A comparison of the two instruments is shown in Figure 6-1. Image A was captured with the hand held and image B is the result of post-processing with the UTD system.

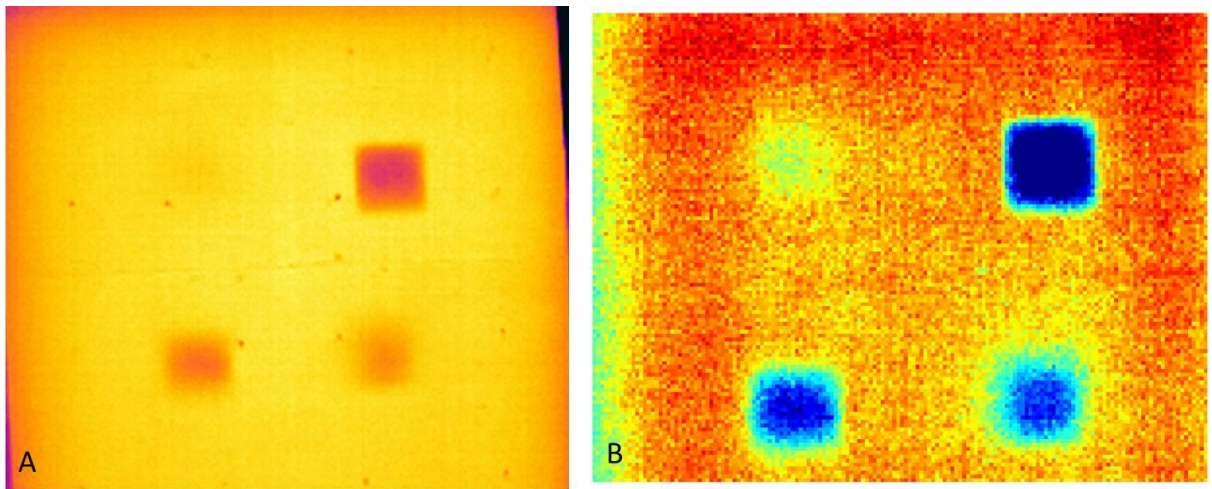


**Figure 6-1: Hand held (A) and IR-UTD (B) results of the Phase I test block**

The environmental conditions were conducive to thermographic testing in both situations. The 5 inch deep target is barely visible in the hand held image and would have a high probability of going undetected. The same target is more readily apparent in the processed image, which demonstrates the increased capability of the UTD technology.

A disadvantage of the hand held infrared camera is its inability to produce quantifiable results. It is unable to detect the total area and depth of delamination during a typical inspection and it is usually accompanied by either chain dragging or hammer sounding for verification. The IR-UTD system was developed to better address the quantification barrier of infrared bridge inspection.

Delaminated areas can be approximately calculated using post processing methods. This is done by determining the number of pixels a delaminated area occupies in an image. The infrared lens of the IR-UTD camera head contains an array of 640 x 512 pixels. The percentage of delamination in a test specimen can be determined using pixel areas. Typically, the field of view of the infrared image extends beyond the edges of the test area. The approximate number of pixels occupying the test area can be found using the post-processing capabilities of the technology. The same method can be used to determine the number of pixels each delamination occupies. The percentage of delaminated area can then be calculated using Equation 6-1.

$$\frac{\text{\# of delaminated pixels}}{\text{\# of test specimen pixels}} \times 100 = \text{percentage of delamination}$$

**Equation 6-1**

An image used for calculating the total delaminated area is shown in Figure 6-2 below.

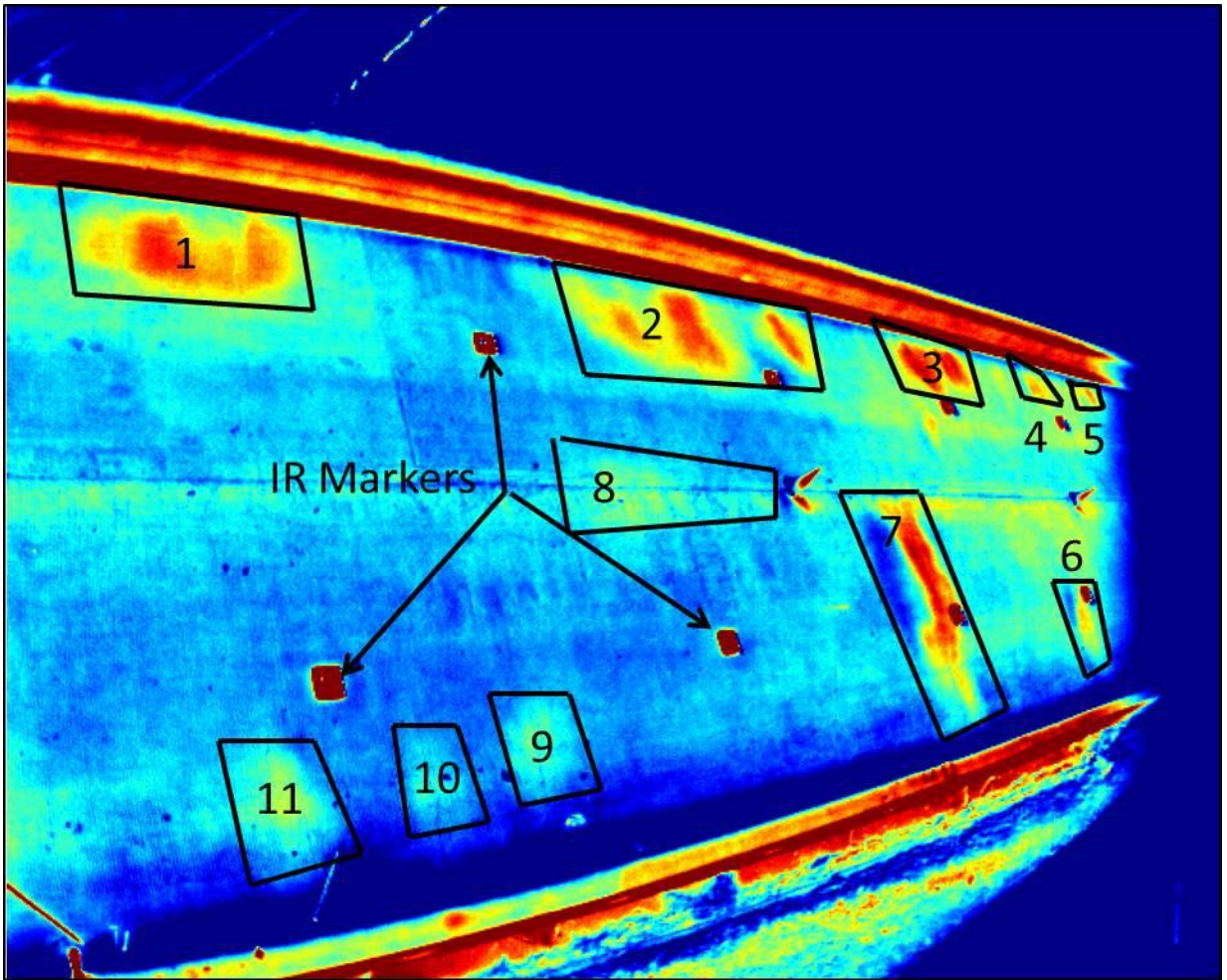


**Figure 6-2: Areas used to calculate total delamination of the Lamoni, IA bridge deck**

The processed image showed areas that appeared to be delaminated; these areas were estimated by the number of pixels they occupied. The approximate area of the deck was found using the same method. The number of pixels occupied by each delamination from Figure 6-2 are shown in Table 6-2.

**Table 6-2: Number of pixels from areas marked in Figure 6-2**

<b>Area</b>	<b>Number of Pixels Occupied</b>
1	6,043
2	5,880
3	1,187
4	329
5	147
6	790
7	4,825
8	4,501
9	2,140
10	1,424
11	2,020
Total Delaminated	29,286
Testing Area	173,190

Delaminations located closer to the camera head will occupy more pixels than a delamination of the same size farther away. The reason for this is because pixels imaging an area farther away cover a greater area based on field of view. There is also some edge distortion, but because relative areas are being figured, it is not a concern. Using Equation 6-1, the percentage of delaminated concrete in the testing field of view is 16.91%.

The depth of delamination is also a point of interest when conducting bridge inspections. If an overlay exists, evaluating the depth of delamination is important to know whether it exists between the overlay and concrete or in the concrete at the level of steel reinforcement. The IR-UTD system is able to determine the relative depth of delamination. Areas of shallow delamination will show up

differently in a processed image than those that are deeper. Although exact depth is not determined in the processed images, engineers typically have plans that provide information about overlay thickness and depth of reinforcement when inspecting a bridge. This information, along with processed data from an infrared test, allows inspectors to determine approximate depths the delaminations occur. A processed image of the Lamoni, IA bridge deck is shown in Figure 6-3 as an example.



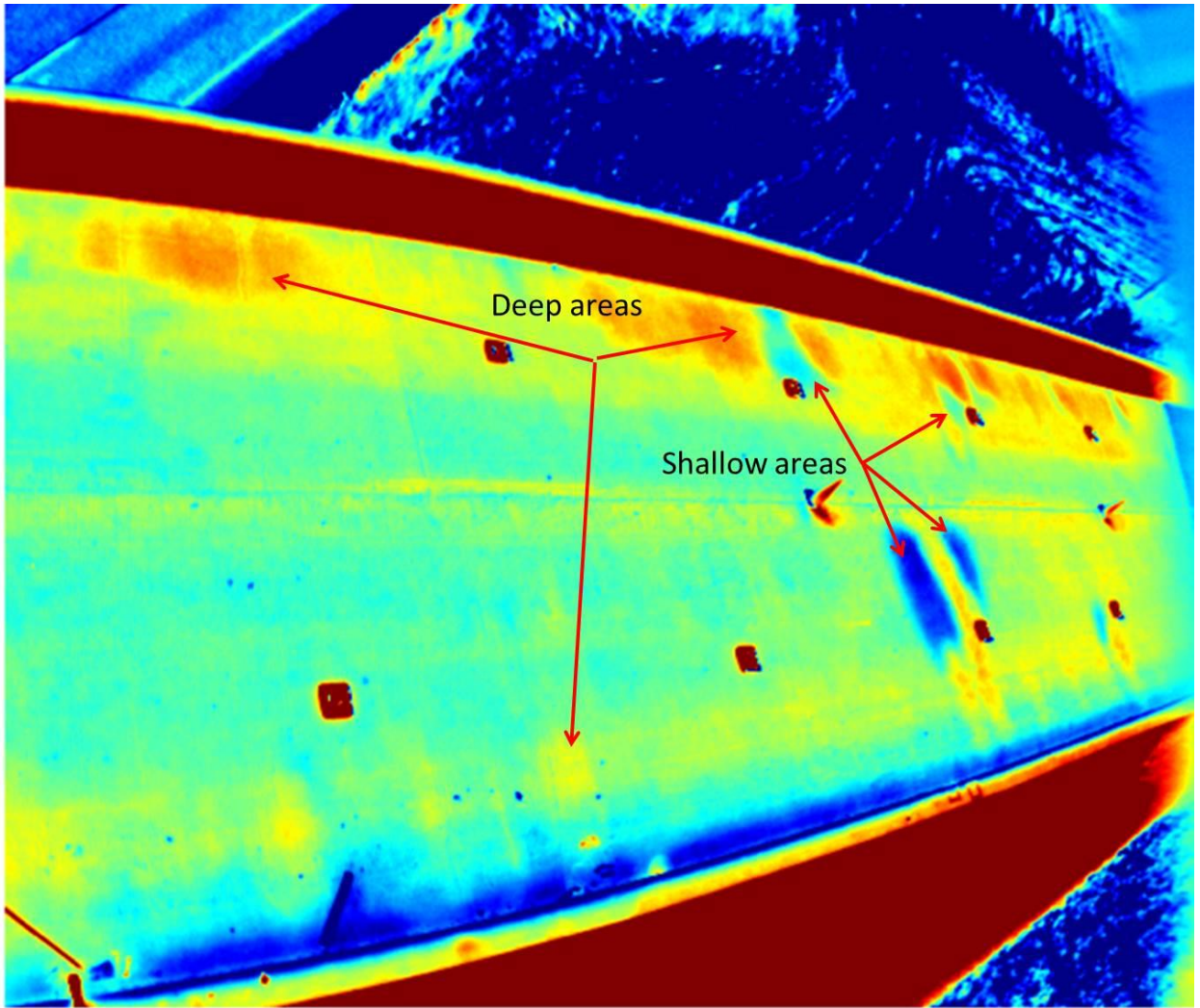


**Figure 6-3: Processed image of Lamoni, IA bridge deck showing relative depths of delamination**

The image above is a result of testing that included both a heating and cooling trend. Many images are produced from the data when processing is completed, but some contain better results than others. The best result produced depends on the heating cycle surrounding the test and the color scale set during post-processing. The best results for determining relative depth of delamination are achieved when testing experiences both heating and cooling cycles. This is

because when both cycles occur during a testing situation, shallow and deep areas of delamination behave differently relative to thermal conductivity. In relation to the sound concrete in surrounding areas, areas of shallow delamination appear to be cool and deeper areas appear to be warmer. The color scale is set based on the area being tested. Utilizing a color scale that includes the entire image could skew results due to objects with different emissivity values than concrete.

Another advantage of the IR-UTD system is the ability to achieve repeatable test results. Reliable, repeatable test results are important is because this information can be used to determine how much a delamination may have grown over an interval of time. This would benefit a DOT that is in the process of making a decision to replace a bridge deck. They would be able to conduct multiple tests over an extended period of time to monitor delamination propagation. This would allow for an accurate determination of when the deck should be replaced. Testing to monitor has not been utilized at this time, but repeat test results were performed on the Kansas City bridge in chapter 5.

## 7 IMPLEMENTATION

One goal of the project was to identify implementation barriers for infrared technology as a bridge inspection tool. Surveys were given to participating states early in the project to determine inspectors' perceptions on what would provide the largest barrier for implementation. The results of the survey included two major points of concern - staff time constraints and difficulty using the technology (Washer 2014).

Phone surveys were conducted from November 2013 through 2014 to determine possible implementation barriers after the participating states had been given time to utilize the technology further. Questions asked in the survey included the following:

1. How often are the cameras used? (weekly, monthly, semi-annually?)
2. Are the cameras used by multiple inspectors? Are those inspectors in a single organizational unit or distributed across different units?
3. When are the cameras most often used? (month, time of year)
4. Where are camera images stored?
5. What other destructive or nondestructive evaluation systems are used in conjunction with IR cameras?
6. Which bridge elements are being imaged most commonly?

Overall, the phone interviews provided positive feedback in relation to what the states viewed as possible implementation barriers. One finding was that participants did not find the technology difficult to use as was perceived early in

the project. The major concerns that participants of the project encountered were lack of staff time, as predicted during the initial surveying, and weather dependency. Weather conditions may not allow for detection of deep delaminations (3-4 inches) in bridge decks. This was identified as a problem in some states where concrete overlays are utilized.

Another concern identified by participants was the inability of the hand held infrared camera to determine depth and area of a delamination. States would want to know this information to know when replacing a bridge deck would be feasible. Quantification of a delamination is difficult without conducting further investigation. Steps are being made towards developing infrared technology that is easily quantifiable utilizing multiple infrared images over time and post-processing methods.

## 8 CONCLUSIONS

### 8.1 Results

The objectives of this research are to: field test and validate inspection guidelines for the application of thermal imaging for bridge inspection, quantify the capability and reliability of thermal imaging technology in the field, and identify implementation barriers faced by inspectors in the field.

Training and verification inspections were determined to be successful if delaminations in concrete could be detected with the hand held infrared camera. The environmental conditions surrounding each inspection are provided in Table 6-1.

When guidelines were met for hand held inspection:

- 1/1 training trips were successful
- 9/9 verification opportunities were successful
  - Delaminations were detected in substructures in two cases where environmental conditions were not conducive to deck inspection.

When guidelines were not met for hand held inspection:

- 2/2 training opportunities were successful
- 0/2 verification opportunities were successful

Although environmental conditions for two of the training trips did not meet the inspection guidelines, the trips were successful. For that reason, it was determined that the inspection guidelines are conservative.

An analysis was performed between infrared imaging and hammer sounding to compare detection area of damaged concrete. The results of the analysis showed that hammer sounding results in larger area of detection by approximately 9%. This is due to the fact that inspectors are conservative when marking hammer sounding results to avoid repairing a smaller area of concrete than is necessary.

Infrared can be used effectively as a bridge inspection tool. Its greatest advantage is the ability to scan large areas in a short time period with no disruption to traffic. It is, however, environmentally dependent and conditions must be favorable for successful inspections. Conducive conditions for inspection include sufficient ambient temperature change, low wind speeds during the deck inspections, and no precipitation. These conditions are not always available, which provides some limitation to the technology. Hand held cameras are also unable to detect subtle thermal contrasts produced by deeper delaminations. For these reasons, IR may not always be the best method, but it can be very effective under conducive inspection conditions.

The IR-UTD system was developed as a new technology for the purpose of producing quantifiable infrared results. Hand held cameras are effective for delamination detection, but are not able to determine area and depth without further physical inspection, such as hammer sounding or coring. The IR-UTD system captures multiple images over a period of time rather than a single image. Post processing capabilities of the system are used to determine the rate of change of infrared radiation and produce an image of the results. The most

significant advantage of the IR-UTD system is the ability to quantify results. The percentage of delamination can be calculated when performing deck inspections and relative depth of delamination can be determined. This information plays an important role in determining when a deck should be replaced. The IR-UTD system is also less dependent on environmental conditions, is able to detect deeper defects due to processing capabilities, and does not require an inspector after test initiation. The UTD system is a highly effective inspection tool and can achieve more comprehensive results that are not possible with the hand held camera.

Implementation challenges of the hand held camera were identified utilizing surveys and phone interviews with participating states of the project. Initial concerns prior to training included staff time constraints and difficulty operating the technology. After training and experience with the technology, phone interviews were conducted to see if the view of possible implementation barriers had changed. It was determined that staff time constraints were still providing problems with performing IR inspections, but difficulty using the technology did not seem to be a problem. Another concern identified during the phone interviews was the environmental dependency.

Both technologies can be used as effective tools for bridge inspection, individually. They could be used more effectively as a combination. The hand held camera serves as a good initial inspection tool and the UTD system can be used for more in depth analysis. These technologies would be easy to implement into a bridge program because of their effectiveness and relative ease of use.

## 8.2 Future Work

Further inspection with the IR-UTD system is in the scope of work for the rest of the project. Additional testing is to be conducted on bridge components not exposed to solar loading and decks with asphalt overlays. Testing in other participating states would also be beneficial to the project to show them how effective the IR-UTD technology is. That would be the first step to further exposing the technology, and possibly leading to wider use.

A wind study using a variable wind source, test block, and infrared heaters will be conducted to gain a more accurate analysis of how wind affects surface temperature. A test block will be heated over a period of time, and then thermal contrast will be measured while varying wind speeds are blown over the surface. This test will determine how much thermal contrast is lost with varying wind speeds and at what speed wind becomes detrimental to thermographic inspection.

A system is currently being developed for vehicle mounted inspections. A fifth wheel would be attached to the back of a vehicle for mounting an infrared camera head. The wheel would contain an encoder that would signal the camera to capture an image after a given distance had been traveled. This would allow for a full infrared bridge survey to be conducted in a short amount of time and without leaving a vehicle. The vehicle would only be able to travel approximately 5 mph while inspecting, and for that reason, it is expected that traffic control would be necessary on bridges with higher traffic volumes.



## REFERENCES

1. Alqannah, H. (2000). "Detection of Subsurface Anomalies in Composite Bridge Decks Using Infrared Thermography". West Virginia University.
2. Arnold, R. H., Furr, H. L., Rouse, J. W. (1969). "Infrared Detection of Concrete Deterioration. College Station, TX, Texas A&M University Remote Sensing Center 14.
3. ASTM (2007). "Standard Test Method for Detecting Delaminations in Bridge Decks Using Infrared Thermography". Standard ASTM D4788-03(2007). West Conshohocken, PA, ASTM International.
4. Bertolini, L., et al (2004). ""Effectiveness of a Conductive Cementitious Mortar Anode for Cathodic Protection of Steel in Concrete"." Cement & Concrete Research.
5. Cady, P. D., Weyers, R.E. (1992). ""Predicting Service Life of Concrete Bridge Decks Subject to Reinforcement Corrosion"." Corrosion Forms and Control for Infrastructure.
6. Clark, M. R., McCann, D. M., Forde, M. C. (2003). ""Application of Infrared Thermography to the Nondestructive Testing of Concrete and Masonry Bridges:." NDT&E International **36**: 265-275.
7. Clemena, G. G., Mckeel, W. T. (1978). ""Detection of Delamination in Bridge Decks with Infrared Thermography"." Transportation Research Board **664**: 180-182.
8. Fenwick, R. (2009). "Development of Handheld Thermographic Inspection Technologies". Department of Civil and Environmental Engineering, University of Missouri-Columbia.
9. FHWA (2014). "National Bridge Inventory Deck Structure Type".
10. Huston, D., et al (2002). "Nondestructive Testing of Reinforced Concrete Bridges Using Radar Imaging Techniques". Final Research Report NETC: 92-94.
11. Kee, S., et al (2012). ""Nondestructive Bridge Deck Testing with Air-Coupled Impact-Echo and Infrared Thermography"." Journal of Bridge Engineering **17**(6): 928-939.
12. Leinhard, J., Eichhorn, R. (1981). A Heat Transfer Textbook. Englewood Cliffs, NJ, Prentice-Hall.

13. Maierhofer, C. (2003). "Nondestructive Evaluation of Concrete Infrastructure with Ground Penetrating Radar." Journal of Materials in Civil Engineering **15**: 287.
14. Maldague, X. (2000). "Applications of Infrared Thermography in Nondestructive Evaluation." Trends in Optical Nondestructive Testing: 591-609.
15. Manning, D. G., Holt, F. B. (1980). "Detecting Delamination in Concrete Bridge Decks." Concrete International **2**(11): 34-41.
16. Manning, D. G., Holt, F. B. (1983). "Detecting Deterioration in Asphalt-Covered Bridge Decks." Transportation Research Record **899**.
17. Manning, D. G., Masliwec, T. (1990). "Application of Radar and Thermography to Bridge Deck Condition Surveys." Bridge Management: Inspection, Maintenance, Assessment and Repair.
18. Maser, K. R., Roddis, W. M. K. (1990). "Principles of Thermography and Radar for Bridge Deck Assessment." Journal of Transportation Engineering **116**(5): 583-601.
19. Masliwec, T. (1988). "An Experimental and Theoretical Evaluation of IR Thermography for Surveying the Condition of Bridge Decks." Proc. SPIE Thermosense X **934**.
20. Nelson, S. (2013). "Training and Field Verification for Hand-Held Thermographic Inspection Technologies." Department of Civil and Environmental Engineering, University of Missouri-Columbia.
21. Roddis, W. M. K. (1987). "Concrete Bridge Deck Assessment Using Thermography and Radar." Department of Civil Engineering, Massachusetts Institute of Technology.
22. Scott, M. L. (1999). "Automated Characterization of Bridge Deck Distress Using Pattern Recognition Analysis of Ground Penetrating Radar Data."
23. Shirkey, R. C., Sauter, B. J. (2001). "Weather Effects on Target Acquisition Part I: Sensor Performance Model Infrared Algorithms". Adelphi, MD, Army Research Laboratory: 9-14.
24. Simonen, J., Green, T., Anderson, E. (2013). "Specialized Post-Tensioning Void Testing". Portland, OR, Wiss, Janney, Elstner Associates, Inc.: 8.

25. Sohangpurwala, A. A. (2006). "Bridge Inspection Practices". Washington D.C., Transportation Research Board National Research, NCHRP Synthesis. **558**.
26. Srinivasan, P., Ravisankar, K., Thirugnanasambandam, S. (2012). "Nondestructive Evaluation of Concrete Structures with Ground Penetrating Radar and Influencing Parameters." IUP Journal of Structural Engineering **5(4)**: 43-52.
27. UMC (2015). "History of the Columns." from <http://missouri.edu/about/history/columns.php>.
28. Usamentiaga, R., et al (2014). "Infrared Thermography for Temperature Measurement and Nondestructive Testing." Sensors **14(7)**: 12305-12348.
29. Vaghefi, K., Ahlborn, T., Harris, D., and Brooks, C. (2013). "Combined Imaging Technologies for Concrete Bridge Deck Condition Assessment." J. Perform. Constr. Facil.
30. Vu, K., Stewart, M. (2000). "Structural Reliability of Concrete Bridges Including Improved Chloride-Induced Corrosion Models." Structural Safety **22(4)**: 313-333.
31. Washer, G., Bolleni, N. K., Fenwick, R. (2010). "Thermographic Imaging of Subsurface Deterioration in Concrete Bridges." Transportation Research Board **2201**: 27-33.
32. Washer, G., Fenwick, R., Harper, J. (2009). "Effects of Environmental Variables on the Infrared Imaging of Subsurface Features in Concrete Bridges." Transportation Research Board **2108**: 107-114.
33. Washer, G., Trial, M., Jungnitsch, A., Nelson, S. (2014). "Field Testing of Hand-Held Infrared Thermography, Phase II", University of Missouri-Columbia. **1**.
34. Wunderground (2013-2015). Accessed multiple times for weather data corresponding to testing.
35. Yehia, S., Abudayyeh, O., et al (2007). "Detection of Common Defects in Concrete Bridge Decks Using Nondestructive Evaluation Techniques." Journal of Bridge Engineering **12**: 215-225.
36. Yu, J. (1989). "Using Infrared Thermography to Measure the Maturity of Concrete". Department of Civil Engineering. Massachusetts Institute of Technology.

## **APPENDIX A**

### **Development of Hand held Thermographic Inspection Technologies**

# **Revised Guidelines for Thermographic Inspection of Concrete Bridges**

**August 19, 2009**

**Revised January, 2014**

**Revised October, 2014**

**DRAFT**

*RI06-038*

*TPF-5 (247)*

Principal Investigator: Dr. Glenn Washer, Ph.D., P.E.

Department of Civil and Environmental Engineering  
University of Missouri – Columbia  
E2503 Lafferre Hall  
Columbia, MO 65211



1 **Guidelines for Thermographic Inspection of Concrete Bridges**

2 The following are suggested guidelines for the thermographic inspection of  
3 highway bridges, based on the results of the research.

4 1.0 Surfaces exposed to Direct Solar Loading

5 1.1 Solar loading

6 1.1.1 Conduct inspections on days when there is direct,  
7 uninterrupted solar loading. Cloud cover should be minimal.

8 1.1.2 Summer days are preferred over winter days due to more  
9 intense and longer solar exposure.

10 1.2 Wind Conditions

11 1.2.1 Lower wind speeds will result in improved thermal contrast for  
12 surfaces exposed to solar loading. In general, wind reduces  
13 the effect of radiant heating from the sun and reduces the  
14 thermal contrast resulting from subsurface defects.

15 1.2.2 Average wind speeds should be 15 mph or less prior to and  
16 during the inspection period. These data can be obtained  
17 based on National Weather Service (NWS) hourly wind  
18 reports<sup>(5.1)</sup>.

19 1.3 Inspection Period

20 1.3.1 Inspections should be conducted starting no sooner than 4  
21 hours after sunrise to allow for thermal contrast to develop  
22 when anticipated depth of the delamination is approximately  
23 2 in. from the surface of the concrete. The useful inspection

24 period is expected to last approximately 6 hours. If the  
25 anticipated depth is 3 inches, inspection should be conducted  
26 starting 5 to 6 hours after sunrise. The useful inspection  
27 period will last approximately 5 hours<sup>(5.2)</sup>.

## 28 2.0. Shaded Surfaces – Daytime inspection

### 29 2.1 Ambient Temperature Changes:

30 2.1.1 Inspection should be conducted on days when the ambient  
31 temperature differential is expected to be at least 15°F.

32 2.1.2 The measured ambient temperature differential should be at  
33 least 10°F within the first 6 hours after sunrise.

34 2.1.3 In general, more rapid increases in ambient temperature will  
35 result in improved thermal contrast.

36 2.1.4 When ambient temperatures begin to decrease, thermal  
37 contrasts will also begin to decrease for a 2 in. deep  
38 delamination.

39 2.1.5 Local environment: The indicated ambient temperature  
40 differentials must be applied at the surface to be inspected. If  
41 the location and geometry of the bridge results in reduced  
42 ambient temperature changes at the surface to be inspected,  
43 this should be considered in determining if adequate  
44 conditions exist for detection of subsurface defects. A simple  
45 temperature monitoring device that stores hourly

46 temperatures can be used to assess the local conditions at a  
47 bridge.

## 48 2.2 Wind Speed

49 2.2.1 A practical limit of 25 mph average wind speed is suggested,  
50 based on NWS data<sup>(5.1)</sup>. High average wind speeds are not  
51 necessarily detrimental to the development of thermal  
52 contrast for shady conditions.

## 53 2.3 Inspection Periods

54 2.3.1 Inspections should be conducted starting 4 to 5 hours after  
55 sunrise to allow for thermal contrast to develop when  
56 anticipated depth of the delamination is approximately 2 in.  
57 from the surface of the concrete. The useful inspection period  
58 is expected to last approximately 8 hours. If the anticipated  
59 depth is 3 in., inspection should be conducted starting  
60 approximately 7 hours after sunrise. The useful inspection  
61 period is expected to last approximately 4 hours.

## 62 2.4 Deck Soffit Inspections

63 2.4.1 Solar loading on the surface of a bridge deck affects the  
64 detection of delamination in the soffit of the deck due to  
65 thermal conduction. As a consequence, delamination in the  
66 soffit may appear colder than surrounding concrete rather  
67 than warmer, as would typically be expected during a warming  
68 cycle. The approximate timing of when this may occur can be

69 estimated with knowledge of the deck thickness (t, in.). The  
70 reversal, from warm to cold, of a delamination in the soffit will  
71 occur t hours after the solar loading begins. For example, for  
72 a bridge deck 7 inches thick, assuming sunrise at 6 am, the  
73 reversal will occur at ~1 pm. Care should be taken in the  
74 preceding 2 hrs, because thermal contrast may be minimal  
75 during this time period.

### 76 3.0 Shaded Surfaces – Nighttime inspections

#### 77 3.1 Ambient Temperature Changes:

78 3.1.1 Inspection should be conducted on nights when the ambient  
79 temperature differential is expected to be at least -15°F. This  
80 value is measured from the highest temperature in the  
81 afternoon to the coldest temperature in the overnight period.

82 3.1.2 The measured ambient temperature differential should be at  
83 least -10°F during the 6 hours preceding sunset for the  
84 previous day.

85 3.1.3 In general, more rapid decreases in ambient temperature will  
86 results in improved thermal contrast.

87 3.1.4 When ambient temperatures begin to increase, thermal  
88 contrasts will begin to decrease for a 2 in. deep delamination.

89 3.2 Local environment: The indicated ambient temperature differentials  
90 must be applied at the surface to be inspected. If the location and  
91 geometry of the bridge result in reduced ambient temperature changes



92 at the surface to be inspected, this should be considered in determining  
93 if adequate conditions exist for detection of subsurface defects.

### 94 3.3 Wind Speed

95 3.3.1 A practical limit of 25 mph average wind speed is suggested,  
96 based on NWS data<sup>(5.1)</sup>. High average wind speeds are not  
97 necessarily detrimental to the development of thermal  
98 contrast for shady conditions.

### 99 3.4 Inspection Periods

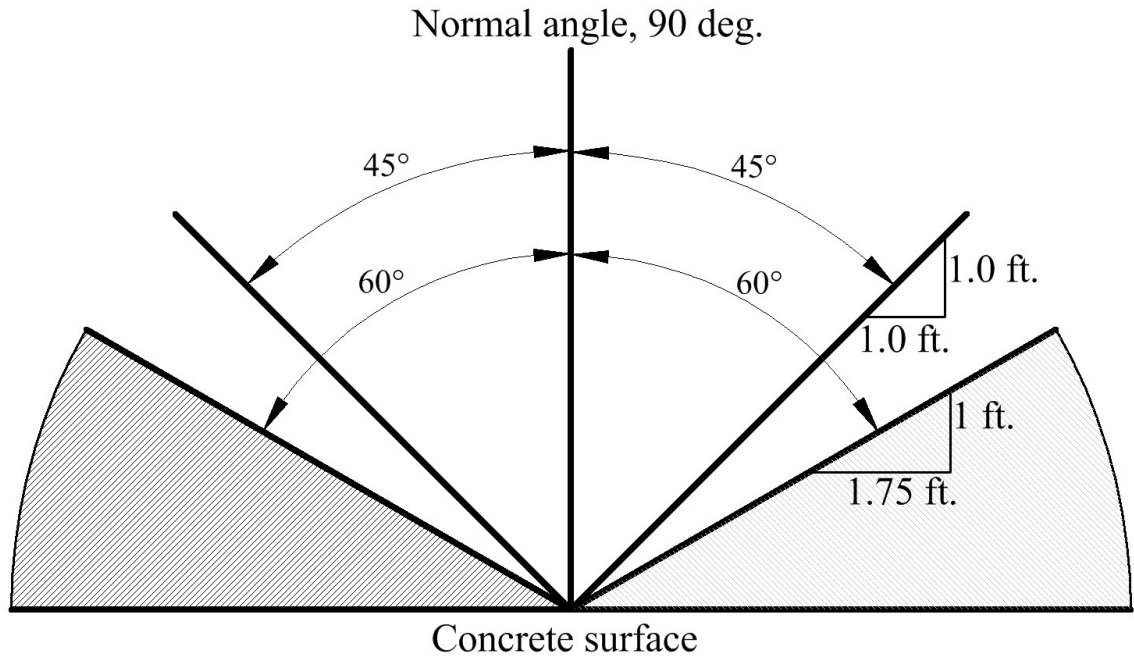
100 3.4.1 Inspections should be conducted starting 1 hour after sunset  
101 when the anticipated depth of the delamination is  
102 approximately 2 in. from the surface of the concrete. The  
103 useful inspection period is expected to last approximately 9  
104 hours. If the anticipated depth is 3 inches, inspection should  
105 be conducted starting approximately 3 hours after sunset. The  
106 useful inspection period is expected to last approximately 7  
107 hours.

## 108 4.0 Camera Settings

109 4.1 Focus: To allow for small temperature contrasts at delaminations to be  
110 detected, cameras should be properly focused on the inspection surface.  
111 Placement of a regularly shaped object, such as a tool or a coin, on the  
112 surface to be inspected can be used to assist in focusing the camera  
113 properly. Well defined edges or an object on the structure surface, such  
114 as utility connections, can also be used.

115 4.2 Level and span: Level and span settings for the camera should be  
116 manually adjusted. Contrast levels for delaminations are typically small,  
117 ~1-2°F. As such, span settings in the range of 4 to 8°F are recommended  
118 for applications where solar loading is not applied. For solar loaded  
119 areas, a span of up to ~10°F may be warranted, but consideration should  
120 be given to the associated loss in sensitivity to thermal contrast in the  
121 image. The level setting should be adjusted to allow for images to be  
122 properly interpreted based on the span. This may require frequent  
123 adjustment when temperatures vary across a structure.

124 4.3 Angle of Observation: Observing surfaces at a low angle can increase  
125 ambient reflections and frequently produces an apparent thermal  
126 gradient across the image. Inspections should be conducted as close to  
127 normal angles (90°) as practical. A practical guideline is to try to stay  
128 within +/- 45 degrees from normal. Angles of more than 60° from normal  
129 should be avoided. Utilization of a wide angle lens can assist in  
130 maintaining normal angles when deck inspections are being conducted.  
131 Figure A-1 below shows the indicated angles for reference.



132

133

**Figure A-0-1: Schematic diagram of observation angles**

134

4.4 Lens Selection: Lens selection is based on inspector distance from surface being inspected, assuming a critical dimension of 6 inches for the damage to be identified. If closer than 35 feet to the delamination, the wide angle lens (45°) is suggested. If 7 further than 35 feet, the regular lens (25°) is suggested. For distance greater than 65 ft., a telephoto lens may be used.

135

136

137

138

139

140 5.0 Commentary

141

5.1 Wind Speed for Sunny Conditions: High wind speeds are detrimental to thermographic inspection under conditions where radiant heating from the sun is involved. Wind speed guidelines have been configured to match NWS data, based on averages provided on an hourly basis. These data were determined by correlating 6 hour averages of the

142

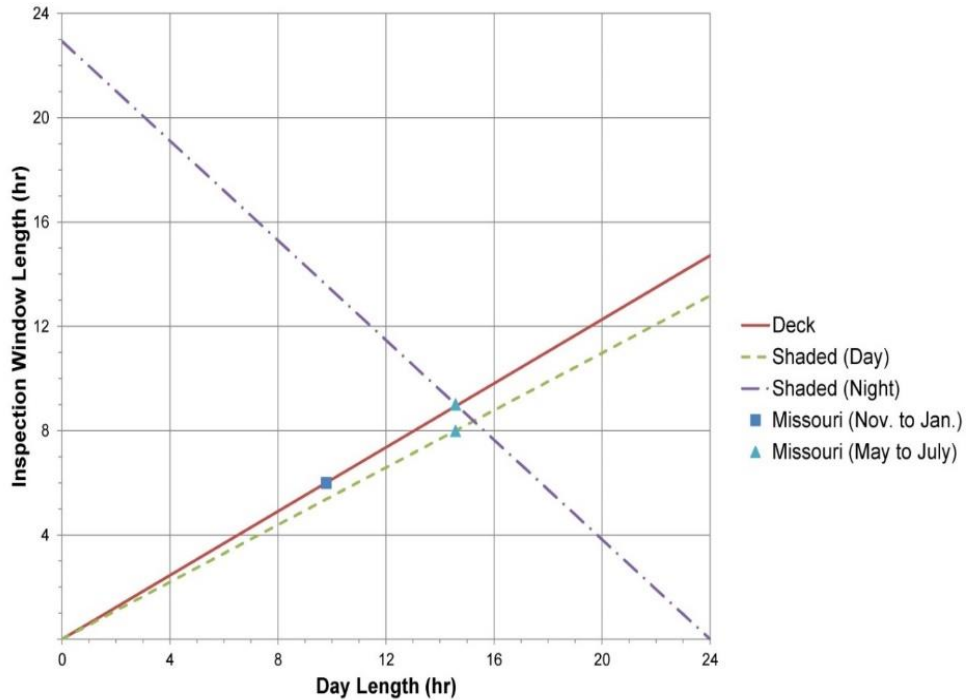
143

144

145

146 second and third quarters of the day, used in the original research, with  
147 wind data provided by the National Weather Service (NWS).

148 5.2 Inspection time periods are based on observations in the research  
149 conducted. For solar exposed surface, measurements were made  
150 during the months of November, December and January, when there  
151 are fewer hours of sunlight than other times of the year. For shaded  
152 surfaces, measurements were made during the months of May, June  
153 and July, when there are more hours of sunlight than other times of the  
154 year. As a result, the inspection intervals suggested are for general  
155 guidance; the time of year in which the inspection is actually conducted  
156 should be considered in applying this guidance. Figure A-2 can be used  
157 to estimate the inspection time periods, based on a delamination depth  
158 of 2 in. below the surface. To utilize this graph, the length of the day  
159 (sunrise to sunset) (horizontal axis) can be used to estimate the length  
160 of the inspection window on the vertical axis.



161

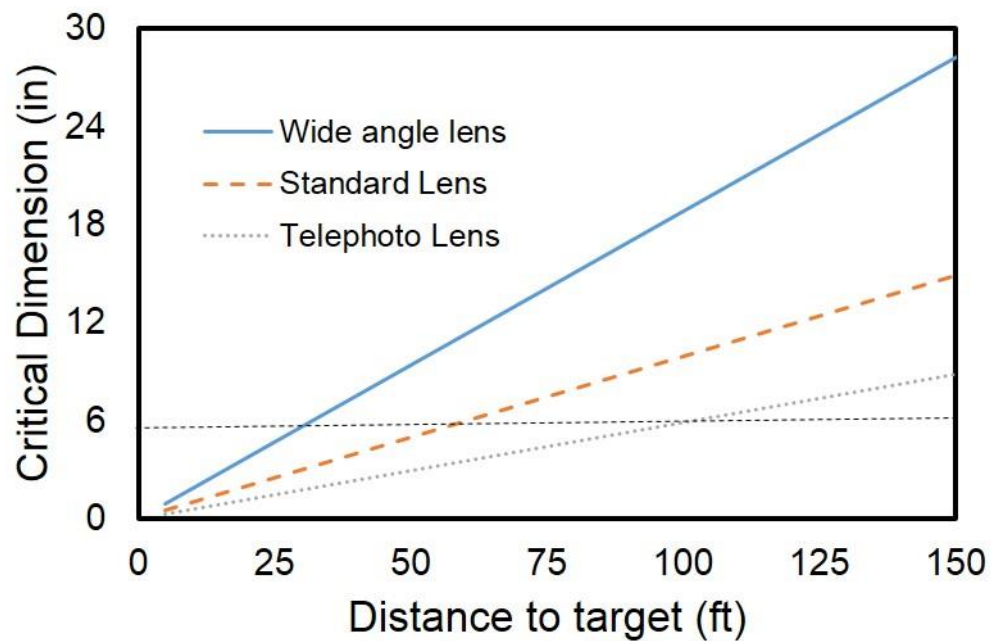
162 **Figure A-0-2: Graph showing inspection windows as a function of day length**

163 5.3 Effect of material in the delamination: If the void is filled with ice, water  
 164 or epoxy, the increased thermal conductivity across the void will  
 165 diminish the thermal contrast between the void and the surrounding  
 166 intact concrete. Under such conditions, the subsurface void may not be  
 167 detectable.

168 5.4 Moisture on the surface of the concrete as a result of precipitation may  
 169 diminish the thermal contrast between voided areas and intact areas of  
 170 concrete, due to evaporation.

171 5.5 Figure A-3 shows the critical dimension as a function of distance for a  
 172 wide angle, standard and telephoto lens. These data are based on  
 173 criteria for identification of a delamination appearing as a thermal

174 contrast in an image. Identification is based on an object occupying at  
175 least 12 pixels across its smallest dimension which was taken from  
176 Johnson's criteria for image forming systems. Based on these data, it is  
177 suggested that a wide-angle lens is suitable for inspections conducted  
178 from a distance of 35 ft. or less, a standard lens is suitable at distance  
179 of up to 65 feet, and a telephoto lens is suitable at distances greater  
180 than 65 ft.



181

182 **Figure A-0-3: Graph showing critical dimension as a function of distance**